

# Oil And Gas Geoscience Reports 2011



**BC Ministry of Energy and Mines**  
Geoscience and Natural Gas Development Branch



© British Columbia Ministry of Energy and Mines  
Oil and Gas Division  
Geoscience and Natural Gas Development Branch  
Victoria, British Columbia, April 2011

Please use the following citation format when quoting or reproducing parts of this document:

Huntley, D. H., Hickin, A. S. and Ferri, F. (2011): Provisional surficial geology, glacial history and paleogeographic reconstructions of the Toad River (NTS 094N) and Maxhamish Lake map areas (NTS 094O), British Columbia; in Geoscience Reports 2011, *BC Ministry of Energy and Mines*, pages 37–56.

Colour digital copies of this publication in Adobe Acrobat PDF format are available, free of charge, from the BC Ministry of Energy and Mines website at:

<http://www.em.gov.bc.ca/subwebs/oilandgas/pub/reports.htm>

## FOREWORD

Geoscience Reports is the annual publication of the Geoscience and Natural Gas Branch (formerly Resource Development and Geoscience Branch) of the Oil and Gas Division, BC Ministry of Energy and Mines (BCMÉM). This publication highlights petroleum related geosciences activities carried out in British Columbia by ministry staff and affiliated partners. All of the studies in the 2011 volume were conducted as part of a collaborative Provincial-Federal partnership between the Geological Survey of Canada (GSC) and BCMÉM. The studies are a component of the Yukon and Liard Basins Project under the GSC's Geo-mapping for Energy and Minerals (GEMs) initiative. This initiative is in cooperation with the Provinces and Territories and designed to provide geoscience knowledge necessary to sustain investment through socially and environmentally responsible energy resource development.

The 2011 volume includes five articles. The first four papers relate to recent field activities in the Horn River and Liard basins. Two contributions are thematic shale gas outcrop studies from the Liard Plateau. Another two papers relate to the application of surficial geology with implications for gas infrastructure development, surface engineering and completion operations. The final paper focuses on laboratory experiments involving hydraulic fracture proppant from a northeast BC sand source.

The first two papers in this volume by Ferri et al. highlight results of recent fieldwork in the Selwyn Mountains. These rocks are the equivalent to those currently being explored for shale gas in the subsurface. The first paper focuses on the Devonian-Mississippian Besa River and Exshaw formations that contain intervals equivalent to the Horn River Group, the target for shale gas development in the Liard and Horn River basins. Cretaceous Garbutt Formation is the subject of the second paper, as these rocks may have natural gas potential. Both of these studies describe and discuss lithostratigraphy, geochemistry, and gamma-ray spectrometer response from the outcrop. The papers examine the relationship between organic preservation and redox conditions at the time of deposition.

The papers by Huntley and Hickin and Huntley et al. focus on surficial geology and glacial history. These papers provide geoscience information on surficial earth materials, geohazards and resource potential for granular aggregate, frac sand and groundwater that is critical for infrastructure development, surface engineering and completion operations. The first paper presents the provisional distribution of surficial deposits and landforms, and describes the sedimentology, surface morphology and facies associations. The second paper describes remote predictive digital terrain mapping and field-based reconnaissance studies in the Horn River and Liard basins. It provides new insight into limits of glaciation, the range of subglacial processes, the patterns of ice flow and the history of ice retreat and glacial lake formation during the late Quaternary and Holocene.

The final paper in the volume is by Hickin and Huntley and examines beneficiation of potential hydraulic fracture sand from northeast BC. Several experiments are presented that focus on washing, sizing and attrition to improve the quality of a promising aeolian sand deposit. This work is part of an initiative to promote the development of a local frac sand industry in BC thereby reducing completion costs and making BC a more competitive jurisdiction.

### **Adrian S. Hickin**

Senior Project Geologist  
Geoscience and Natural Gas Development Branch  
Oil and Gas Division  
British Columbia Ministry of Energy and Mines



# TABLE OF CONTENTS

## GEOSCIENCE REPORTS 2011

BESA RIVER FORMATIONS, WESTERN LIARD BASIN, BRITISH COLUMBIA (NTS 094N): GEOCHEMISTRY AND REGIONAL CORRELATIONS .....	1
<i>by Filippo Ferri, Adrian S. Hickin and David H. Huntley</i>	
GEOCHEMISTRY AND SHALE GAS POTENTIAL OF THE GARBUTT FORMATION, LIARD BASIN, BRITISH COLUMBIA (PARTS NTS 094N, O; 095B, C) .....	19
<i>by Filippo Ferri, Adrian S. Hickin and David H. Huntley</i>	
PROVISIONAL SURFICIAL GEOLOGY, GLACIAL HISTORY AND PALEO GEOGRAPHIC RECONSTRUCTIONS OF THE TOAD RIVER (NTS 094N) AND MAXHAMISH LAKE MAP AREAS (NTS 094O), BRITISH COLUMBIA (NTS 094B/14) .....	37
<i>by David H. Huntley, Adrian S. Hickin and Filippo Ferri</i>	
GEO-MAPPING FOR ENERGY AND MINERALS PROGRAM (GEM-ENERGY): PRELIMINARY SURFICIAL GEOLOGY, GEOMORPHOLOGY, RESOURCE EVALUATION AND GEOHAZARD ASSESSMENT FOR THE MAXHAMISH LAKE AREA (NTS 094O), NORTHEAST BRITISH COLUMBIA .....	57
<i>by David H. Huntley and Adrian S. Hickin</i>	
ATTRITION EXPERIMENTS FOR THE BENEFICIATION OF UNCONSOLIDATED SAND SOURCES OF POTENTIAL HYDRAULIC FRACTURE SAND, NORTHEAST BRITISH COLUMBIA .....	75
<i>by Adrian S. Hickin and David H. Huntley</i>	





# BESA RIVER FORMATION, WESTERN LIARD BASIN, BRITISH COLUMBIA (NTS 094N): GEOCHEMISTRY AND REGIONAL CORRELATIONS

Filippo Ferri<sup>1</sup>, Adrian S. Hickin<sup>1</sup> and David H. Huntley<sup>2</sup>

---

## ABSTRACT

*The Besa River Formation in the northern Toad River map area contains correlatives of the subsurface Muskwa Member, which is being exploited for its shale gas potential. In the Caribou Range, more than 285 m of fine-grained carbonaceous siliciclastic sediments of the Besa River Formation were measured along the northwestern margin of the Liard Basin (the upper 15 m and lower 25 m of the section are not exposed). The formation has been subdivided into six informal lithostratigraphic units comprised primarily of dark grey to black, carbonaceous siltstone to shale. The exception is a middle unit comprising distinctive pale grey weathering siliceous siltstone. A handheld gamma-ray spectrometer was used to produce a gamma-ray log across the section, which delineated two radioactive zones that are correlated with the Muskwa and Exshaw markers in the subsurface. Rock-Eval geochemistry indicates that there are several zones of high organic carbon, with levels as high as 6%. Abundances of major oxides and trace elements show distinct variability across the section. The concentration of major oxides generally correlates with lithological subdivisions, whereas some of the trace-element abundances display a relationship with organic carbon content, suggesting that these levels are tied to redox conditions at the time of deposition.*

Ferri, F., Hickin, A. S. and Huntley, D. H. (2011): Besa River Formation, western Liard Basin, British Columbia (NTS 094N): geochemistry and regional correlations; in *Geoscience Reports 2011, BC Ministry of Energy and Mines*, pages 1-18.

<sup>1</sup>Geoscience and Natural Gas Development Branch, Oil and Gas Division, BC Ministry of Energy and Mines, Victoria, BC; Fil.Ferri@gov.bc.ca

<sup>2</sup>Geological Survey of Canada, Natural Resources Canada, Vancouver, BC

**Key Words:** Liard Basin, Horn River Basin, Liard River, Toad River, Caribou Range, Besa River Formation, Horn River Formation, Muskwa Member, Fort Simpson Formation, Exshaw Formation, Mattson Formation, geochemistry, gamma ray, Rock-Eval, total organic content, oil, gas, sulphides

---

## INTRODUCTION

The Geoscience and Natural Gas Development Branch of the British Columbia Ministry of Energy and Mines, in conjunction with the Geological Survey of Canada, undertook an examination of outcrop exposures of Middle Devonian to early Mississippian siltstone sequences of the Besa River Formation, which are equivalent, in part, to rocks currently being exploited for natural gas resources in the Horn River Basin and to sections being examined for similar potential in the Liard Basin (Figures 1 and 2). The main objective of this examination was to delineate shale gas-equivalent horizons in outcrop so that they could be used as potential reference sections to aid in understanding the subsurface geological setting in the Horn River Basin. Characterization of the section was accomplished through lithological description and collection of samples for lithological, organic geochemical and geochronological analysis. In addition, a gamma-ray spectroscopic survey of the outcrop was performed for use in correlating the section with subsurface sequences in the Liard and Horn River basins.

This study is part of a collaborative program between the Geological Survey of Canada and the British Columbia Ministry of Energy and Mines, and is under the umbrella of the federal government's Geo-mapping for Energy and Minerals program (GEM), which is examining petroleum-related geoscience of the Liard and Horn River basins. A major focus of this program has involved mapping resources associated with surficial geology that will assist with operational aspects of resource development (infrastructure, surface engineering, drilling and completion; Huntley and Hickin, 2010; Huntley and Sidwell, 2010; Huntley and Hickin, 2011; and Huntley et al., 2011).

## LOCATION AND REGIONAL GEOLOGY

The Liard Basin is located in northeastern British Columbia, straddling the British Columbia–Yukon–Northwest Territories border (Figures 1 and 2), spanning NTS map areas 094N and O, and 095B and C. It is traversed by the Liard River and defines a relatively high plateau between the southern Selwyn Mountains and the northern Rocky

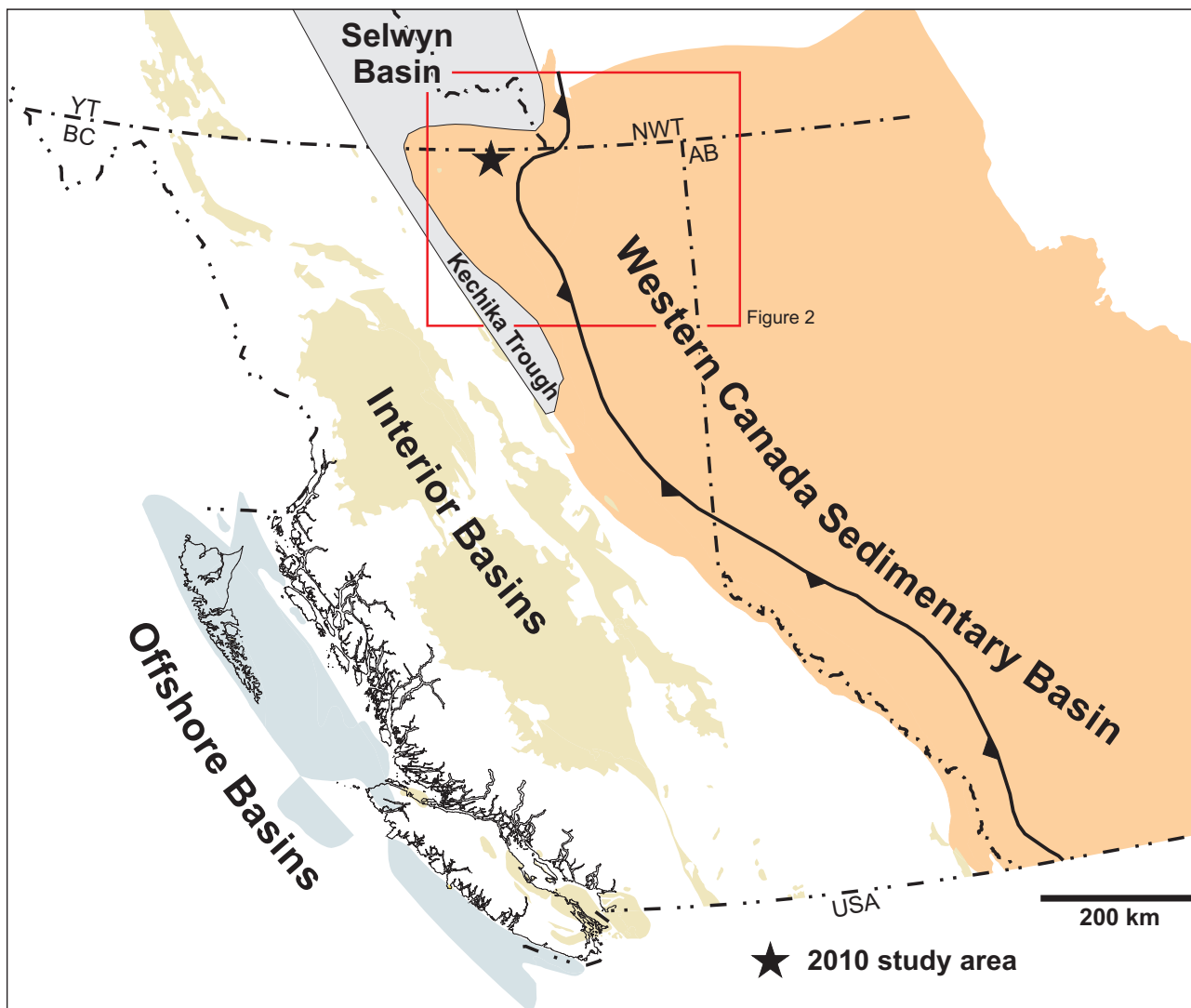


Figure 1. Location of the Liard Basin with respect to the primary sedimentary basins of Western Canada. Also shown are the Early Paleozoic offshore depocentres of the Selwyn Basin and the Kechika Trough. The red box outlines the area shown in Figure 2. Basin outlines are from Mossop et al. (2004).

Mountains. Highway 77 runs along the eastern half of the basin and joins with the Alaska Highway, which cuts across the southern margin. Numerous petroleum activity roads and forestry access roads extend from these two main highways across the basin. Vehicle access across the Liard River is provided by a barge that originates at Fort Liard, NWT and terminates south of the confluence of La Biche River, where a road connects to the Beaver River gas field (Figure 3).

The Liard Basin is defined on the basis of its thick Late Paleozoic succession (Gabrielse, 1967; Figures 4 and 5). The Bovie Lake structure marks the eastern margin of the basin, west of which is an anomalously thick section of the Mississippian Mattson Formation (Figure 4). Subsequent Late Cretaceous movement on this fault has also preserved a thick sequence of Early to Late Cretaceous rocks (Leckie et al., 1991). Although the development of the Liard Basin had no influence on depositional facies and thicknesses of

shale gas units within the older Horn River Basin (i.e., Horn River Formation), its initiation effectively marked the current western limit of shale gas development in the Horn River Basin. Prospective shale horizons in the eastern Horn River Basin, west of the Bovie fault (Figure 2), have been dropped deeper by approximately 2000 m (Figure 4), imposing drilling and completion challenges. A consequence of this has been a shift to the exploitation of the stratigraphically higher Exshaw Formation within the Liard Basin, which is at a depth that can be potentially economically developed for its shale gas resources.

The Middle Devonian to mid-Mississippian Besa River Formation represents the western basinal equivalents of predominantly carbonate successions between the Upper Keg River and Debolt formations (Figures 4 and 5). Farther west, in the Selwyn Basin and Kechika Trough, these rocks correlate with the Devonian-Mississippian Earn Group (Figure 6). The Selwyn Basin and the Kechika Trough are



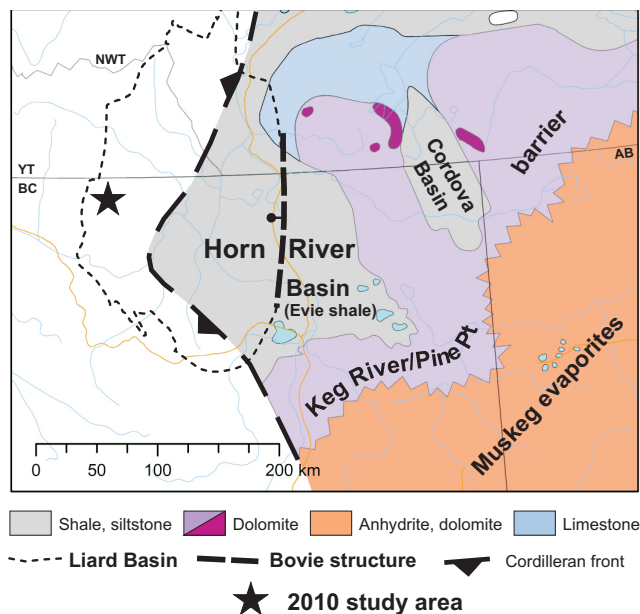


Figure 2. Schematic representation of the Horn River Basin (and Cordova Basin) during upper Keg River times (Givetian). Superimposed on this is the outline of the Liard Basin. This reef-carbonate-shale basin configuration persisted until the end of Slave Point times (end of Givetian; modified from Meijer Drees, 1994). Liard Basin outline is from Mossop et al. (2004).

deep-water equivalents to Early Paleozoic carbonate shelf deposition along the Western Canada Sedimentary Basin (MacDonald Platform; Ferri et al., 1999) and are filled primarily by shale and siltstone of the Kechika and Road River groups.

In the study area, Besa River shale and siltstone sit above carbonate rocks of the Middle Devonian Dunedin Formation, which can be traced westward into the subsurface where it is equivalent to parts of the Chinchaga and Lower Keg River formations (Figure 5; Meijer Drees, 1994). During Upper Keg River and Slave Point deposition, a well-defined barrier reef complex was developed, which marked the eastern limit of the Horn River Basin (Figures 2 and 3; Oldale and Munday, 1994). West of the barrier edge, shales of the Horn River Formation include a stratigraphically lower radioactive, bituminous shale assigned to the Evie Member, overlain by shale of the Otter Park Member (Figures 4 and 5). A transgression followed the Slave Point deposition and pushed the shallow carbonate edge eastward (Leduc facies), leading to deposition of the highly bituminous shale of the Muskwa Formation (Duvernay equivalent; Switzer et al., 1994). Carbonate conditions were re-established to the west during Frasnian and Famennian times, resulting in deposition of Kakiska to Kotcho formations along a broad shelf (Figures 4 and 5). A major transgression occurs across the Devonian-Mississippian boundary, represented by deposition of the highly radioactive and bituminous shale of the Exshaw Formation. Carbonate deposition again migrated westward in Early Carboniferous times, with the deposition of the

Banff Formation and the succeeding Rundle Group.

In the subsurface, the shale of the Fort Simpson Formation encompasses the westward shale-out of the carbonate units above the Muskwa Formation. Carbonate rocks of the Banff Formation and the Rundle Group disappear into basinal shale above the Exshaw Formation and finally into the Besa River Formation (Figures 4 and 5). Approximately 300 m of Besa River siltstone and shale equates to more than 2000 m of the carbonate and siltstone section along the Keg River barrier edge.

The upper part of the Besa River Formation interfingers with the Middle to Late Mississippian sandstone, siltstone and minor carbonate rocks of the Mattson Formation. These exceed 1000 m in thickness within the Liard Basin west of the Bovie fault structure. This fault has been interpreted as a Late Paleozoic extensional structure that was later reactivated during the Laramide compression (Wright et al., 1994). This is based on the preservation of thick Mattson sandstone and the succeeding Kindle Formation below the Permian Fantasque Formation west of the Bovie fault, whereas only a thin Mattson section occurs below the Fantasque Formation east of the fault (Monahan, 2000; MacLean and Morrow, 2004). In addition, the westerly directed thrust associated with the Bovie fault structure is likely related to compressional reactivation of this graben structure (McClay and Buchanan, 1992). This pre-existing fault allowed compressional structures to form outboard of major Laramide structures (Figure 3). Using seismic data, MacLean and Morrow (2004) interpret the Bovie fault as having Late Paleozoic and Mesozoic compressional tectonics followed by extension during the Cretaceous.

Mattson clastic rocks are part of a slope-to-delta plain and shallow marine sandstone succession that was sourced from the north (Bamber et al., 1991). These rocks correlate with similar deposits of the Carboniferous Stoddart Group, which was deposited within the Late Paleozoic Dawson Creek graben complex (Barclay et al., 1990). Deltaic deposits of the Mattson Formation disappear westward and are replaced by the upper Earn Group siltstone and shale within the Kechika Trough.

To the west, within the Kechika Trough and the Selwyn Basin, the Besa River shale and siltstone correlate with the Middle Devonian to Early Mississippian Earn Group (MacIntyre, 1998; Paradis et al., 1998; Ferri et al., 1999). These deeper-water siliciclastic strata overlie Middle Ordovician to Middle Devonian siltstone, shale and minor carbonate rocks of the Road River Group, representing basinal equivalents of coeval carbonate of the MacDonald Platform (Figure 6).

Besa River rocks examined during the 2010 field season are located within the northern part of the Caribou Range, part of the southern Hyland Highlands, occupying the southernmost extent of the Mackenzie Mountains (Mathews, 1986). The broad highland represented by the

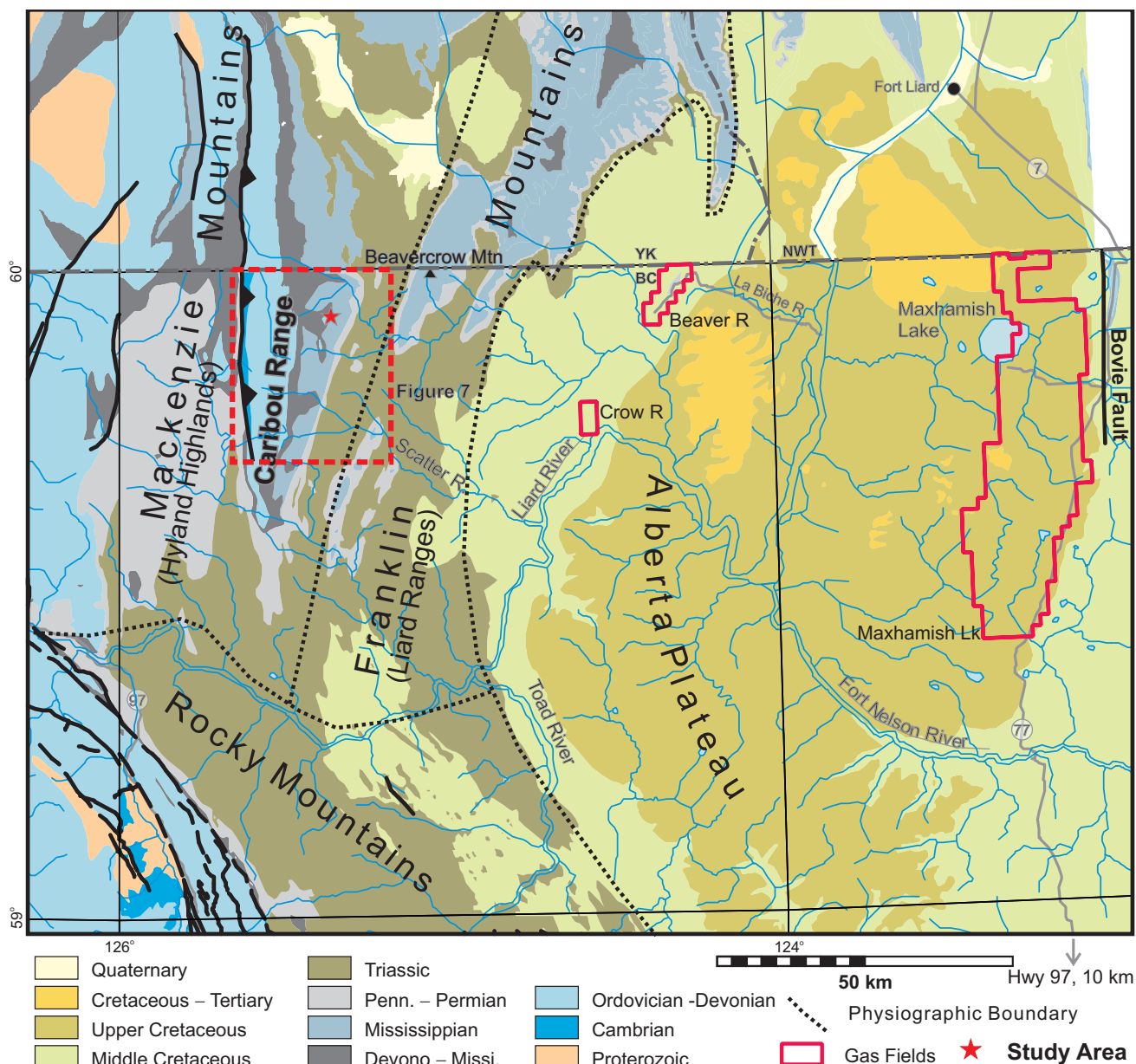


Figure 3. Geology of the western portion of the Liard Basin. The red box outlines the geology depicted in Figure 7. Geology is from MapPlace.ca (BC Geological Survey, 2011).

Caribou Range is underlain by a westwardly directed thrust panel of gently east-dipping Paleozoic rocks (Figures 2 and 7). These north- to northeast-striking rocks follow the general trend of structures within the Mackenzie and Franklin mountains and are at almost right angles to the northwest structural grain of the Rocky Mountains, resulting in the large bend in the trace of major structures across the Liard River (Figure 3). Furthermore, the southern portion of the Mackenzie and Franklin mountains represents a portion of the Foreland Belt dominated by west-verging structures, compared to overall northeast vergence seen within the Rocky Mountains (see Fallas et al., 2004).

Rocks as old as Cambrian are mapped within the Caribou Range, although these can be traced northward into

the Yukon Territory where they are assigned a Proterozoic age (Taylor and Stott, 1999; Fallas et al., 2004). Generally, rocks of the Besa River Formation overlie the Dunedin Formation, although in the north, all of the Dunedin and parts of the upper Stone formations shale out and are included in the Besa River Formation (Figure 7; Taylor and Stott, 1999).

In British Columbia, the regional geological database in the vicinity of the section includes mapping within the Toad River (Taylor and Stott, 1999), the Tuchodi Lakes (Stott and Taylor, 1973) and the Rabbit River (Gabrielse, 1963; Ferri et al., 1999) map areas. In the Yukon and Northwest Territories, La Biche River (NTS 095C) has been compiled at 1:50 000 (Fallas, 2001; Fallas and Evenchick,

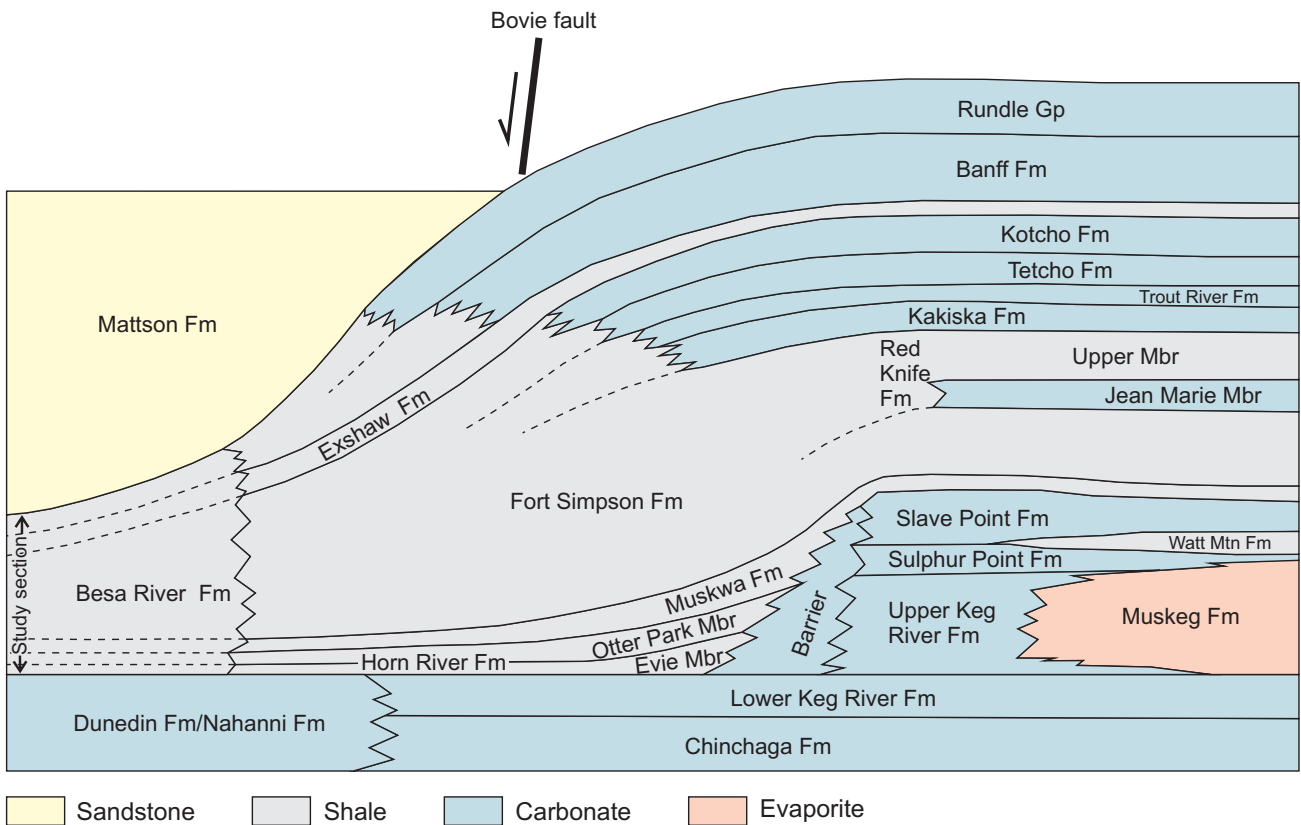


Figure 4. Schematic diagram showing relative thickness variations between Middle to Upper Paleozoic shelf and offshore sequences depicted in Figure 2.

2002) and 100 000 scales (Fallas et al., 2004). The Besa River Formation was first defined by Kidd (1963) north of the Muskwa River; later, Pelzer (1966) further described its mineralogy and broad stratigraphy. The organic petrography and thermal maturity of similar rocks in the Yukon and Northwest Territories were described by Potter et al. (1993) and Morrow et al. (1993). A recent subsurface evaluation of Devonian-Mississippian fine clastic sequences was published by Ross and Bustin (2008), which included Besa River rocks within the Liard Basin area. An assessment of the conventional hydrocarbon resources of the Liard Basin was produced by Monahan (2000).

## METHODOLOGY AND RESULTS

A nearly complete section of the Besa River Formation was measured and described through the use of a 1.5 m staff along a west-facing valley, some 22 km southwest of Beaver Mountain (base of section: UTM 367107E, 6643192N; top of section: 367496E, 6642948N; zone 10, NAD 83; Figure 7). Representative chip samples were acquired across 2 m intervals along the entire section. Samples were split, with one group being analyzed for whole-rock, trace- and rare earth element abundances by inductively coupled plasma–emission spectroscopy (ICP-ES) and

inductively coupled plasma–mass spectrometry (ICP-MS) via a lithium metaborate-tetraborate fusion at Acme Analytical Laboratories (Vancouver, BC), and a second group, at 4 m spacing, for Rock-Eval analysis at the Geological Survey of Canada (GSC) laboratories (Calgary, Alberta). A smaller subset of these samples will also be analyzed by X-ray diffraction (XRD) at the GSC laboratories for semi-quantitative determination of mineral abundances. Another subset will be processed for their potential to contain palynomorphs for biostratigraphy. Separate samples were collected for thermal maturity determination at the GSC laboratories in Calgary through reflected light microscopy. Data not presented or discussed in this paper will be presented in later publications. In addition, a handheld gamma-ray spectrometer (RS-230 by Radiation Solutions, Inc.) was used to measure natural gamma radiation every 1 m during a 2 minute time interval allowing the calculation of K (%), U (ppm), Th (ppm) and total gamma-ray count. The resulting diagram shows the variation in total natural radiation along the section and is approximately equivalent to conventional gamma-ray readings collected from boreholes in the subsurface. Results of this exercise were used to assist in the correlation of the outcrop section with equivalent rocks in the subsurface.

Approximately 285 m of siltstone and shale of the Besa River Formation were measured (Figure 8). The upper and

			Liard Basin	Horn River Basin	Platform			
Carboniferous	Penn.	U	Fantasque Formation			Fantasque Formation		
		M	Kindle Formation					
		L						
	Mississippian	U	Mattson Fm	Mattson Fm				
		M	Golata Fm	Golata Fm				
		L	Rundle Group	Rundle Group	Debolt Fm	Rundle Group	Debolt Formation	
					Shunda Fm		Shunda Formation	
	Devonian	Upper	Frasnian	Besa River Formation	Banff Fm	Banff Formation	Banff Formation	
					Exshaw Fm	Exshaw Formation	Exshaw Formation	
					Fort Simpson Formation	Kotcho Fm	Kotcho Formation	Kotcho Formation
Tetcho Fm						Tetcho Formation	Tetcho Formation	
Trout River Fm						Trout River Formation	Trout River Formation	
Kakiska Fm		Kakiska Formation	Kakiska Formation					
Middle		Givetian	Besa River Formation	Red Knife Fm	Upper Mbr	Fort Simpson Formation		
					Jean Marie Mbr			
				Muskwa Fm	Muskwa Formation	Muskwa Formation		
				Horn River Fm	Slave Point Fm	Slave Point Fm		
	Otter Park Mbr			Watt Mtn Fm	Watt Mtn Fm			
L	Em	Besa River Formation	Sulphur Point Fm	Upper Keg River Fm	Muskeg Fm			
			Evie Mbr	Evie Mbr				
			Dunedin Fm - Nahanni Fm	Keg River Fm	Lower Keg River Fm			
			Chinchaga Fm	Chinchaga Fm				
			Stone Fm					

Figure 5. Time stratigraphic chart of the Middle to Upper Paleozoic showing the main stratigraphic units along the northwestern part of the Western Canada Sedimentary Basin within northeastern British Columbia and the relationship between shelf and offshelf sequences. The legend for this figure is shown in Figure 4.

lower parts of the Besa River Formation were not exposed, but examination of rocks to the north indicate approximately 15 m of missing Besa River rocks are below the base of the Mattson Formation, and a structural section suggests approximately 25 m of covered rocks are above the Dunedin Formation.

Broadly, the Besa River Formation consists of dark grey to black, carbonaceous siltstone and shale (Figure 8).

Besa River Formation rocks along the measured section can be subdivided into six lithostratigraphic units consisting of, from the base (Figure 9): 1) dark grey to black carbonaceous siltstone to blocky siltstone with shale partings, showing tan to orange-brown or beige weathering (34 m thick, Figure 10a); 2) dark grey to black, fissile to blocky carbonaceous siltstone showing dark grey to beige weathering (34 m thick, Figures 10b, c); 3) dark grey to black

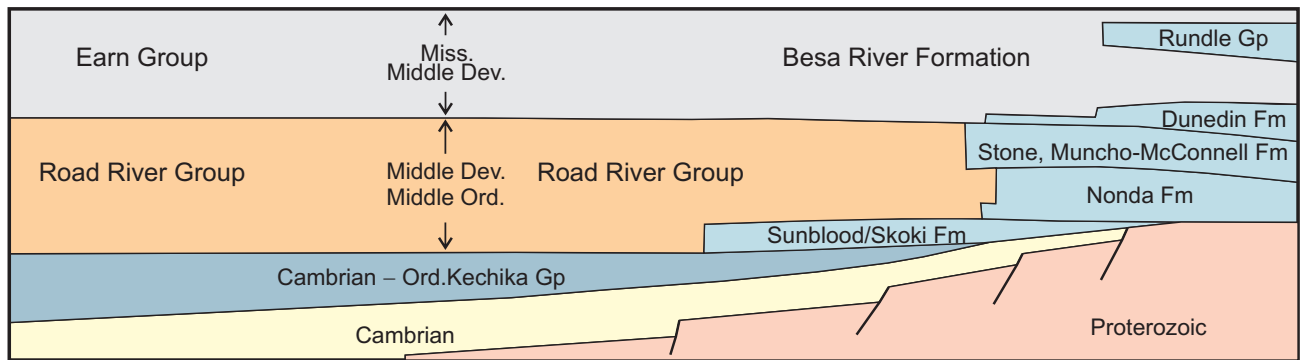


Figure 6. Schematic representation of the westward shale-out of Lower Paleozoic carbonate rocks into Road River siltstone and shale within the Kechika Trough and the Selwyn Basin, and the relationship between the Besa River Formation and the Earn Group.

carbonaceous blocky siltstone and shale, showing rusty to grey or dark grey weathering (32 m thick, Figures 10c, d); 4) rusty to light grey weathering, grey to light grey, blocky to platy and laminated siliceous siltstone showing rusty to light grey weathering (34 m thick, Figure 10e); 5) dark grey to black, blocky to platy and laminated, carbonaceous and siliceous siltstone showing rusty to dark grey weathering (51 m thick, Figures 10f, g); 6) dark grey to black crumbly siltstone to shale showing dark grey to rusty weathering with uneven partings, and with lesser blocky siltstone in the lower and middle parts (100 m thick, Figures 10g, h).

Exposures of the Besa River Formation in the Caribou Range display the distinctive light grey weathering of unit 4 together with the recessive, crumbly nature of the upper part of unit 6 (Figures 8 and 10h). Distinctive rusty to ochre-coloured run-off channels emanating from exposures of unit 6 are also observed within the central part of the Caribou Range.

The upper part of the section contains several thin horizons (5–20 cm) of disseminated and massive pyrite, together with a horizon containing barite nodules of more than 30 cm in diameter (Figure 9). These occurrences are more fully described by Ferri et al. (2011).

Comparison of the broad lithological composition; total gamma-ray counts; K, Th and U contents; and total organic carbon (TOC) contents from Rock-Eval analysis along the section are shown in Figure 11. Values of other elements based on litho geochemistry are shown in Figure 12. Total organic carbon levels are quite high across several portions of the formation, reaching more than 6% by weight in some parts and they are consistently more than 2% for the upper half of the section. The  $S_2^1$  values across the section are less than 0.1 mg HC<sup>2</sup> /g rock, with corresponding hydrogen index (HI) values averaging approximately 2 mg HC/g TOC. These values indicate that the rocks are mature to overmature and contain little to no generative capacity. Although the low  $S_2$  values calls into

question the reliability of  $T_{max}^3$  in determining thermal maturity (Peters, 1986), some of the higher  $S_2$  values have corresponding  $T_{max}$  values in the range of 480 to 500°C, suggesting the upper wet gas window. This is consistent with HI levels within organic matter. This data also suggests that these organic-rich horizons were likely two to four times richer in organic matter prior to the expulsion of hydrocarbons during maturation (Jarvie, 1991).

There is excellent correlation between relative abundances of U and organic carbon content, suggesting either syngenetic precipitation of U during periods of higher anoxia or diagenetically within horizons rich in organic material. Although U concentrations appear to generally decrease towards the upper part of the section, Th shows an increase in abundance. The concentration of K does not appear to correlate with the abundances of the other elements, and is probably tied to the mineralogy of the sediments being deposited.

The carbonaceous (i.e., organic-rich) nature of these sediments is a reflection of the reducing conditions present during deposition. These very low oxygen conditions did not permit any aerobic organic activity, which led to the preservation of organic matter (Fowler et al., 2005). In these anoxic waters, bacteria that respire through the reduction of sulphur became abundant, producing a large amount of reduced sulphur that was used in the precipitation of metal sulphides from metalliferous brines expelled on the seafloor (Goodfellow and Lydon, 2007). Even if these brines had sufficient reduced sulphur, this anoxic environment favoured the preservation of any precipitated sulphides. Oxygenated bottom waters, as in today's oceans, would have led to the oxidation of sulphides in the water column or along the seafloor, negating or eliminating any sizable sulphide accumulations (Force et al., 1983).

1 Represents the amount of hydrocarbons resulting from the cracking of sedimentary organic matter in the sample.

2 Hydrocarbons

3 Temperature of maximum  $S_2$  production

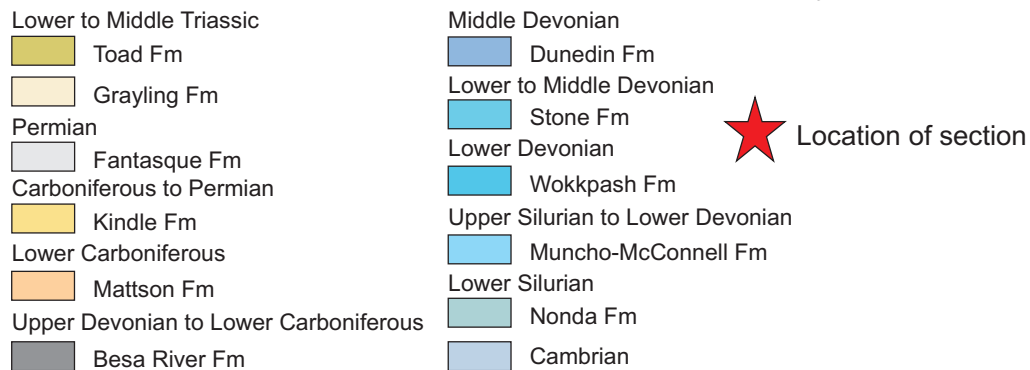
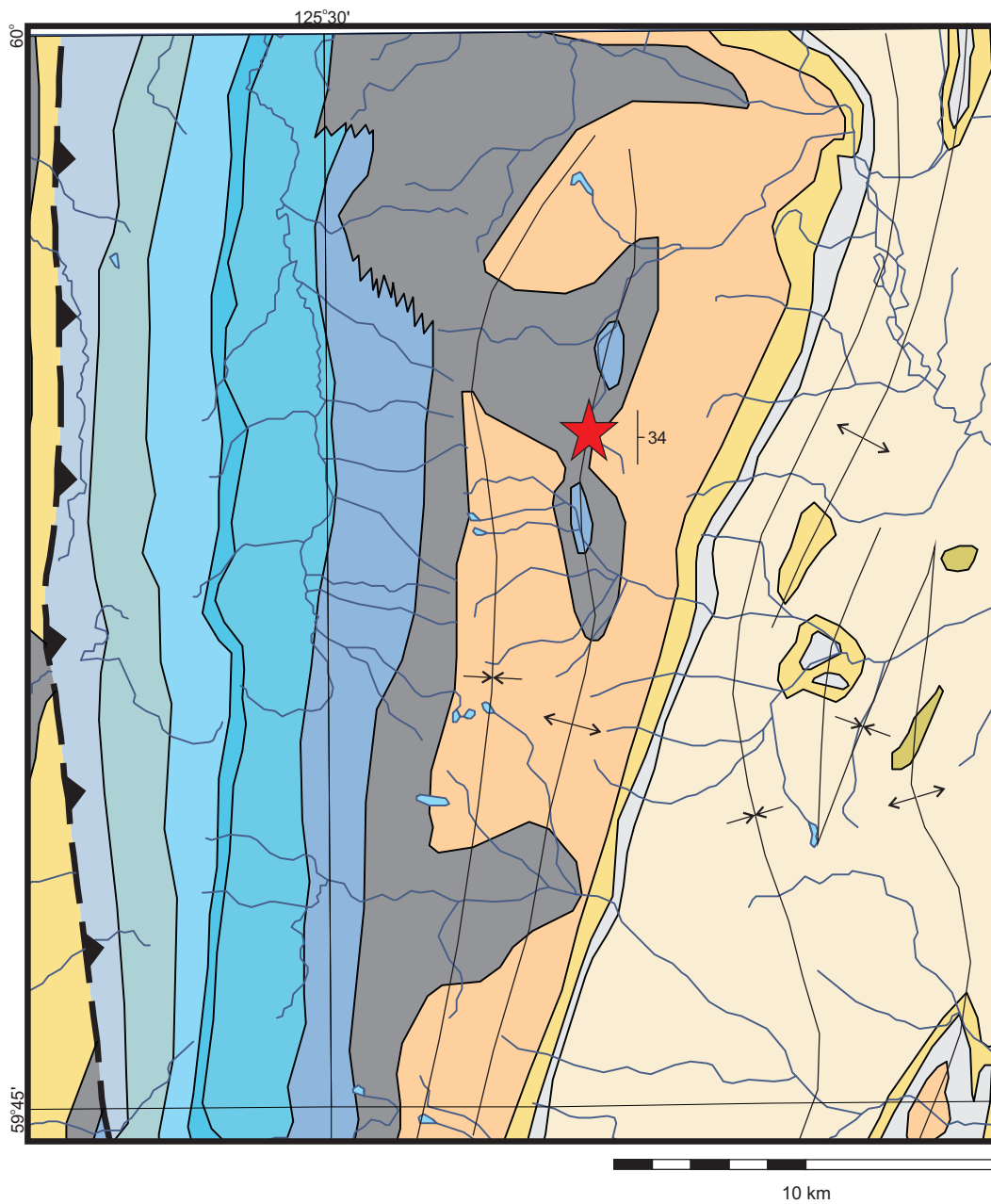


Figure 7. Geology of the Caribou Range, showing the location of the measured section. Geology is from MapPlace.ca (BC Geological Survey, 2011).

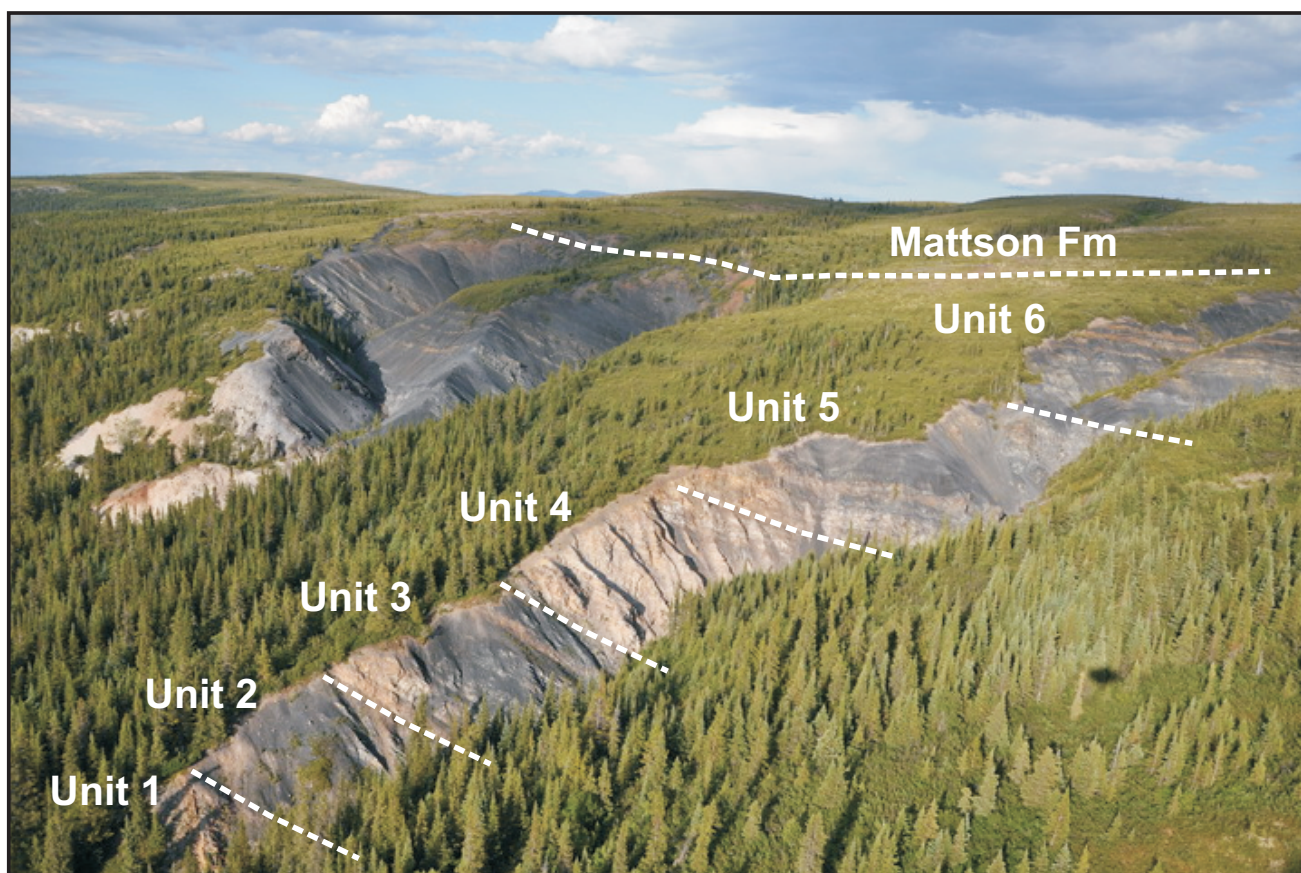


Figure 8. Photograph of the measured section of Besa River Formation showing the character of exposed rock. The light-coloured material is produced by the more siliceous siltstone of unit 4. The upper Besa River siltstone (unit 6) appears somewhat more recessive than the siltstone of unit 5.

Lithochemical abundances of select major oxides and trace elements are shown in Figure 12 in comparison to the main units defined during the logging of the section. Several of the units, particularly units 4, 5 and 6, show distinct elemental concentrations. Unit 4 is elevated in  $\text{SiO}_2$  and depleted in  $\text{Al}_2\text{O}_3$ ,  $\text{K}_2\text{O}$  and  $\text{MgO}$ , which contrasts with the other units. Unit 6 also shows a general decrease in  $\text{SiO}_2$  contents towards its upper part. The concentration of  $\text{Al}_2\text{O}_3$  shows an inverse relationship to  $\text{SiO}_2$ , suggesting that clay increases in abundance at the expense of silica. There is also a general increase in  $\text{MgO}$ ,  $\text{CaO}$  and  $\text{Na}_2\text{O}$  towards the top of the Besa River Formation. Although the concentration of  $\text{Fe}_2\text{O}_3$  remains at approximately 1–2% across much of the formation, it increases substantially in the upper part, as reflected lithologically by the presence of disseminated to bedded pyrite mineralization. In general, it is likely that major oxide concentrations reflect the mineralogy of the sediments being deposited, although the chemistry of the waters during deposition (i.e., redox conditions) could affect the concentrations of certain elements (e.g.,  $\text{Fe}_2\text{O}_3$  and  $\text{MnO}$ ; see following sections).

Abundances of several trace elements appear to correlate with organic carbon concentrations, suggesting a

genetic link (Figures 11 and 12). This is particularly true for U, Mo, V and to some extent Pb. As with U, there is a suggestion of either syngenetic precipitation of U during periods of higher anoxia or diagenetically within horizons rich in organic material. The elemental logs in Figure 12 indicate that Mo, V, and to a lesser extent Pb, may be good inorganic proxies for the relative abundance of organic carbon and the reducing nature of the water column during the deposition of the sediments. Nickel, zinc and to some extent lead have higher concentrations in the upper and lower parts of the Besa River section and correspond to higher concentrations of  $\text{Fe}_2\text{O}_3$ . The higher level of these elements may be tied to either changes in reducing conditions, or, as inferred in the case of  $\text{Fe}_2\text{O}_3$  and Ba, higher input from metalliferous brines that were active during this time.

The preservation of organic matter in these sediments attests to the reducing environment during deposition. The concentration of Mn in sedimentary rocks is suggested by Goodfellow (2000) and Quinby-Hunt and Wilde (1994) to be related to redox conditions of the water column. Quinby-Hunt and Wilde (1994) have shown that in low-calcic shale ( $\text{CaO} < 0.6\%$ ), under specific pE and pH conditions, MnO concentrations of less than 0.1% signify anoxic conditions.

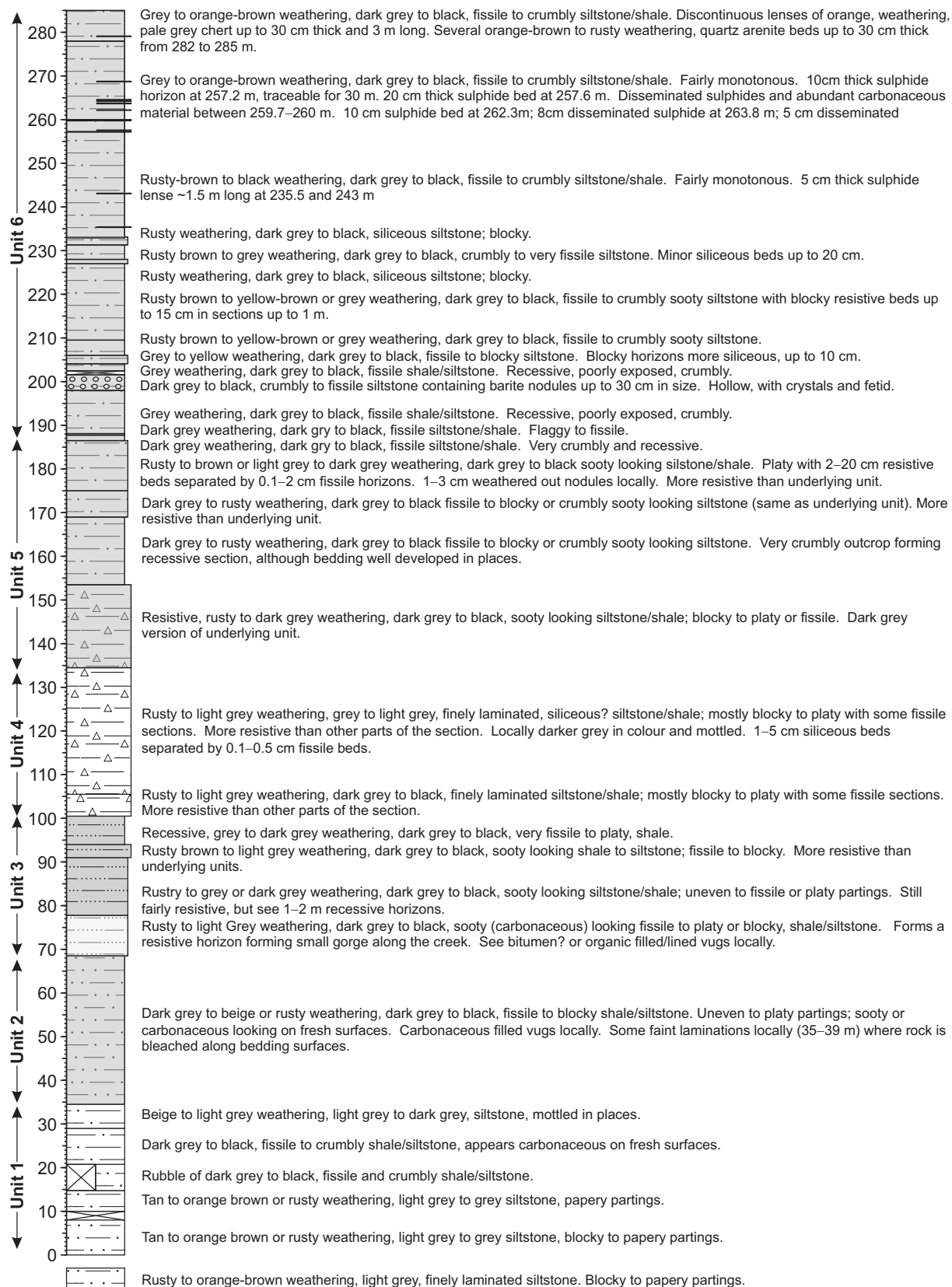


Figure 9. Lithological section of the Besa River Formation measured along the eastern part of the Caribou Range.





a)



b)



c)



d)



e)



f)



g)



h)

Figure 10. a) Rusty weathering siltstone of unit 1 at the 5 m level; b) beige to grey weathering, dark grey siltstone of unit 2 between 37 and 41 m; c) contact between units 2 and 3, showing the slightly more resistive nature of the siltstone in unit 3; d) general shot of grey to dark grey weathering siltstone of unit 3 at the 80 m level; e) light grey and rusty weathering siltstone of unit 4, 116 m level; f) dark grey and resistive siltstone with shaly partings within unit 5 at the 150 m level; g) transition from more resistive ribs of siltstone in unit 5 into more recessive siltstone of unit 6; h) crumbly dark grey siltstone of unit 6, 238–250 m level.

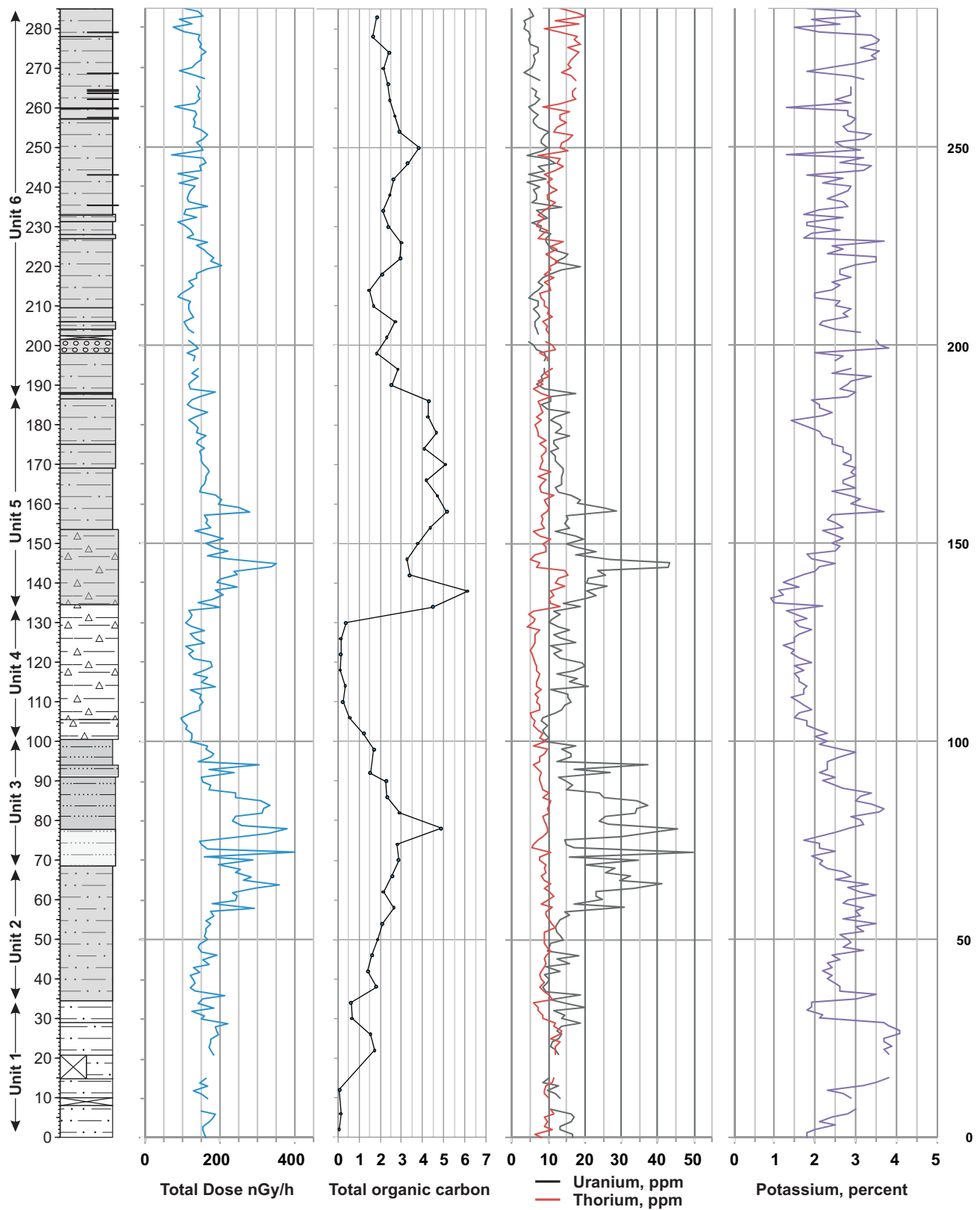


Figure 11. Comparison of main lithological units of the measured Besa River Formation section with measured levels of total gamma-ray counts, U, Th, K and total organic carbon.

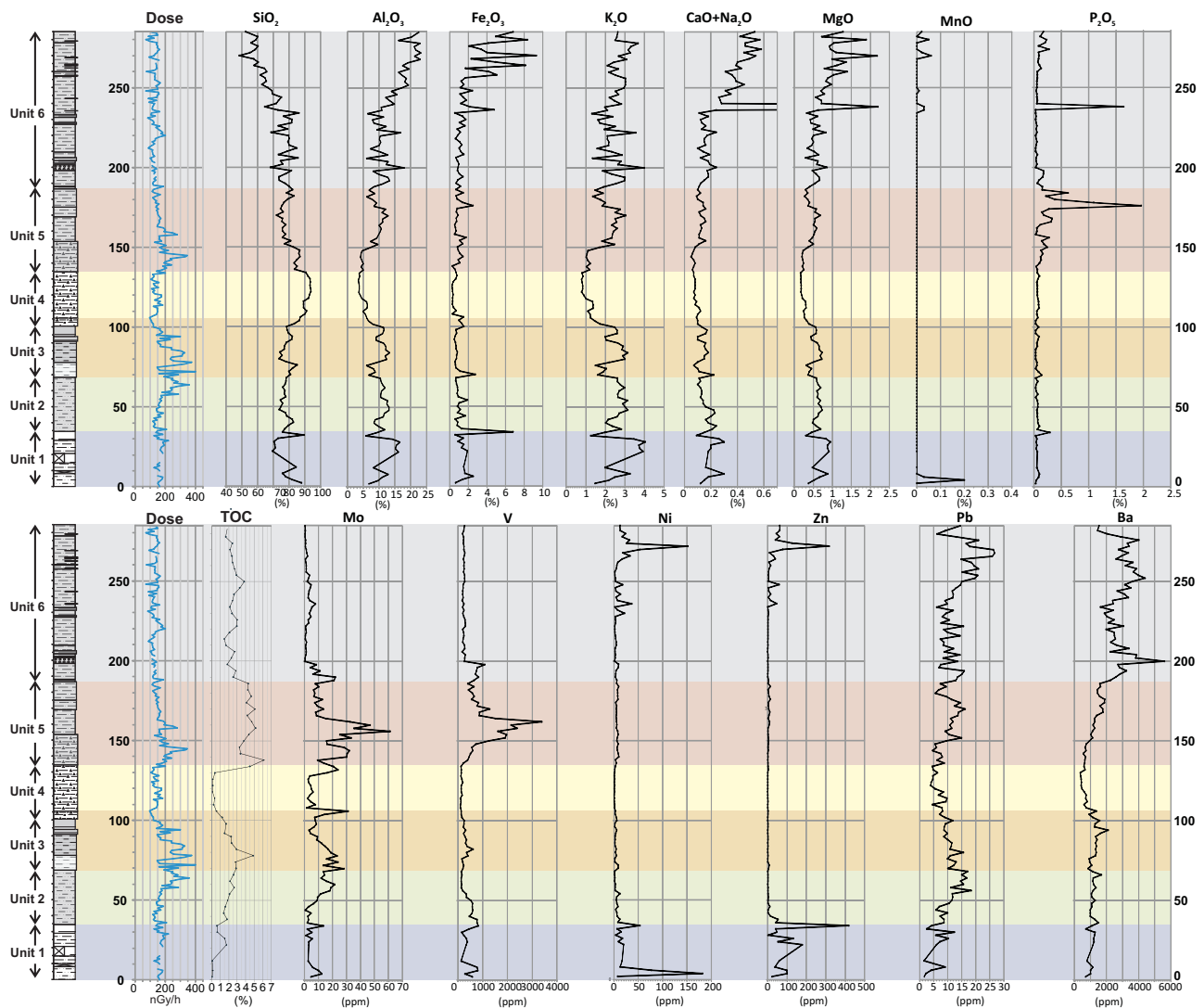


Figure 12. Abundances of select major oxides and trace elements within rocks of the Besa River Formation within the study area. The lithological log with units is shown on the right. The colour banding is provided as a guide to the unit boundaries.

Furthermore, these authors have further subdivided shales deposited within the anoxic environment based on the relative abundances of V and Fe. In the least-reducing environment (less anoxic), Fe is found as oxides (less insoluble) and will occur in rocks in concentrations greater than 3.75%. Under these conditions, V levels are low (<320 ppm). Where Eh conditions are lower (more anoxic), Fe is reduced, soluble concentrations in rocks will fall below 3.75%, and MnO concentrations average approximately 0.02%. Under the most reduced conditions, MnO concentration is approximately 0.01% and V concentration averages 1500 ppm.

Litho geochemistry (and the carbonaceous nature of the sediments) of the Besa River rocks suggests deposition under anoxic conditions. High V, low Fe and corresponding elevated levels of organic matter within parts of the section also suggest reducing conditions during deposition.

Quinby-Hunt and Wilde (1994) also note that the concentration of V can be used as an inorganic indicator of the organic content of the shale. Vanadium in the water column can form organic compounds that are best preserved under low pH and highly reducing conditions. It is clear that the concentrations of Mo and U relative to those of C shown in Figure 12 suggest a similar origin.

## CORRELATIONS

Besa River rocks in the study area can be broadly correlated with the Earn Group of the Kechika Trough (Figure 5). Units 1–5 most likely correlate with cherty argillite, carbonaceous siliceous shale, and lesser black carbonaceous siltstone and shale of the Middle to Late Devonian Gunsteel Formation (MacIntyre, 1998). The succeeding more recessive and crumbly siltstone and shale of unit 6 are

probably correlative to recessive dark grey siltstone of the Akie Formation, postulated to be Late Devonian to Early Mississippian in age (MacIntyre, 1998).

Correlation of the outcropping Besa River Formation with subsurface formations to the east is suggested based on the total gamma-ray trace across the measured section (Figures 13 and 14). In the subsurface, as the Keg River reef and successive Devonian and Mississippian carbonate successions shale-out westward into fine clastic rocks of the Horn River, Fort Simpson and Besa River formations, the distinctive radioactive shales of the Evie, Muskwa and Exshaw successions can be traced across into the thick, monotonous siltstone sequence. The Exshaw Formation can be traced with confidence because it forms a regional marker horizon throughout a large part of the Western Canada Sedimentary Basin. The Evie shale above the Lower Keg River carbonate also defines a distinctive package, and together with the succeeding Muskwa horizon, they characterize a recognizable sequence.

Correlations of the outcrop section with several wells west of the Liard River are depicted in Figure 14. To the east of these wells, the Fort Simpson Formation increases in thickness to more than 400 m. The Exshaw Formation can be traced into the strongly radioactive central part of the Besa River section and the lowermost radioactive zone equates with the Muskwa Formation. Approximately 25 m of basal Besa River Formation siltstone is covered; they are assumed to represent the Evie Member of the Horn River Formation. The siltstone below Muskwa-equivalent rocks would be equivalent to the Otter Park siltstone, and those between the Muskwa and Exshaw horizons to the Fort Simpson Formation. These correlations also correspond broadly to the main lithological units described previously: unit 1 corresponds to the Otter Park Member, units 2 and 3 to the Muskwa Formation, unit 4 to the Fort Simpson Formation and unit 5 to the Exshaw Formation (Figure 14). Note that the distinctive light grey weathering panel within the Besa River Formation exposures in the Caribou Range,

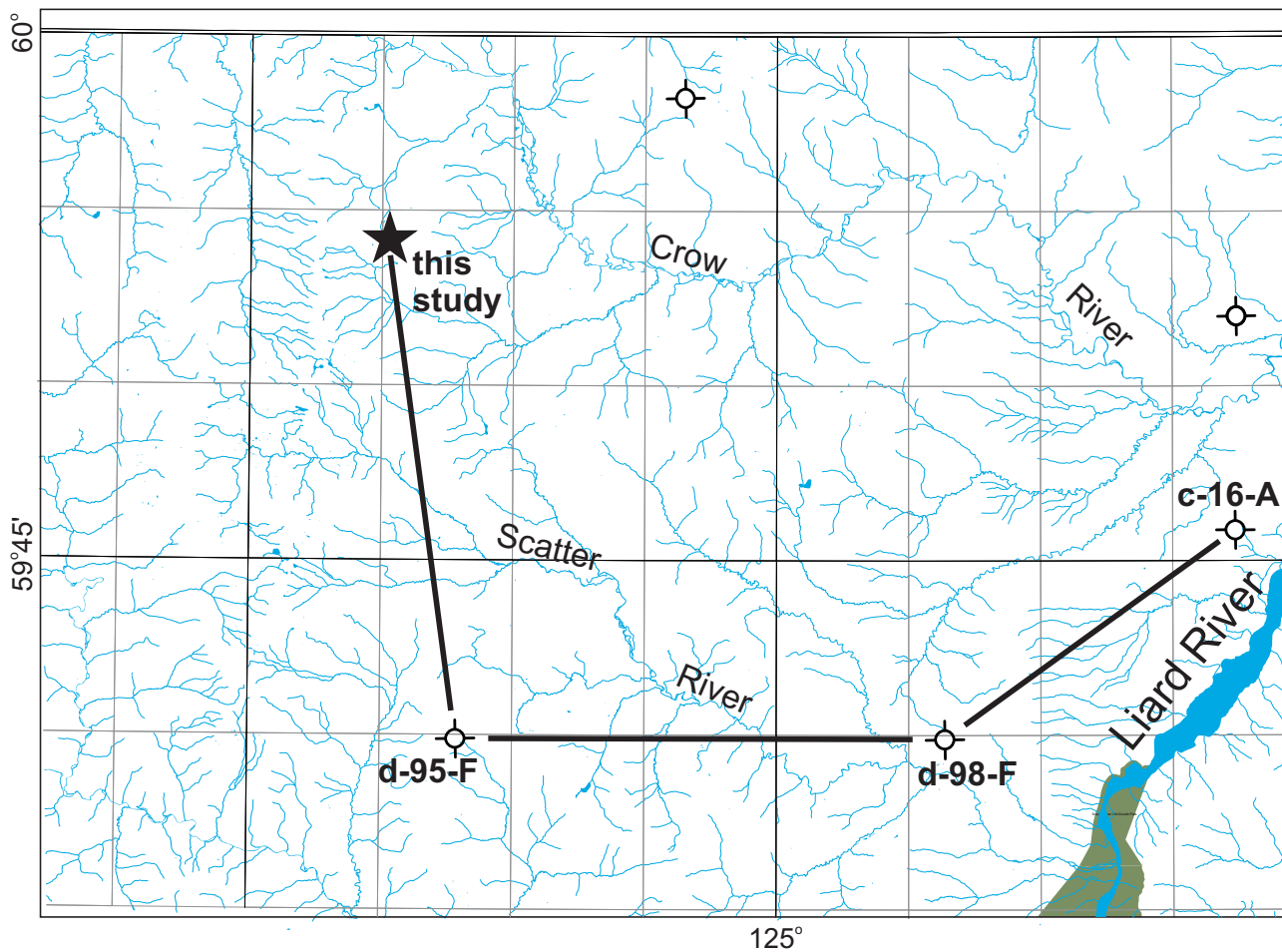


Figure 13. Map showing well locations used in the correlations depicted in Figure 14. The study area is shown by a star.

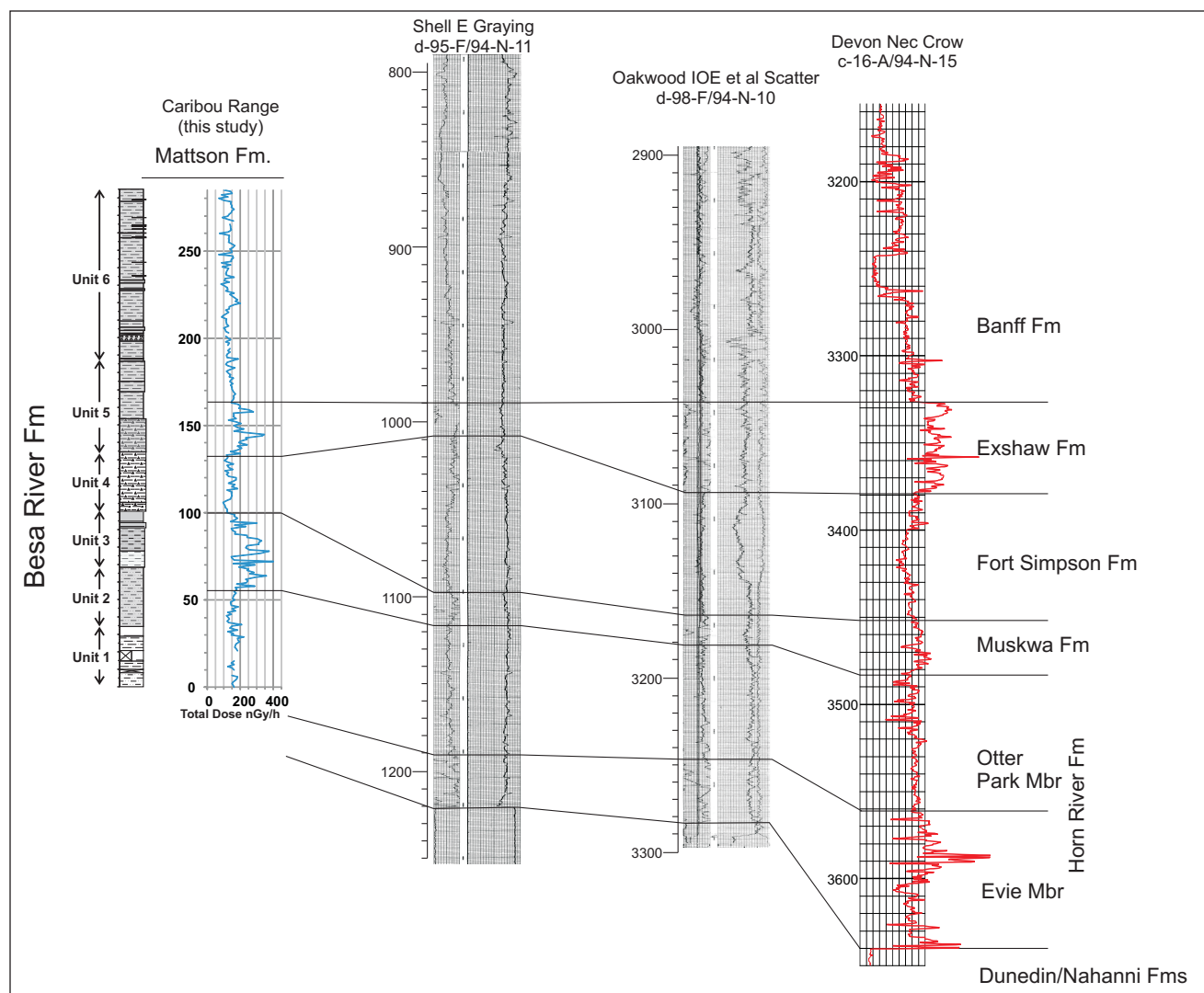


Figure 14. Correlation of the measured Besa River section, using the trace of total gamma-ray counts, with several subsurface sections, the locations of which are shown in Figure 13. Only the gamma-ray log is shown for the c-16-A well. The bulk density is shown for the d-98-F well and the acoustic log for the d-95-F well.

which corresponds to the Fort Simpson–equivalent horizon, is only approximately 25–35 m in thickness, attesting to the extremely condensed nature of this section, compared to the previously mentioned Fort Simpson interval with a thickness of more than 400 m. In outcrop, the section above unit 4 that correlates with the Exshaw Formation appears as siliceous as the underlying Fort Simpson–equivalent strata, but is considerably darker and more carbonaceous. This is confirmed by litho geochemistry (Figure 12).

Although the overall trace of the gamma-ray log across the outcrop is very similar to subsurface gamma-ray logs, the unit boundaries defined by this methodology do not necessarily correspond to those defined within the lithological log (Figures 11 and 14). The relatively sharp contacts of unit 4 correlate with breaks in the gamma-ray trace (Fort Simpson Formation equivalent, Figure 11). The upper boundary of the Exshaw marker, as defined by the gamma-ray trace,

falls within the upper part of unit 5. This unit is also defined by high organic contents and higher U concentrations than the base of unit 6 (Figure 11), suggesting that this may be the upper contact of the Exshaw marker.

The contact between units 2 and 3 occurs within the lower part of the Muskwa marker. Furthermore, the contact between units 1 and 2 is not distinctive on the gamma-ray trace, although total organic carbon contents are higher in unit 2 and K levels are higher in unit 1. There is an increase in organic content (and U levels) in unit 2 up-section, whereas its overall lithological character stays relatively uniform.

It is not surprising that unit boundaries of these fine-grained sediments defined within outcrop do not conform precisely to radioactive marker boundaries delineated in the subsurface or with radioactive zones in the outcrop. The high levels of radioactivity (i.e., U content) within specific

sedimentary sections appear linked to reducing conditions during deposition and preservation of produced organic matter, and may not necessarily correlate to the lithological composition of sediments being deposited. A change in redox conditions and/or organic production during otherwise uniform deposition will lead to concentration of organic matter within the bulk inorganic composition, thus altering its gamma-ray signature. This is evident between units 4 and 5; the base of unit 5 is still fairly siliceous (as in unit 4) but is more carbon-rich than unit 4, thus more radioactive. In some horizons, the production and preservation of organic matter will correlate very well with other lithological compositions (i.e., unit 4), suggesting a link between mineralogical input and organic productivity.

## CONCLUSIONS

- Approximately 285 m of the Besa River Formation outcrops along the western margin of the Liard Basin and consists of light grey to black weathering carbonaceous siltstone to siliceous siltstone. The lower 25 m and upper 15 m of the unit are not exposed.
- The Besa River Formation has been subdivided into six informal lithostratigraphic units based on overall outcrop composition.
- Rock-Eval analysis of representative samples on 4 m spacing across the outcrop indicate two zones of high organic carbon content, with levels reaching 6% by weight. Little generative capacity remains in these rocks as peak thermal maturities are inferred to be in the upper wet gas window.
- A gamma-ray spectroscopic log across the outcrop defines several zones of higher radiation that correlate to higher concentrations of U and organic carbon.
- Litho-geochemistry across the section displays distinct variability with respect to major oxides and trace-element abundances. Generally, the concentration of major oxides correlates with lithological subdivisions, whereas some of the trace-element abundances show a relationship with organic carbon content, suggesting that these levels are tied to redox conditions during deposition.
- Correlation of the gamma-ray trace with subsurface sections to the east suggests that the lower and upper radioactive zones in the outcrop correlate with the Muskwa and Exshaw markers, respectively.

## ACKNOWLEDGMENTS

The authors thank Lauren Wilson and Lisa Fodor for competent and cheerful assistance in the field. We acknowledge Lisa Fodor for having compiled the scintillometer data. We acknowledge Great Slave Helicopters of Fort Liard for the efforts in transporting us to our field localities. The senior author thanks Sarah Saad at Geological Survey of Canada laboratories in Calgary for her patience and knowledge in the preparation and analysis of Rock-Eval samples. We also thank JoAnne Nelson of the BC Geological Survey for carefully reviewing an earlier version of this manuscript and Warren Walsh for comments on various aspects of the stratigraphy.

## REFERENCES

- Bamber, E.W., Henderson, C.M., Richards, B.C. and McGugan, A. (1991): Carboniferous and Permian stratigraphy of the Foreland Belt, part A. Ancestral North America; in Upper Devonian to Middle Jurassic Assemblages, Chapter 8 of *Geology of the Cordilleran Orogen in Canada*, Gabrielse, H. and Yorath, C.J., Editors; Geological Survey of Canada, *Geology of Canada*, Number 4, pages 242–265.
- Barclay, J.E., Krause, F.F., Campbell R.I. and Utting, J. (1990): Dynamic casting and growth faulting; Dawson Creek graben complex, Carboniferous-Permian Peace River Embayment, Western Canada; *Bulletin of Canadian Petroleum Geology*, Volume 38A, pages 115–145.
- BC Geological Survey (2011): MapPlace GIS internet mapping system; *BC Ministry of Forests, Mines and Lands*, MapPlace website, URL <<http://www.MapPlace.ca>> [February 2011].
- Fallas, K.M. (2001): Preliminary geology, Mount Martin, Yukon Territory—British Columbia—Northwest Territories; *Geological Survey of Canada*, Open File 3402, scale 1:50 000.
- Fallas, K.M. and Evenchick, C.A. (2002): Preliminary geology, Mount Merrill, Yukon Territory—British Columbia; *Geological Survey of Canada*, Open File 4264, scale 1:50 000.
- Fallas, K.M., Pigage, L.C. and MacNaughton, R.B. (2004): Geology, La Biche River southwest (95C/SW), Yukon Territory—British Columbia; *Geological Survey of Canada*, Open File 4664, scale 1:100 000.
- Ferri, F., Hickin, A. and Huntley, D. (2011): Bedded barite-pyrite occurrences in upper Besa River Formation, western Liard Basin, British Columbia and regional correlations with Devonian to Mississippian sub-surface formations; in *Geological Fieldwork 2010, BC Ministry of Forests, Mines and Lands*, Paper 2011-1, pages 13–30.
- Ferri, F., Rees, C., Nelson, J. and Legun, A. (1999): Geology and mineral deposits of the northern Kechika Trough between Gataga River and the 60th parallel; *BC Ministry of Energy and Mines*, Bulletin 107, 122 pages.

- Force, E., Cannon, W.F., Koski, R.A., Passmore, K.T. and Doe, B.R. (1983): Influences of ocean anoxic events on manganese deposition and ophiolite-hosted sulphide preservation; in Cronin, T.M., Cannon, W.F. and Poore, R.Z., Editors, Paleoclimate and mineral deposits; *U.S. Geological Survey, Circular 822*, pages 26–29.
- Fowler, M., Snowdon, L. and Stasiuk, V. (2005): Applying petroleum geochemistry to hydrocarbon exploration and exploitation; *American Association of Petroleum Geologists, Annual Convention, Short Course Handbook*, 300 pages.
- Gabrielse, H. (1963): Geology, Rabbit River, British Columbia; *Geological Survey of Canada, Preliminary Map 46-1962*, scale 1:250 000.
- Gabrielse, H. (1967): Tectonic evolution of the northern Canadian Cordillera; *Canadian Journal of Earth Sciences*, Volume 4, pages 271–298.
- Goodfellow, W.D. (2000): Anoxic conditions in the Aldridge Basin during formation of the Sullivan Zn-Pb deposit: implications for the genesis of massive sulphides and distal hydrothermal sediments; Chapter 12 in *The Geological Environment of the Sullivan Deposit*, British Columbia, Lydon, J.W., Hoy, T., Slack, J.F. and Knapp, M.E., Editors, *Geological Association of Canada, Mineral Deposits Division, Special Publication Number 1*, pages 218–250.
- Goodfellow, W.D. and Lydon, J.W. (2007): Sedimentary exhalative (SEDEX) deposits; in *Mineral Deposits of Canada*, Goodfellow, W.D., Editor, *Geological Association of Canada, Special Publication*, Volume 5, pages 163–184.
- Huntley, D.H. and Hickin, A.S. (2010): Surficial deposits, landforms, glacial history and potential for granular aggregate and frac sand: Maxhamish Lake map sheet (NTS 94O), British Columbia; *Geological Survey of Canada, Open File 6430*, 17 pages.
- Huntley, D.H. and Hickin, A.S. 2011. Geo-Mapping for Energy and Minerals program (GEM-Energy): preliminary surficial geology, geomorphology, resource evaluation and geohazard assessment for the Maxhamish Lake map area (NTS 094O), northeastern British Columbia; *Geoscience Reports 2011*, BC Ministry of Energy, pages 57-73.
- Huntley, D.H., Hickin, A.S. and Ferri, F. (2011): Provisional surficial geology, glacial history and paleogeographic reconstructions of the Toad River (NTS 94N) and Maxhamish Lake map areas (NTS 94O), British Columbia; *Geoscience Reports 2011*, BC Ministry of Energy, pages 37-55.
- Huntley, D.H. and Sidwell, C.F. (2010): Application of the GEM surficial geology data model to resource evaluation and geohazard assessment for the Maxhamish Lake map area (NTS 94O), British Columbia; *Geological Survey of Canada, Open File 6553*, 12 pages.
- Jarvie, D.M. (1991): Total organic carbon (TOC) analysis; in *Source Migration Processes and Evaluation Techniques*, Merrill, R.K., Editor, *American Association of Petroleum Geologists, Treatise of Petroleum Geology*, pages 113–118.
- Kidd, F.A. (1963): The Besa River Formation; *Bulletin of Canadian Petroleum Geology*, Volume 11, Issue 4, pages 369–372.
- Leckie, D.A., Potocki, D.J. and Visser, K. (1991): The Lower Cretaceous Chinkeh Formation: a frontier-type play in the Liard Basin of Western Canada; *American Association of Petroleum Geologists Bulletin*, Volume 75, Number 8, pages 1324–1352.
- MacIntyre, D.G. (1998): Geology, geochemistry and mineral deposits of the Akie River area, northeast British Columbia (NTS 094F01, 02, 07, 10, 11); *BC Ministry of Forests, Mines and Lands, Bulletin 103*, 99 pages.
- MacLean, B.C. and Morrow, D.W. (2004): Bovie Structure; its evolution and regional context; *Bulletin of Canadian Petroleum Geology*, Volume 52, Issue 4, Part 1, pages 302–324.
- Mathews, W.H. (1986): Physiography of the Canadian Cordillera; *Geological Survey of Canada, Map 1701A*, scale 1:5 000 000.
- McClay, K.R. and Buchanan, P.G. (1992): Thrust faults in inverted extensional basins; in *Thrust Tectonics*, McClay, K.R., Editor, *Chapman and Hall*, pages 93–104.
- Meijer Drees, N.C. (1994): Devonian Elk Point Group of the Western Canada Sedimentary Basin; in *Geological Atlas of the Western Canada Sedimentary Basin*, Mossop, G.D. and Shetsen, I., Compilers, *Canadian Society of Petroleum Geologists and Alberta Research Council, Special Report 4*, URL <[http://www.ags.gov.ab.ca/publications/wcsb\\_atlas/atlas.html](http://www.ags.gov.ab.ca/publications/wcsb_atlas/atlas.html)> [December 2010].
- Monahan, P. (2000): Liard Basin area; *BC Ministry of Energy, special report*, URL <<http://www.empr.gov.bc.ca/OG/oilandgas/petroleumgeology/ConventionalOilAndGas/Pages/NortheasternBCBasin.aspx>> [December 2010].
- Morrow, D.W., Potter, J. Richards, B. and Goodarzi, F. (1993): Paleozoic burial and organic maturation in the Liard Basin region, northern Canada; *Bulletin of Canadian Petroleum Geology*, Volume 41, Issue 1, pages 17–31.
- Mossop, G.D., Wallace-Dudley, K.E., Smith, G.G. and Harrison, J.C., Compilers (2004): Sedimentary basins of Canada; *Geological Survey of Canada, Open File Map 4673*, scale 1:5 000 000.
- Oldale, H.S. and Munday, R.J. (1994): Devonian Beaverhill Lake Group of the Western Canada Sedimentary Basin; in *Geological Atlas of the Western Canada Sedimentary Basin*, Mossop, G.D. and Shetsen, I., Compilers, *Canadian Society of Petroleum Geologists and Alberta Research Council, Special Report 4*, URL <[http://www.ags.gov.ab.ca/publications/wcsb\\_atlas/atlas.html](http://www.ags.gov.ab.ca/publications/wcsb_atlas/atlas.html)> [December 2010].
- Paradis, S., Nelson, J.L. and Irwin, S.E.B. (1998): Age constraints on the Devonian shale-hosted Zn-Pb-Ba deposits, Gataga District, northeastern British Columbia, Canada; *Bulletin of the Society of Economic Geologists*, Volume 93, Issue 2, pages 184–200.
- Pelzer, E.E. (1966): Mineralogy, geochemistry, and stratigraphy of Besa River shale, British Columbia; *Bulletin of Canadian Petroleum Geology*, Volume 14, Issue 2, pages 273–321.
- Peters, K.E. (1986): Guidelines for evaluating petroleum source rock using programmed pyrolysis; *American Association of Petroleum Geologists Bulletin*, Volume 70, Number 3, pages 318–329.

- Potter, J., Richards, B.C. and Goodarzi, F. (1993): The organic petrology and thermal maturity of Lower Carboniferous and Upper Devonian source rocks in the Liard Basin, at Jackfish Gap-Yohin Ridge and North Beaver River, northern Canada; *Implications for Hydrocarbon Exploration, Energy Sources*, Volume 15, Issue 2, pages 289–314.
- Quinby-Hunt, M.S. and Wilde, P. (1994): Thermodynamic zonation in the black shale facies based on iron-manganese-vanadium content; *Chemical Geology*, Volume 113, Issue 3–4, pages 297–317.
- Ross, D.J.K. and Bustin, R. (2008): Characterizing the shale gas resource potential of Devonian-Mississippian strata in the Western Canada Sedimentary Basin; application of an integrated formation evaluation; *American Association of Petroleum Geologists Bulletin*, Volume 92, Issue 1, pages 87–125.
- Stott, D.F. and Taylor, G.C. (1973): Tuchodi Lakes map area, British Columbia; *Geological Survey of Canada*, Memoir 373, 37 pages.
- Switzer, S.B., Holland, W.G., Christie, D.S., Graf, G.C., Hedinger, A.S., McAuley, R.J., Wierzbicki, R.A. and Packard, J.J. (1994): Devonian Woodbend-Winterburn strata of the Western Canada Sedimentary Basin; in Geological Atlas of the Western Canada Sedimentary Basin, Mossop, G.D. and Shetsen, I., Compilers, *Canadian Society of Petroleum Geologists and Alberta Research Council*, Special Report 4, URL <[http://www.ags.gov.ab.ca/publications/wcsb\\_atlas/atlas.html](http://www.ags.gov.ab.ca/publications/wcsb_atlas/atlas.html)> [December 2010].
- Taylor, G.C. and Stott, D.F. (1999): Geology, Toad River, British Columbia; *Geological Survey of Canada*, Map 1955A, scale 1:250 000.
- Wright, G.N., McMechan, M.E. and Potter, D.E.G. (1994): Structure and architecture of the Western Canada Sedimentary Basin; in Geological Atlas of the Western Canada Sedimentary Basin, Mossop, G.D. and Shetsen, I., Compilers, *Canadian Society of Petroleum Geologists and Alberta Research Council*, Special Report 4, URL <[http://www.ags.gov.ab.ca/publications/wcsb\\_atlas/atlas.h](http://www.ags.gov.ab.ca/publications/wcsb_atlas/atlas.h)



# GEOCHEMISTRY AND SHALE GAS POTENTIAL OF THE GARBUTT FORMATION, LIARD BASIN, BRITISH COLUMBIA (PARTS NTS 094N, O; 095B, C)

Filippo Ferri<sup>1</sup>, Adrian S. Hickin<sup>1</sup> and David H. Huntley<sup>2</sup>

---

## ABSTRACT

*An examination of the Garbutt Formation was undertaken in the Liard Basin of British Columbia to better understand the geochemical composition of the unit and how it relates to overall lithostratigraphy and shale gas potential. The Garbutt Formation is approximately 285 m thick in the Toreva–Scatter River area and consists of dark grey to black or dark grey brown shale, siltstone and lesser fine sandstone. Sedimentary structures suggest deposition by turbiditic flows below the storm wave base, which is consistent with a position near the shelf edge or prodelta environment. Rock-Eval data show average total organic carbon contents of 1.12 wt.% with peaks between 1.2 and 1.67%. The kerogen is type III in nature and average hydrocarbon abundances in kerogen are 60 mg HC/g TOC. The  $T_{max}$  maturation levels suggest the beginning of the dry gas generation window. The concentration of Mn, Fe, V and other elements suggest the sediments were deposited near the boundary between anoxic and oxic water conditions.*

Ferri, F., Hickin, A. S. and Huntley, D. H. (2011): Geochemistry and shale gas potential of the Garbutt Formation, Liard Basin, British Columbia (parts of NTS 094N, O; 095B, C); in Geoscience Reports 2011, *BC Ministry of Energy and Mines*, pages 19–36.

<sup>1</sup>Geoscience and Natural Gas Development Branch, Oil and Gas Division, BC Ministry of Energy and Mines, Victoria, BC; Fil.Ferri@gov.bc.ca

<sup>2</sup>Geological Survey of Canada, Natural Resources Canada, Vancouver, BC

**Key Words:** northeast BC, Liard River, Liard Basin, Fort St. John Group, Garbutt Formation, Scatter Formation, Rock-Eval, litho-geochemistry, gamma ray, shale gas, correlations

---

## INTRODUCTION

British Columbia has an abundance of shale intervals with unconventional gas potential and their recent exploration has increased British Columbia's natural gas resources by several trillion cubic feet (Adams, 2009). Although Triassic and Middle Devonian shale sequences have been the focus of exploration and development (e.g., Groundbirch area and Horn River Basin), other organic-rich shale and siltstone successions, such as rocks of Jurassic and Cretaceous ages, may hold potential for shale gas.

This report details the results of an examination of an Early Cretaceous shale sequence, the Garbutt Formation, found along the western margin of the Liard Basin in the Toad River map area (NTS 094N). The main objective is a characterization of this formation through lithological description and lithological and organic geochemistry. In addition, a gamma-ray spectroscopic survey of the outcrop is used to assist with correlating the section with subsurface sequences in the Liard and Horn River basins. We hope that this information will assist in the regional evaluation of this formation for its shale gas potential.

This study is part of a collaborative program between the Geological Survey of Canada and the British Columbia

Ministry of Energy and Mines and is under the federal government's Geo-mapping for Energy and Minerals (GEM) program, which is examining petroleum-related geoscience of the Liard and Horn River basins. A large part of this program has targeted mapping of surficial geology in support of drilling and completion of shale gas wells (Huntley and Hickin, 2010; Huntley and Sidwell, 2010; Huntley and Hickin, 2011; Huntley et al., 2011).

## LOCATION

The Liard Basin is located in northeastern British Columbia and includes the region where British Columbia, the Northwest Territories and the Yukon meet (Figures 1 and 2). The Liard Basin encompasses the corners of NTS map areas 094N and O, and 095 B and C. This area defines a relatively high plateau between the southern Selwyn Mountains and northern Rocky Mountains. Highway 77 runs north-south along the eastern margin of the Liard Basin. The south end of Highway 77 joins the east-west-running Alaska Highway (Highway 97) near Fort Nelson (Figure 2). Numerous petroleum activity roads and forestry access roads extend from these two main highways across the area. Road access

across the Liard River is by barge, which originates at Fort Liard, NWT and ferries vehicles to just south of the confluence of La Biche River, where a road connects to the Beaver River gas field (Figure 3).

## REGIONAL GEOLOGY

The Liard River traverses the Liard Basin, which was originally defined on the basis of the thick Late Paleozoic succession in southeastern Yukon by Gabrielse (1967) and extended into northeastern British Columbia by Morrow et al. (1993) and Richards et al. (1994). The Bovie Lake structure marks the eastern margin of the basin, west of which is an anomalously thick section of the Mississippian Mattson Formation. Late Cretaceous movement on this fault has

also preserved a thick sequence of Early to Late Cretaceous rocks within the confines of the basin (Leckie et al., 1991; Leckie and Potocki, 1998).

In the Liard River region, Cretaceous rocks rest unconformably on Triassic strata. The basal part of this section is represented by Lower to mid-Cretaceous rocks of the Fort St. John Group followed by Upper Cretaceous strata of the Dunvegan, Kotaneelee and Wapiti formations (Figures 2–4). Fort St. John Group strata represent a marine incursion along the western interior of the continent and are dominated by shale and siltstone punctuated by coarser, regressive sandstone sequences reflecting increased tectonism to the west (Chinkeh, Scatter and Sikanni formations; Stott, 1982; Leckie et al., 1991). Coarse clastic rocks of the Dunvegan Formation rest conformably on the Fort St. John Group and represent the last major regression into the

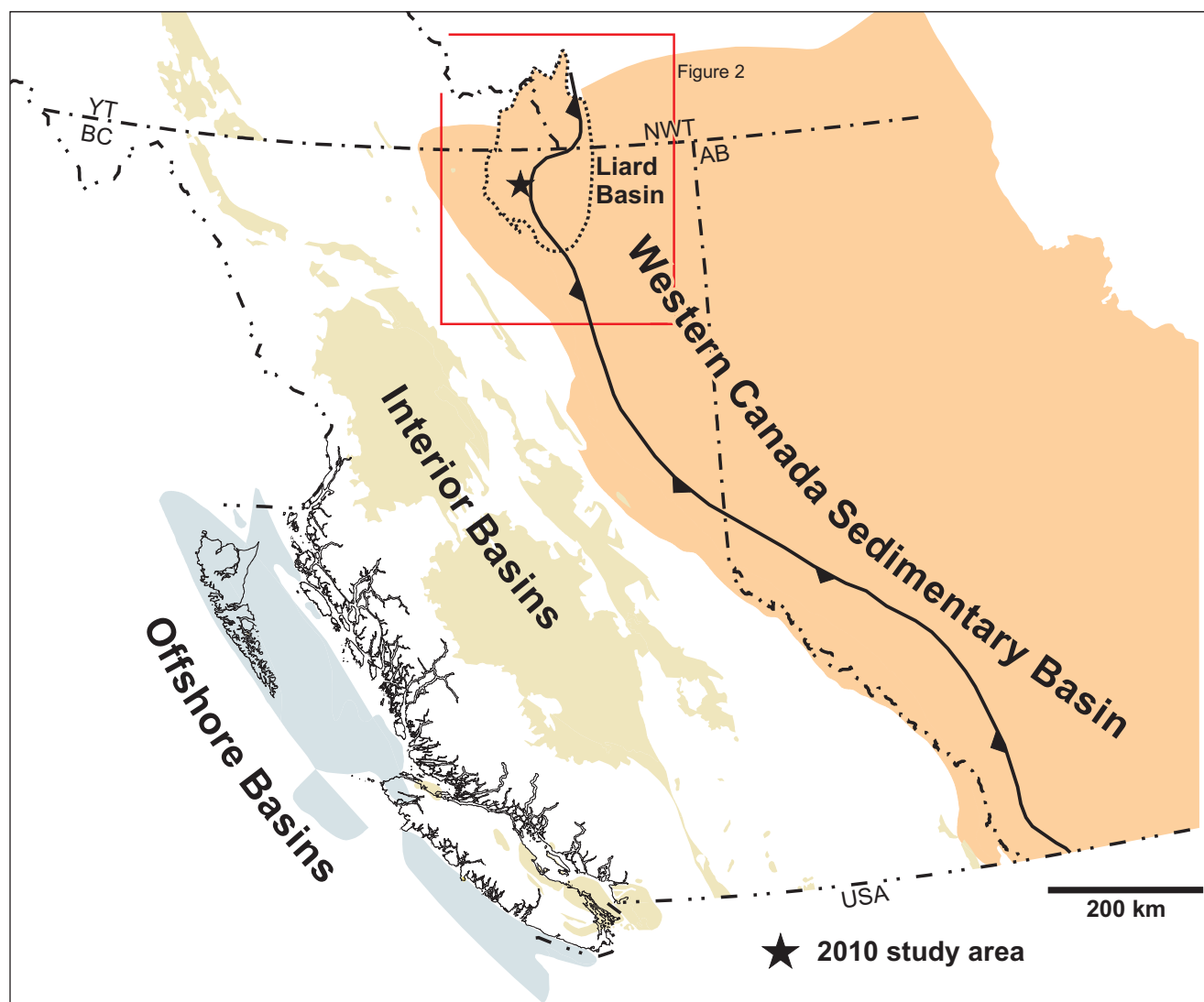


Figure 1. Location of the Liard Basin with respect to the primary sedimentary basins of Western Canada. Also shown are the Early Paleozoic offshelf depocentres of the Selwyn Basin and the Kechika Trough. The red box outlines the area shown in Figure 2. Basin outlines are from Mossop et al. (2004).

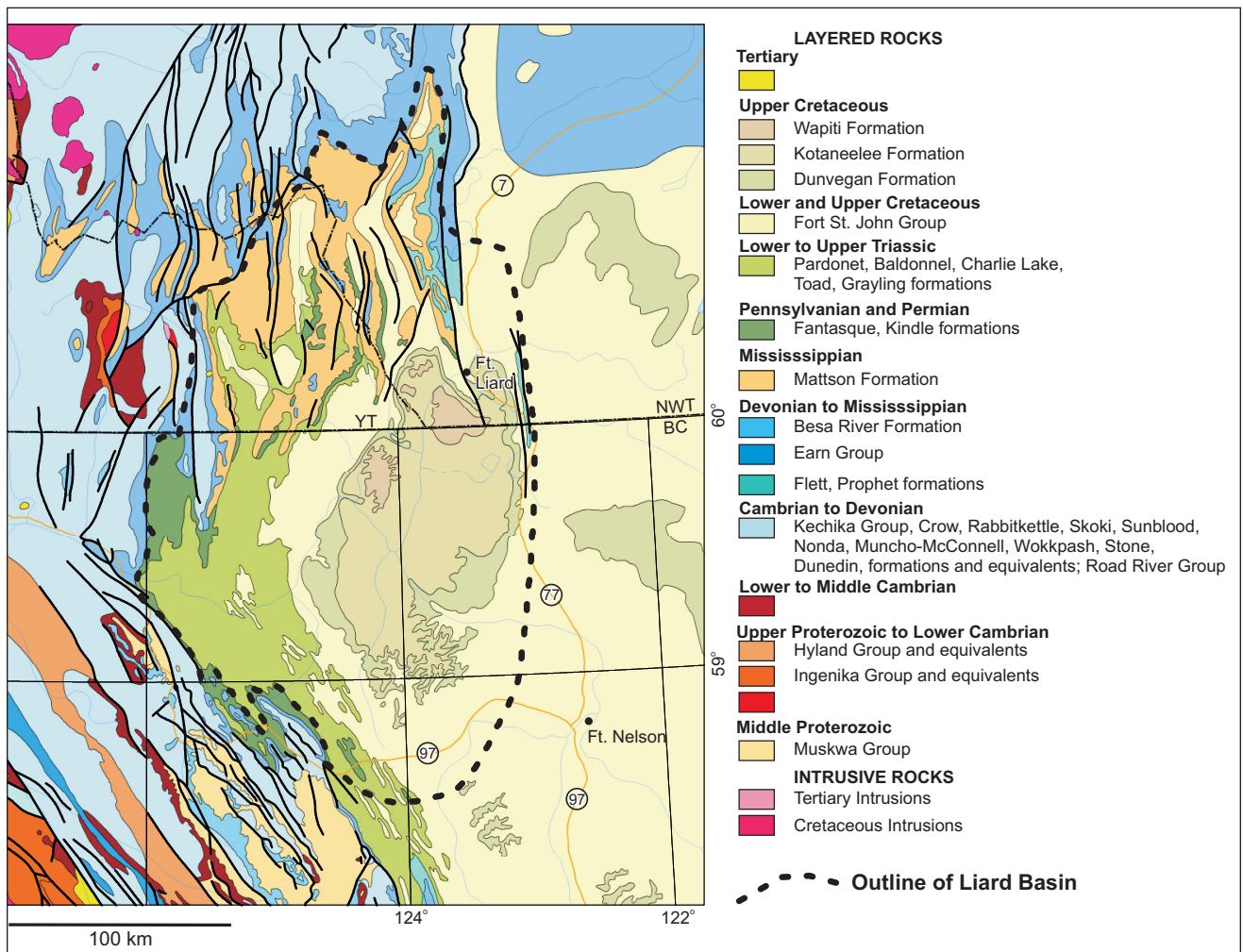


Figure 2. Geology of the Liard Basin and immediate area showing the distribution of Mattson Formation sandstone in the northern part of the Liard Basin.

interior seaway. Marine shale and minor sandstone of the Kotaneleele Formation unconformably overlie the Dunvegan Formation and define a final marine transgression that is succeeded by nonmarine sandstone and mudstone of the Wapiti Formation (Dawson et al., 1992; Taylor and Stott, 1999).

Shale, siltstone and fine sandstone of the Garbutt Formation define a major marine transgression along the Western Canada Sedimentary Basin. These rocks lie above the Chinkeh Formation, which consists of a marine shoreface succession in its upper part resting on nonmarine valley fill in its lower part (Leckie et al., 1991). Basal Garbutt Formation shale or siltstone either lie conformably atop the Chinkeh Formation (when developed) or unconformably above older strata (e.g., Triassic), with or without the presence of a pebble lag at its base (Leckie and Potocki, 1998).

Garbutt Formation rocks are interpreted to have been deposited in a marine environment, largely below the storm wave base (Leckie and Potocki, 1998). Succeeding sandstones of the Scatter Formation suggest an open-water,

shallow marine shelf to shoreface depositional setting (Leckie and Potocki, 1998). Leckie and Potocki (1998) describe wave and combined flow ripples and hummocky cross-stratification in the upper third of the Garbutt Formation, suggesting shallow-water environments affected by storm waves. Slump features within the lower parts of the Garbutt Formation, together with other mass flow deposits, suggest deposition of this unit in deeper waters, downslope from a shelf or slope-margin setting (Leckie and Potocki, 1998) or in a prodelta environment (Stott, 1982).

In British Columbia, the regional geological database in the vicinity of the section includes mapping within the Toad River (Taylor and Stott, 1999), the Tuchodi Lakes (Stott and Taylor, 1973) and the Rabbit River (Gabrielse, 1963; Ferri et al., 1999) map areas. In the Yukon and the Northwest Territories, parts of the La Biche River map area (NTS 095C) have been compiled at 1:50 000 (Fallas, 2001; Fallas and Evenchick, 2002) and 1:100 000 scales (Fallas et al., 2004). Stott (1982) first defined the type sections of the Garbutt Formation as part of a regional investigation of

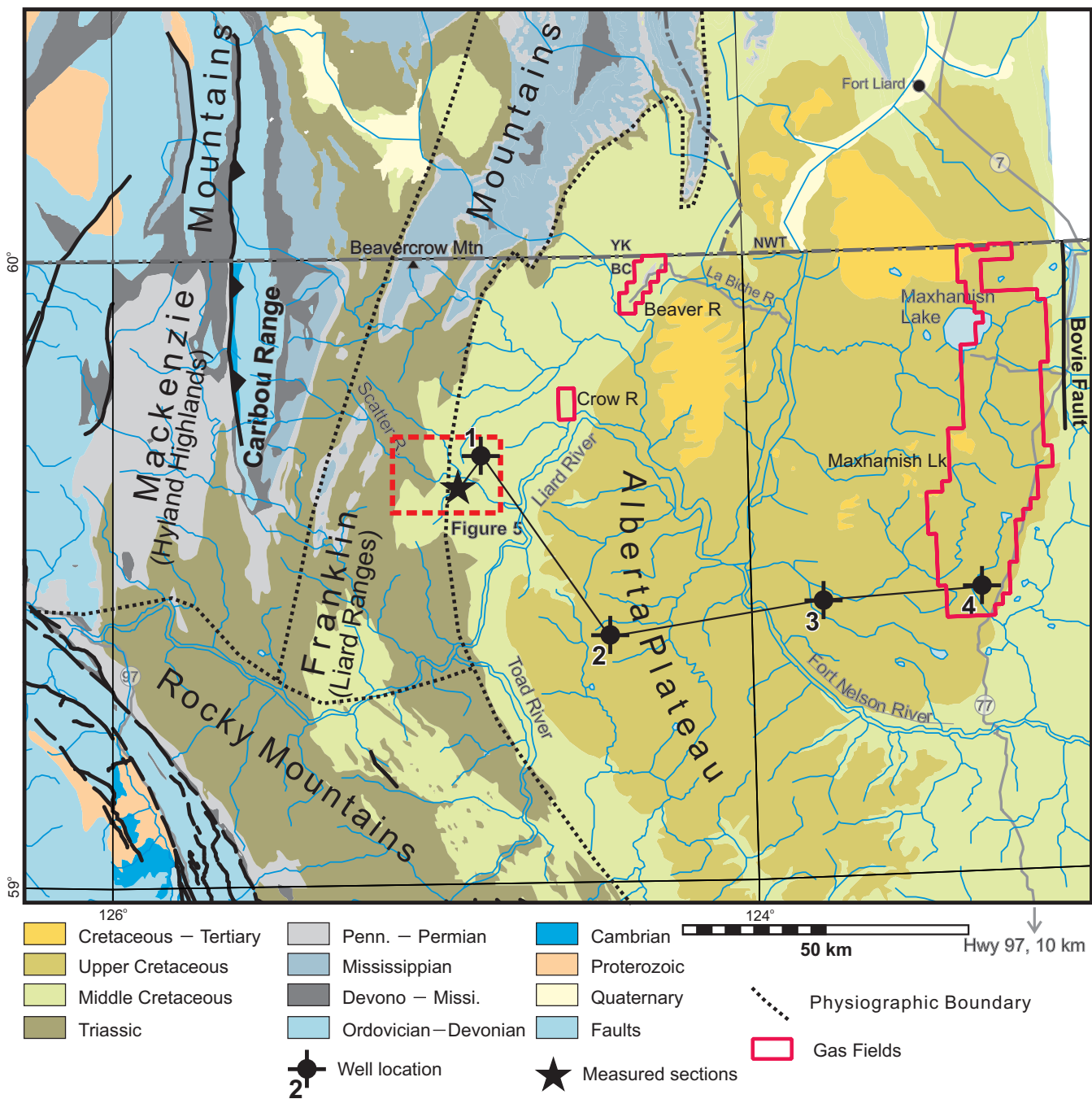


Figure 3. Regional geological setting of the study area showing main geological units and main physiographic boundaries. Wells shown in Figure 23 are marked as 1 (d-98-F), 2 (d-75-E), 3 (b-43-K) and 4 (d-52-K).

Cretaceous rocks in northeastern British Columbia. Leckie et al. (1991) and Leckie and Potocki (1998) further describe the sedimentology of the Chinkeh, Garbutt and Scatter Formations. Jowett and Schröder-Adams (2005) described the paleoenvironments and stratigraphy of the succeeding Lepine Formation. Chalmers and Bustin (2008a, b) examined the Garbutt Formation as part of more regional investigation of the shale gas potential of Lower Cretaceous shale in northeastern British Columbia.

## METHODOLOGY

Several sections of the Garbutt Formation were measured and described through the use of a 1.5 m staff along Toreva Creek and Scatter River (Figures 4 and 5). A continuous section of this unit could not be measured because of limited access and poor exposure; therefore, the five separate segments that were examined represent different, though nearly contiguous parts of the formation (Figure 5; UTM coordinates for the base of each section

	Liard River (Stott, 1982; Leckie et al., 1991)	Sikanni Chief River (Stott, 1982)	Plains, BC (Stott, 1982; Jowett and Schroder-Adams, 2005)	Plains, BC (Stott, 1982; Jowett and Schroder-Adams, 2005)
U Cret	Dunvegan Fm	Dunvegan Fm	Dunvegan Fm	Dunvegan Fm
Lower Cretaceous	Sully Fm	Sully Fm	Shaftesbury Fm	Shaftesbury Fm
	Sikanni Fm	Sikanni Fm	Goodrich Fm	
	Lepine Fm	Buckingham Fm	Hasler Fm	
	Scatter Fm		Boulder Ck Fm	
	Tussock Mbr		Hulcross Fm	
	Wildhorn Mbr		Gates Fm	
	Bulwell Member		Moosebar Fm	
	Garbutt Fm			
	Fort St. John Group	Fort St. John Group	Fort St. John Group	Fort St. John Group
	Peace River Fm		Peace River Fm	
Paddy Mbr		Paddy Mbr		
Cadotte Mbr		Cadotte Mbr		
Harmon Mbr		Harmon Mbr		
Notikewin Mbr		Notikewin Mbr		
Falher Mbr		Falher Mbr		
Spirit River Fm		Spirit River Fm		
Wilrich Mbr		Wilrich Mbr		
Bluesky Fm		Bluesky Fm		
Chinkeh Fm	Gething Fm	Gething Fm	Gething Fm	

Figure 4. Correlation of Early Cretaceous strata in northeast British Columbia.

are: 1, 394932E 6612890N; 2, 394286E 6612364N; 3, 394159E 6612554N; 4, 389260E 6612795N; 5, 389021E 6612714N; Zone 10, NAD83). Representative chip samples were acquired across 2 m intervals along the entire section. Samples were split, with one group being analyzed for whole-rock, trace and rare earth element abundances by inductively coupled plasma–emission spectroscopy (ICP-ES) and inductively coupled plasma–mass spectrometry (ICP-MS) via a lithium metaborate-tetraborate fusion at Acme Analytical Laboratories (Vancouver, BC), and a second group, at 4 m spacings, for Rock-Eval analysis at Geological Survey of Canada (GSC) laboratories (Calgary, Alberta). A smaller subset of these samples will also be analyzed by X-ray diffraction (XRD) at the GSC laboratories for semi-quantitative determination of mineral abundances. Separate samples were collected for thermal maturity determination at the GSC laboratories in Calgary through reflected light microscopy. In addition, a handheld gamma-ray spectrometer (RS-230 by Radiation Solutions Inc.) was used to measure natural gamma radiation every 1 m during a 2 minute time interval allowing the calculation of K (%), U (ppm), Th (ppm) and total gamma-ray count. These data produced a diagram showing the variation in total natural radiation along the section, which is approximately equivalent to the subsurface gamma-ray trace. This was used to assist with the correlation of the outcrop section with equivalent rocks in the subsurface.

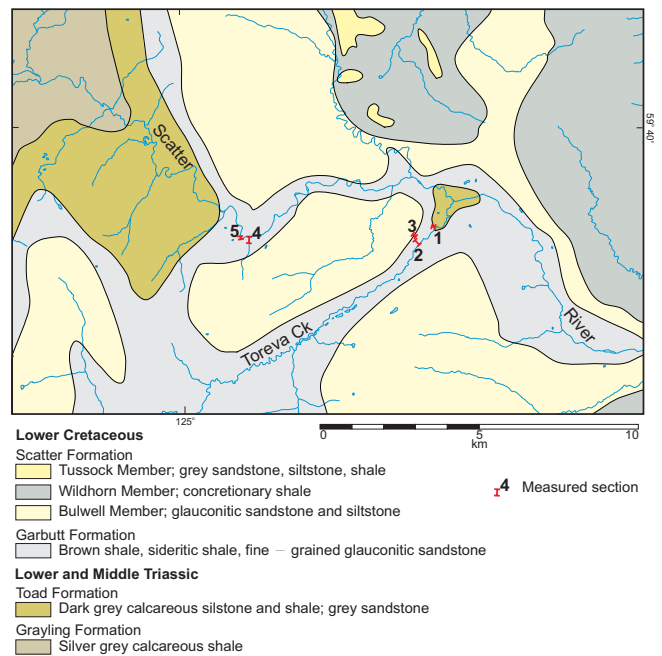


Figure 5. Location of the five measured sections of the Garbutt Formation with respect to local geology.

## LITHOLOGICAL DESCRIPTION

A combined thickness of approximately 221 m of section was measured at five localities (Figures 5–8). A composite section with the relative position of each section (Figure 6) is based on structural sections, relative position of these sections to the Toad (Triassic) and Scatter (Lower Cretaceous) formation contacts and from the 285 m section of measured Garbutt Formation (Stott, 1982) near these localities. The relative position of these sections is supported by a well-defined geothermal gradient produced by plotting  $T_{max}$  versus depth (see discussion below).

The base of the composite section was observed on Toreva Creek where more than 6 m of section is exposed. At the river level, 3 m of Toad Formation is present. It consists of thin bedded, laminated, calcareous siltstone and thin to crossbedded, fine-grained sandstone. The contact between the Toad and the Garbutt formations appears unremarkable except for the presence of 1–3 cm of grey chert nodules. The Garbutt Formation consists of dark grey crumbly shale with uneven partings and a 30 cm thick laminated bed of fine-grained, calcareous and micaceous sandstone containing carbonaceous partings in places.

The succeeding part of the Garbutt Formation was examined on the south side of Scatter River (sections 4 and 5; Figure 5), as most of the lower 60 m of the Garbutt Formation is covered in Toreva Creek (Figure 6). At Scatter River, the unit consists of rusty to dark brown weathering, micaceous shale and siltstone with thin, laminated quartz sandstone (locally glauconitic) horizons that typically comprise less than 10% of the section, but can locally reach

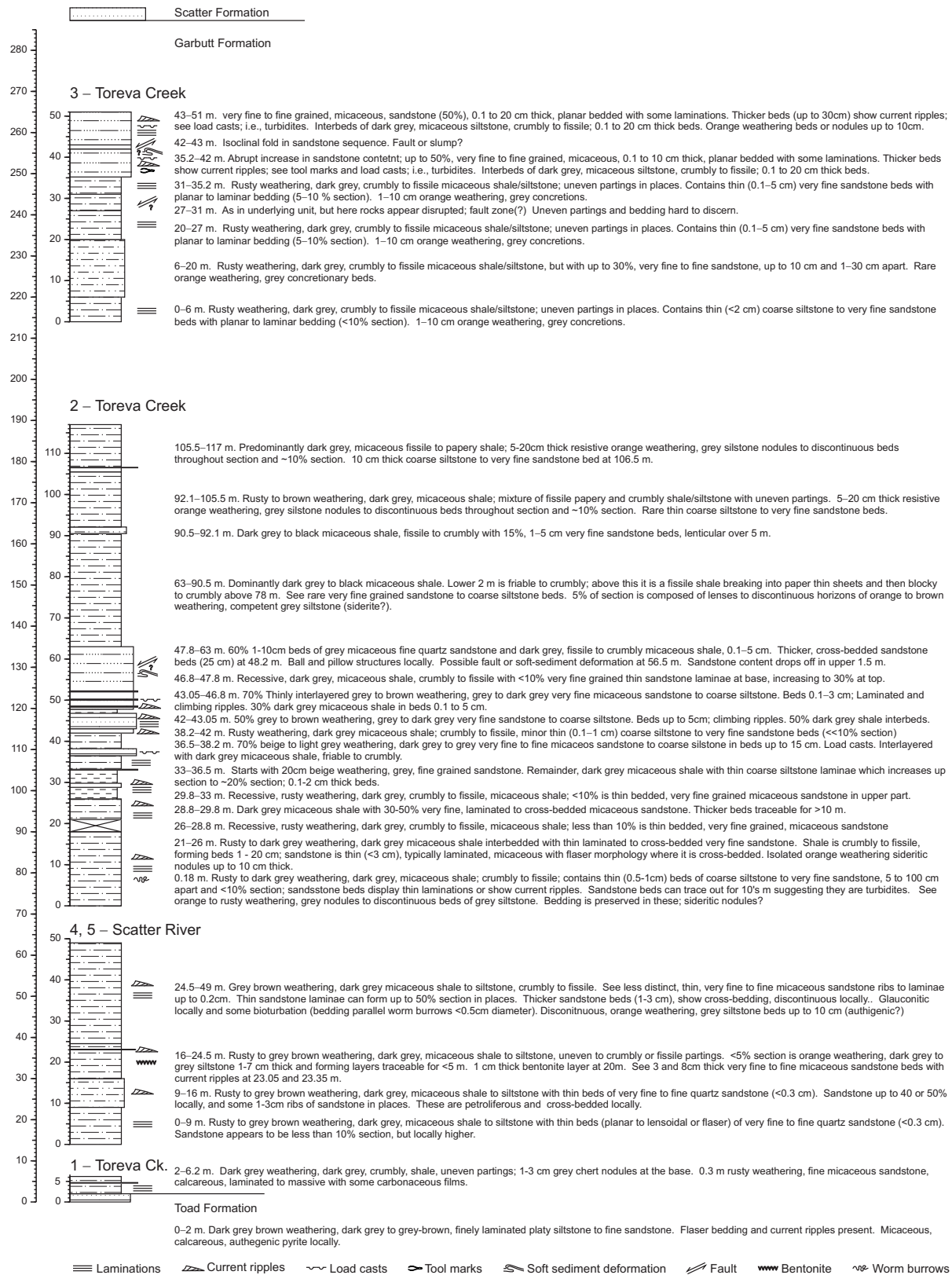


Figure 6. Relative stratigraphic positions of measured sections, with descriptive notes. Numbers refer to the order in which the sections were measured. Sections 4 and 5 are contiguous, section 4 extending from 0 to 16 m.



Figure 7. a) Looking northwest at the contact between the Garbutt and Scatter formations. Note the increase in sandstone in the upper part of the Garbutt Formation until the sandstone becomes dominant within the Scatter Formation (brown weathering sandstone); b) looking northwest at Garbutt Formation rocks measured on the north side of Toreva Creek. Note the tabular nature of the sandstone beds and how they can be traced for many tens of metres. Recessive papery shale in the upper part of section 2 and lower part of section 3 can be seen at the top of the section above the sandstone ribs. Note the structural offset of the topmost, thickest sandstone rib.



Figure 8. Looking south at the section of Garbutt Formation measured along Scatter River. Sandstone ribs seen at the top of this section are believed to be the same as those seen within the lower part of section 2 (Figure 7). Thin bentonite horizons occur at the base of the section.

up to 50%. Sandstone beds in well exposed blocks on the creek bed show lenticular to flaser structures associated with bioturbation and may indicate wave influence (Figure 9, inset). Thicker, current-rippled sandstone beds up to 8 cm thick occur and can have a petroliferous odour when broken. Also present are discontinuous, orange-weathering manganiferous (?) siltstone horizons up to 10 cm thick, comprising 5% of the section. A thin (1–2 cm) bentonite horizon was observed at the 20 m level. Bedding-parallel trace fossils (burrows) were common in the sandy horizons (Figure 9).



Figure 9. Bedding-parallel worm burrows in lower Garbutt Formation siltstone and shale along Scatter River. Inset shows thin-bedded, planar to lenticular nature of bedding in the lower part of the Garbutt Formation, together with worm burrows (to the left of the lens cap).

Similar rock types are found in the lower part of the next stratigraphically higher section examined at creek level along Toreva Creek (section 2; Figure 6). The occurrence of thin bedded and laminated, fine micaceous sandstone begins to increase at the 33 m level of this section. Sandstone beds thicken (10–15 cm) and constitute up to 60% of the section by the 60 m level, and locally up to 70% between 43 and 48 m. Occasionally, the sandstone beds can be up to 25 cm thick and contain climbing to current ripples and load casts at the base (Figure 10). These beds form prominent sheets traceable for tens of metres (Figure 7).

There is a possible fault or soft-sediment deformation structure at the 56.5 m level of section 2 (Figure 11). Flat-lying siltstone and fine sandstone sit abruptly above folded and locally overturned siltstone and sandstone (Figure 11). The tightness of the folding and the manner in which the folded beds are cut off along strike suggests a tectonic feature.

At 63 m of section 2, the sandstone content drops off over 1.5 m, followed by 50 m of dark grey to black, fissile to papery, micaceous shale with rare, thin beds of fine micaceous sandstone (Figures 6 and 12). At the 117 m level, section 2 became obscured by vegetation; as a result, a new



Figure 10. Current ripples in fine sandstone of the Garbutt Formation within the lower part of section 2.

section was initiated approximately 1 km to the west.

The lower part of section 3 (Figure 6) contains fissile shale similar to the lower part of section 2. Lenticular to podiform, orange-weathering, manganiferous (?) siltstone horizons are found within the finer-grained sequences (Figure 13). Thin-bedded, laminated sandstone increases up-section until it comprises approximately 30% of the



Figure 11. Possible fault (or soft-sediment deformation feature?) in the Garbutt Formation at 56.5 m of section 2.

section (6–20 m). At the 35 m level, micaceous sandstone beds increase in abundance and thickness and are locally up to 30 cm thick. Sandstone beds are tabular in nature, commonly laminated and traceable for many metres along the section. Thicker beds show current ripples (Figure 14), load casts and tool marks (Figure 15). Numerous zones of disrupted bedding were observed in the section (Figures 16 and 17) being of either soft-sediment or tectonic origin. The section is too steep to access at the top of section 3, but observations indicate that sandstone abundances continue to increase upsection to the base of the Scatter Formation (i.e., at the first thick sandstone horizon, approximately 20–25 m higher in the section).



Figure 12. Black to dark grey, thin papery shale in the upper part of section 2.

## INTERPRETATION

Overall, the combined sections of the Garbutt Formation define a coarsening-upwards succession to the Scatter Formation. The minor coarsening-upwards interval in the middle of section 2 along Toreva Creek (Figure 6) likely represents a lower-order succession. Generally, the Garbutt Formation appears to represent a shallowing-upward transition from distal shelf/slope margin to inner shelf and shoreface. The lower Garbutt Formation consists of interbedded, laminated mudstone and thin tabular sandstone



Figure 13. Interbedded sandstone, shale and siltstone in the upper part of section 3.





Figure 14. Current ripples in fine sandstone of the Garbutt Formation in the upper part of section 3.



Figure 17. Soft-sediment deformation or folding in Garbutt Formation rocks in the upper part of section 3.



Figure 15. Tool marks (aligned with the pencil) along the base of sandstone beds in the upper part of section 3.



Figure 16. Soft-sediment deformation or faulting in Garbutt Formation rocks in the upper part of section 3 (indicated with the arrow).

with current and climbing ripples, load and tool casts and bedding plane-parallel trace fossils that have low diversity but are abundant. This suggests deposition by turbid flow at the slope margin or possibly distal shelf. The increase in sand content upsection reflects a more proximal position with respect to terrigenous sediment supply. In the upper portion of the Garbutt Formation, sheet sand beds become more common and thicker and may represent sea level lowering or the progradation of a Scatter Formation delta. This succession supports the interpretation that the Garbutt Formation formed initially in a slope-margin setting (Leckie and Potocki, 1998) or a distal shelf, prodelta environment (Stott, 1982). Convoluted bedding in the upper part of the Garbutt Formation (or in the middle coarsening sequence), if of depositional origin, would indicate instability. In these settings, turbidite deposits were shed from the shelf edge or delta into quiescent waters. Though storm beds were not unequivocally identified in this investigation, Leckie and Potocki (1998) report wave-formed structures in the upper part of the Garbutt Formation and conclude they formed as relative sea level became shallower prior to the deposition of the Scatter Formation.

## ROCK-EVAL DATA

Only a summary of the Rock-Eval data will be presented here; the complete dataset will be made available in a later publication. Plotting of total organic carbon (TOC) within the section indicates that the highest TOC levels (1.2–1.67%) are within the central part of the formation (Figure 18), with an average value for the entire sample set of 1.12%. Distribution of other Rock-Eval parameters suggests that the kerogen within these sedimentary rocks is type III in nature; i.e., terrestrial plant in origin (Figures 19a, b) and has an average hydrogen index (HI) of 60 mg HC<sup>1</sup> /g TOC (Figure 19b), although prior to maturation, this would have been slightly higher (Figures 18 and 19c).

Thermal maturation of the sequence can be reasonably deduced from  $T_{max}^2$  values, as  $S2^3$  values are consistently higher than 0.2 mg HC/g rock (Peters, 1986). Plotting  $T_{max}$  versus depth in the section shows a regular increase in  $T_{max}$  values with increase in depth likely related to the paleogeothermal gradient (Figure 18). A regression line through the dataset indicates that the top of the section is at the beginning of the dry gas generation window and the base is at the midpoint (Dow, 1977; Teichmuller and Durand, 1983; cf. Figure 4 in Leckie et al., 1988).

Although organic carbon levels suggests a fair to good source rock (Peters, 1986), HI levels are low due to a type III kerogen and suggest gas-prone kerogen. The presence of trace fossils in parts of the sequence, together

with litho-geochemistry (see below), suggests that optimum reducing conditions (i.e., anoxic) were not present for preservation of all organic material (i.e., some was metabolized by organic activity). This may have also been coupled with low productivity and dilution by sediment supply.

## SCINTILLOMETER DATA

Gamma-ray spectroscopic data (total counts as dose, with calculated U, Th and K concentrations) collected across the various sections of the Garbutt Formation are displayed in Figure 20. At first glance, it appears that the total count rate (i.e., gamma-ray trace) correlates best with

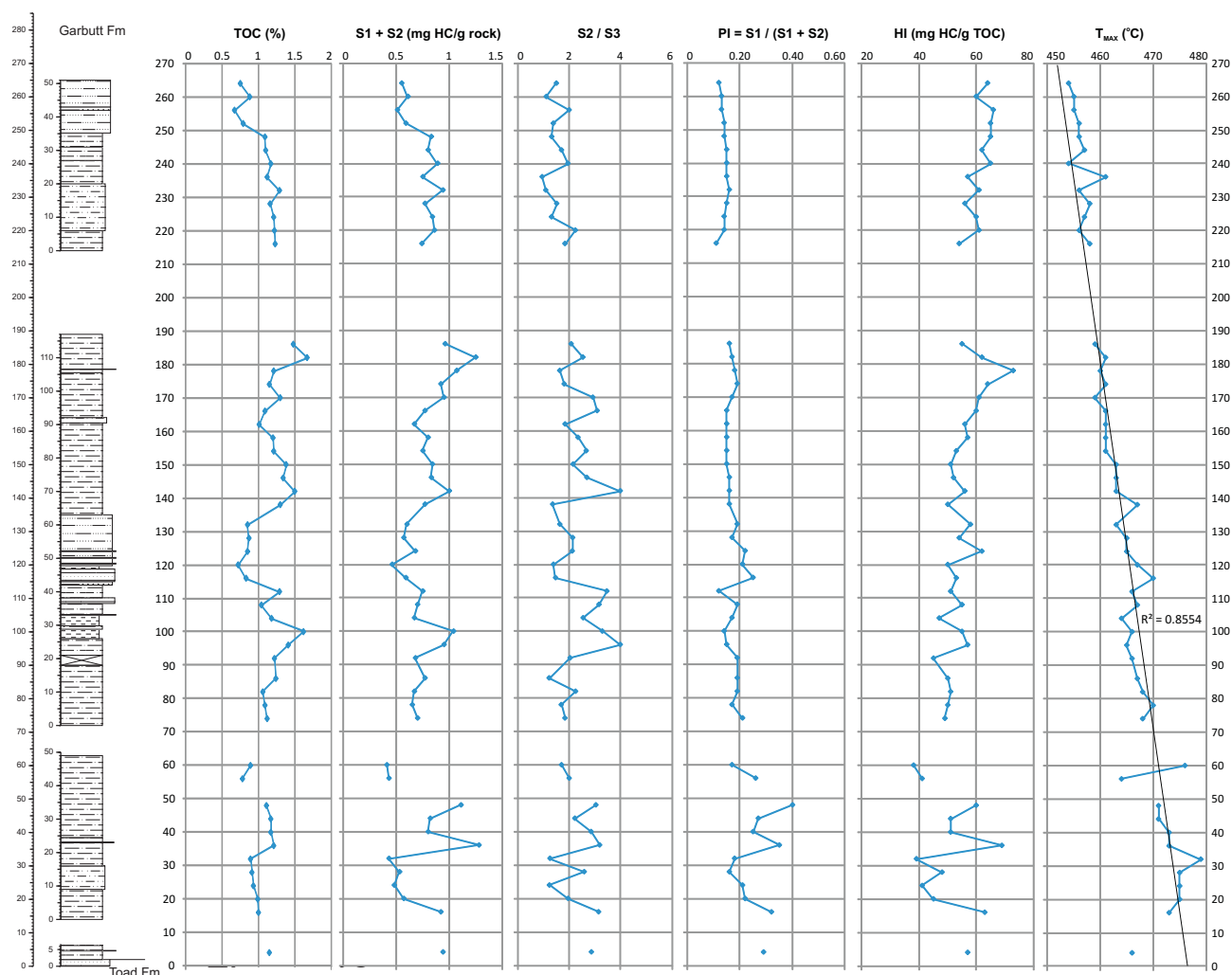


Figure 18. Rock Eval data plotted against the measured sections of the Garbutt Formation.

- 1 Hydrocarbons
- 2 Maximum temperature of hydrocarbon production
- 3 Represents the amount of hydrocarbons resulting from cracking sedimentary organic matter in the sample (mg HC/g rock)

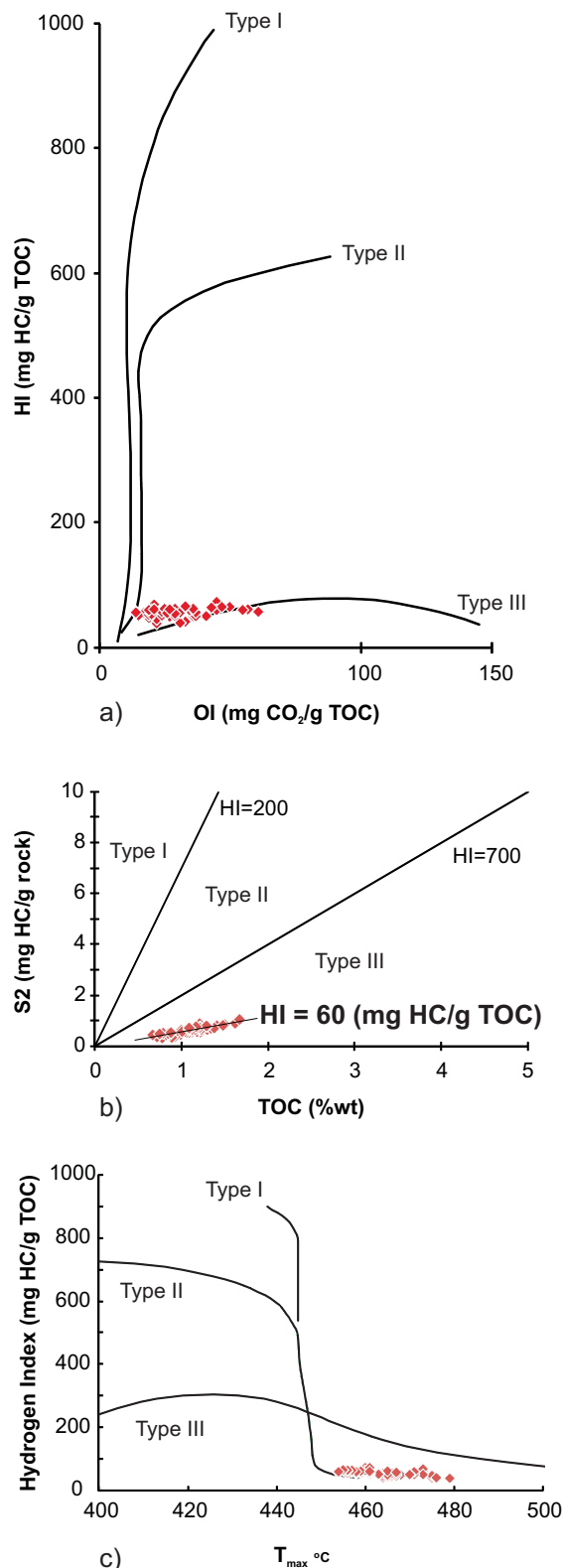


Figure 19. a) Modified van Krevelen diagram (Tissot and Welte, 1984) showing the type III nature of the kerogen from the Garbutt Formation. b) An S<sub>2</sub> versus TOC diagram from Langford and Blanc-Valleron (1990) showing the type III nature of the kerogen from the Garbutt Formation and the level of hydrocarbons in the organic matter (60 mg HC/g TOC); c) Hydrogen index (HI) versus T<sub>max</sub> showing the change in hydrocarbon content with maturation of the kerogen; modified from Bordenave (1993).

K and Th concentrations, suggesting that the overall bulk concentration of the rocks is controlling the signature. This contrasts with similar data from the Triassic Toad Formation and Devonian-Mississippian Besa River Formation, where the total gamma-ray trace is governed by the concentration of U, which is ultimately tied to reducing conditions at the time of deposition (Ferri et al., 2010, 2011). Furthermore, this reducing environment in Toad River and Besa River rock types results in the relative abundance of organic matter (shown as TOC), correlating very well with U concentrations (Ferri et al., 2010, 2011). Although there is a broad correlation between organic carbon content and total gamma-ray levels in the Garbutt Formation (Figure 20), this is likely a function of dilution within the coarser clastic parts of the succession.

## LITHOGEOCHEMICAL DATA

Select major- and trace-element geochemistry across the measured section of the Garbutt Formation is shown in Figures 21 and 22. As expected, SiO<sub>2</sub> content follows gross lithological composition and has inverse relationships with Al<sub>2</sub>O<sub>3</sub> and K<sub>2</sub>O. Concentrations of Fe<sub>2</sub>O<sub>3</sub> are above 15% by weight and average 6%. Levels of MnO and MgO mimic those of Fe<sub>2</sub>O<sub>3</sub> with levels of MnO peaking above 0.1% (averaging 0.027%) and MgO peaking above 2% (averaging 1.12%). The relative abundances of several trace elements shown in Figure 22 appear to correlate with total organic carbon contents (TOC; i.e., V, Pb and to a lesser extent Mo). Barium concentrations are quite high, up to 1500 ppm (0.15 wt.%), and these relative levels also generally follow those of TOC.

The concentration of organic carbon and specific elements within a sedimentary succession is a reflection of reducing conditions during the time of deposition (see Ferri et al., 2011 for further discussion). Quinby-Hunt and Wilde (1994) describe four groups of low-calcic shale (Table 1) based on Mn, Fe and V concentrations, which are primarily a function of the redox conditions during sediment deposition.

Chemical data for shale within the Garbutt Formation suggests they fall within Group 2 as defined by Quinby-Hunt and Wilde (1994; Table 1). These authors caution that the elemental concentrations defining Group 2 shale could form under several reducing environments such that the high Fe concentrations reflects Fe as oxides (least reduced) or sulphides (most reduced). Although the oxidation state of the Fe in the samples was not determined or any mineral speciation carried out, the low concentration of S in these rocks (average of 0.1 wt.%) suggests Fe is not found as sulphides. Furthermore, Quinby-Hunt and Wilde (1994) indicate that shale deposited in the least reducing anoxic environment will contain glauconite and other Fe silicates together with siderite and rhodochrosite and that the shale

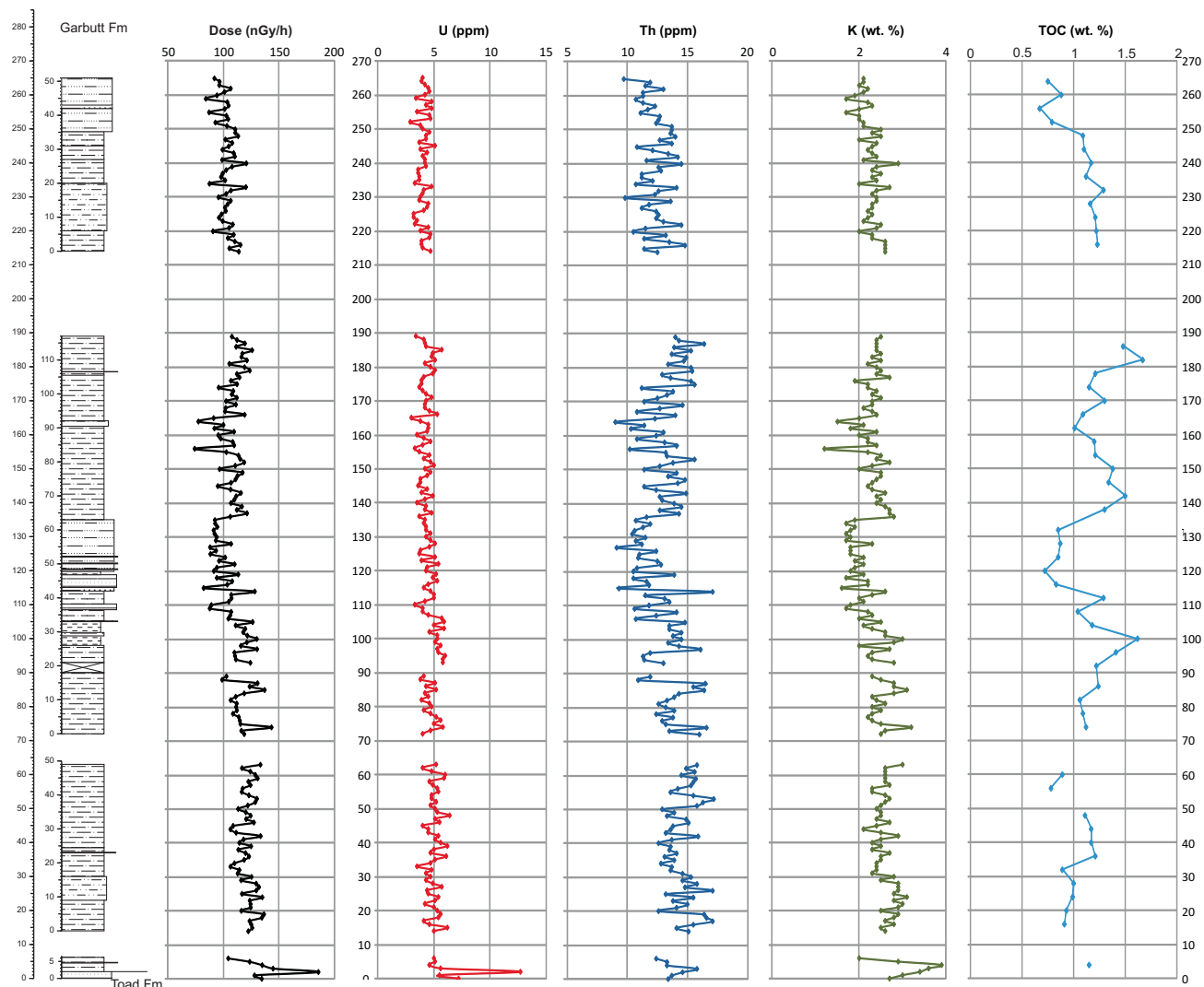


Figure 20. Gamma-ray spectrometer data and total organic carbon contents, and U, Th and K values from the five measured sections of the Garbutt Formation.

would have a browner colour due to the presence of Fe oxides.

Although the Fe concentration in sediments deposited within the oxic zone is comparable to those set down in the least anoxic conditions, the distinguishing feature is the greater abundance of Mn (Table 1), which would be found as oxides (Quinby-Hunt and Wilde, 1994). Manganese levels in Garbutt rocks average approximately 0.03%, suggesting that the bulk of the section is consistent with Group 2 anoxic rocks, but several horizons peak above 0.1% and fall within the oxic zone (Figure 21, Table 1). Also note that parts of the section have MnO levels below 0.01% (suggesting more reduced conditions) and that this roughly corresponds to the 'rad zone' in the subsurface (see below). Possible Mn concretions or Mn horizons were noted in this

study and in other studies of the Garbutt Formation (Stott, 1982; Leckie and Potocki, 1998). In addition, trace fossils were noted at several levels within the Garbutt Formation, suggesting oxygen levels may have been high enough locally or temporally to allow some organisms to survive. These observations can be explained if these rocks were being deposited close to the anoxic-oxic boundary, which may have fluctuated in response to relative sea level variations and sea water mixing leading to incursions of more oxygenated waters.

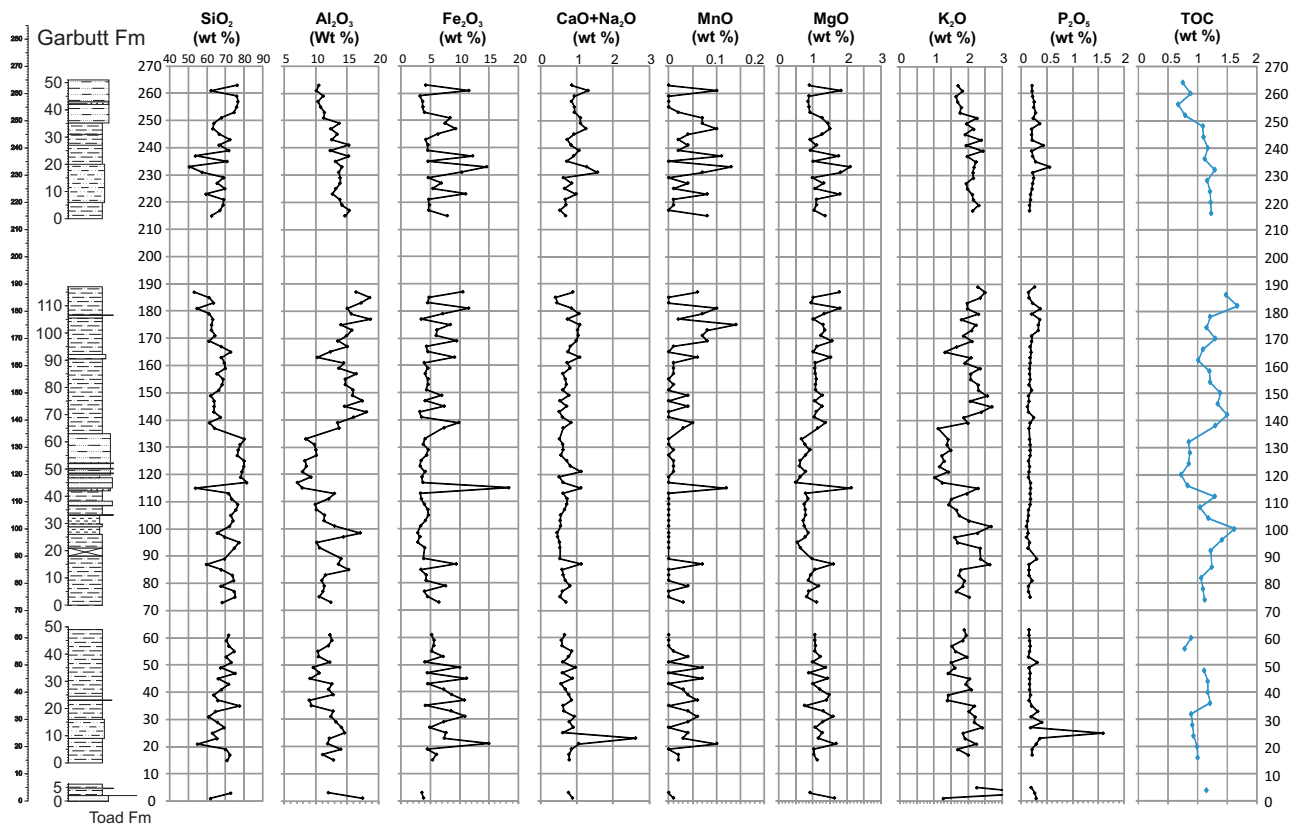


Figure 21. Major oxide geochemical data and total organic carbon contents from the five measured sections of the Garbutt Formation.

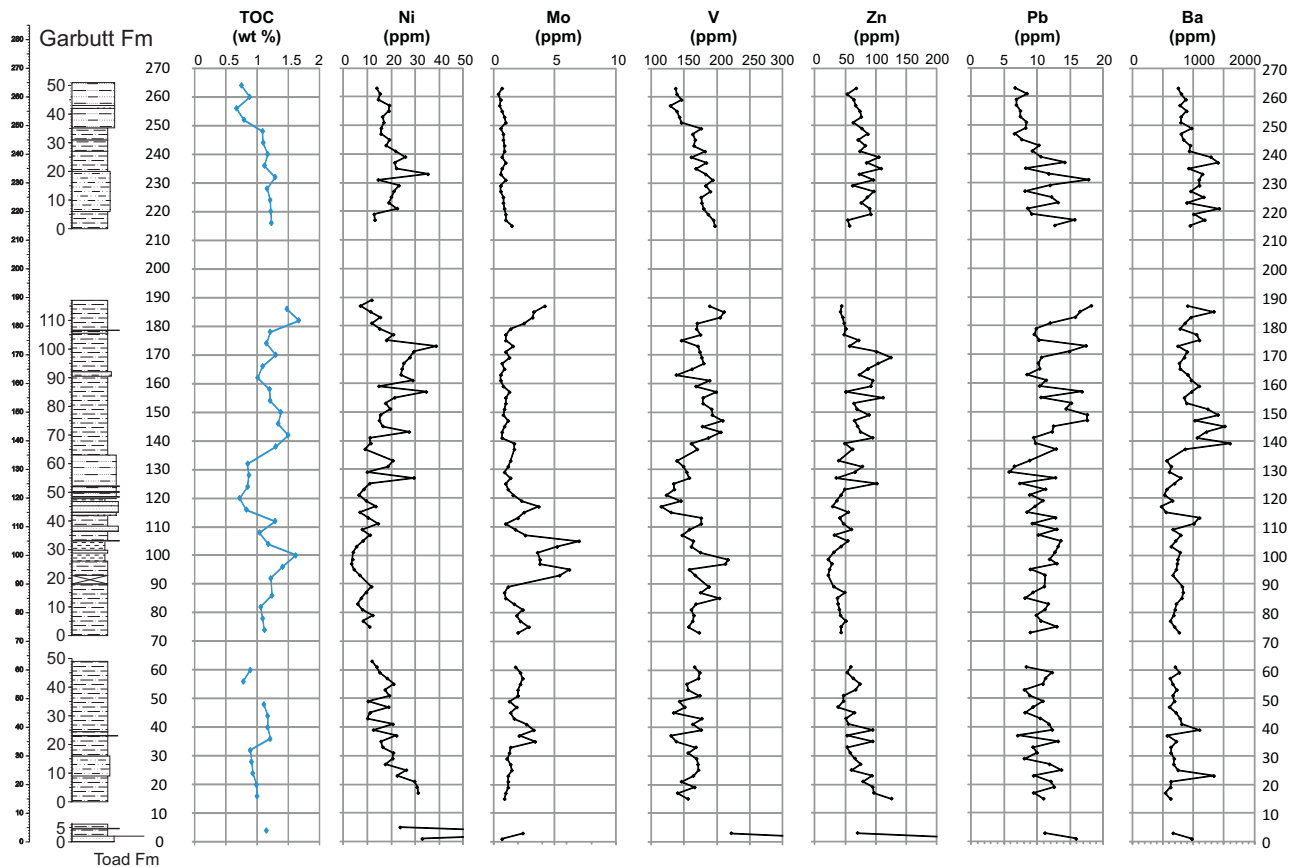


Figure 22. Trace-element data and total organic carbon contents from the five measured sections of the Garbutt Formation.

TABLE 1. SUBDIVISION OF LOW-CALCIC BLACK SHALE BASED ON FE-MN-V CONTENTS.

			Mn ppm	MnO wt. %	Fe ppm	Fe <sub>2</sub> O <sub>3</sub> wt. %	V ppm
Oxygenated waters (Manganese nodules)	Group 1: Oxic Mn>800 ppm, Fe>37,500 ppm, V<320 ppm MnO>0.1%, Fe <sub>2</sub> O <sub>3</sub> >5.36%	Avg.	1,300	0.17	56,000	8.0	130
		Max.	3,600	0.46	87,000	12.4	310
		Min.	830	0.011	38,000	5.4	84
Least Anoxic	Group 2: Mn soluble Mn<750 ppm, Fe<37,500 ppm, V<320 ppm MnO<0.1, Fe <sub>2</sub> O <sub>3</sub> >5.36%	Avg.	310	0.04	52,000	7.4	140
		Max.	730	0.094	100,000	14.3	220
		Min.	46	0.005	39,000	5.6	64
	Group 3: Mn, Fe Soluble Mn<750 ppm, Fe<37,500 ppm, V<320 ppm MnO<0.1%, Fe <sub>2</sub> O <sub>3</sub> <5.36%	Avg.	170	0.022	23,000	3.3	170
		Max.	680	0.088	37,000	5.3	300
		Min.	33	0.004	6,700	0.96	77
Most Anoxic (Maximum preservation of organic matter)	Group 4: V enhanced Mn<750 ppm, Fe<37,500 ppm, V>320 ppm MnO<0.1%, Fe <sub>2</sub> O <sub>3</sub> <5.36%	Avg.	76	0.01	19,000	2.7	1,500
		Max.	260	0.034	36,000	5.1	4,900
		Min.	20	0.003	4,600	0.66	320

(Modified from Quinby-Hunt and Wilde, 1994).

## CORRELATIONS

Correlation of Garbutt Formation rocks examined along Toreva Creek and Scatter River with subsurface sections across the Liard Basin is shown in Figure 23. The constructed gamma-ray trace from this study fits well with the d-98-F well found a few kilometres to the north (Figure 23). Note the change in character of the Garbutt Formation eastward (Figure 23). The most prominent change occurs in the lower third of the formation with the development of the 'rad zone', or radioactive zone, as defined by the anomalous gamma-ray levels at this horizon. The Garbutt Formation also thins and generally becomes finer grained towards the east.

## DISCUSSION

The organic carbon contents and the type of kerogen defined within the Garbutt section of the study area are consistent with those reported by Chalmers and Bustin (2008b). These authors also show organic carbon levels and the type of kerogen within Early Cretaceous sequences changing eastward (i.e., TOC increasing and changing from type III to type II/III and to type I/II kerogen). In the Garbutt Formation, an increase in organic carbon content is indirectly shown by the development of the rad zone in the lower part of the Garbutt Formation, assuming the higher radioactivity is a consequence of an increase in organic carbon.

The eastward increase in TOC levels may be a function of a decrease in sedimentary dilution as one moves away from the western sediment source. Chalmers and Bustin (2008b) suggest that the change from type III to type II/III or type I/II kerogen reflects the proximity of the rock to terrestrial sediment sources (i.e., type III kerogens occurring closer to the sediment supply area). The TOC levels may also increase to the east as a result of better preservation

of organic matter within the deeper, anoxic parts of the basin. Data from this study suggests that Garbutt Formation rocks in the Toreva Creek—Scatter River area were deposited where waters fluctuated between oxic and anoxic conditions. During oxic conditions, organic preservation is likely limited, which may account for lower TOC levels. In addition, organic carbon levels decrease with an increase in thermal maturation as hydrocarbons are produced; this is especially important within type I and II kerogens, where more than half the organic matter is expelled as thermal maturation progresses (Jarvie, 1991). Thermal maturation levels decrease eastward as the sedimentary succession thins, suggesting that residual organic carbon levels should increase if the initial TOC was uniform across the region.

The type (richness) and amount of organic matter within the Garbutt succession appears to decrease towards the Cordilleran front, resulting in a decrease in the amount of adsorbed gas that the sequence can accommodate (see Chalmers and Bustin, 2008a, b). Concurrent with this is an increase in the thickness of the stratigraphic sequence towards the Cordilleran front (i.e., sediment source area), resulting in greater depths of burial and increased formation pressure, which will ultimately increase the amount of gas held within the formations. As a result, the lower adsorbed gas contents due to lower TOC levels will be offset by higher concentrations of pore-space gas.

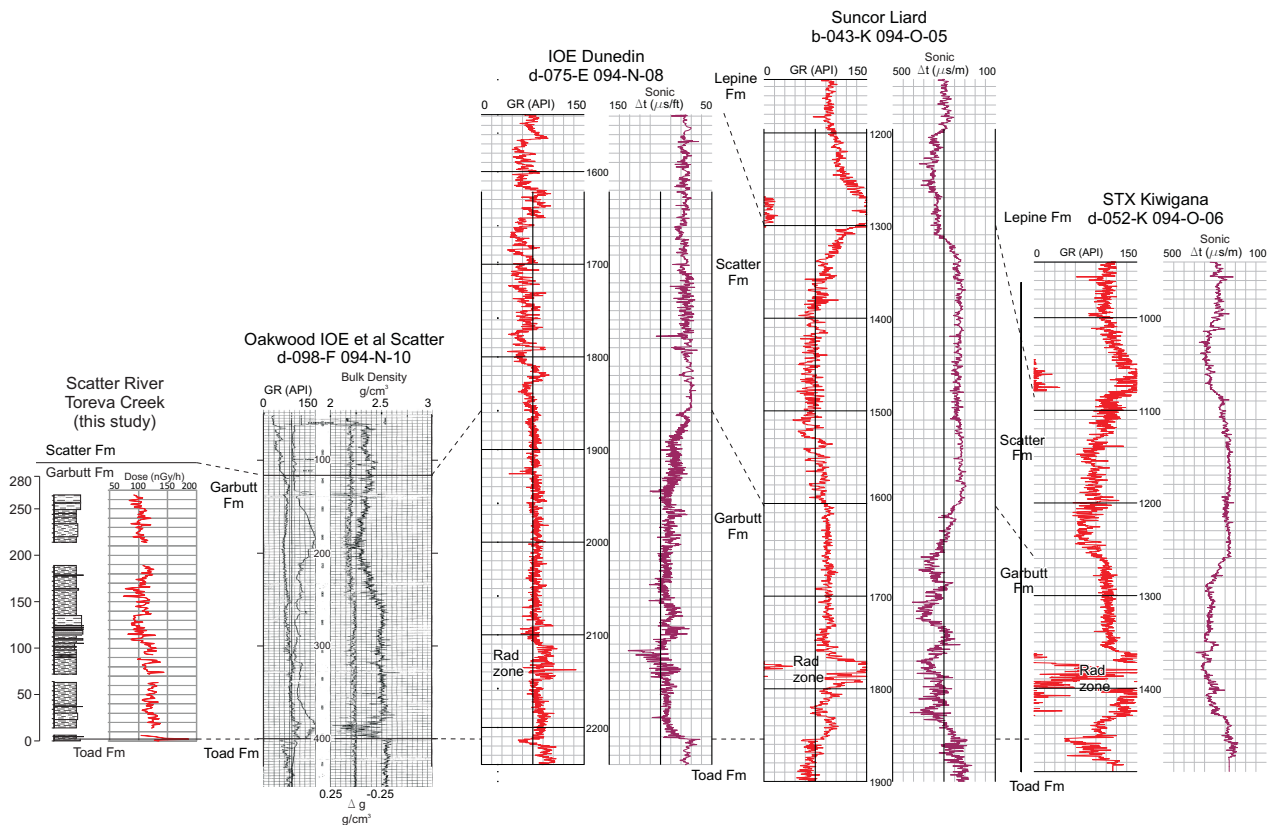


Figure 23. Correlation of the combined five sections of the Garbutt Formation in the study area with several subsurface sections of the unit across the Liard Basin. The location of the wells used in the section can be found in Figure 3.

## CONCLUSIONS

- The Garbutt Formation is approximately 285 m thick in the Toreva—Scatter River area and consists of dark grey to black or dark grey brown shale, siltstone and lesser fine sandstone.
- Sedimentary structures suggest deposition below the storm wave base in a distal shelf, slope-margin or prodelta environment.
- Rock-Eval data show average total organic carbon contents of 1.12 wt.% with peaks between 1.2 and 1.67%. Hydrogen index levels are low and average 60 mg HC/g TOC. Kerogen is type III in nature (terrestrial) and  $T_{max}$  maturation levels suggest the early to mid dry gas generation window.
- The concentration of Mn, Fe, V and other elements suggest that the sediments were deposited near the boundary between anoxic and oxic water conditions.

## ACKNOWLEDGMENTS

The authors thank Lauren Wilson and Lisa Fodor for competent and cheerful assistance in the field. Lisa Fodor is acknowledged for having compiled the scintillometer data. We acknowledge Great Slave Helicopters of Fort Liard for transporting us to our field localities. The senior author thanks Sarah Saad at Geological Survey of Canada laboratories in Calgary for her patience, knowledge in preparation and analysis of Rock-Eval samples.

## REFERENCES

- Adams, C. (2009): Summary of shale gas activity in northeast British Columbia (2008); *BC Ministry of Energy*, Petroleum Geology Open File 2009-1, 17 pages.
- Bordenave, M.L. (1993): Applied Petroleum Geochemistry; *Technip*, 531 pages.
- Chalmers, G.R.L. and Bustin, R.M. (2008a): Lower Cretaceous gas shales in northeastern British Columbia; part I, geological controls on methane sorption capacity; *Bulletin of Canadian Petroleum Geology*, Volume 56, Issue 1, pages 1–21.
- Chalmers, G.R.L. and Bustin, R.M. (2008b): Lower Cretaceous gas shales in northeastern British Columbia; part II, evaluation of regional potential gas resources; *Bulletin of Canadian Petroleum Geology*, Volume 56, Issue 1, pages 22–61.
- Dawson, F.M., Kalkreuth, W.D. and Sweet, A.R. (1992): Stratigraphy and coal resource potential of the Upper Cretaceous to Tertiary strata of northwestern Alberta; *Geological Survey of Canada*, Open File Report 2499, 98 pages.
- Dow, W.G. (1977): Kerogen studies and geological interpretations; *Journal of Geochemical Exploration*, Volume 7, Issue 2, pages 79–99.
- Fallas, K.M. (2001): Preliminary geology, Mount Martin, Yukon Territory—British Columbia—Northwest Territories; *Geological Survey of Canada*, Open File 3402, scale 1:50 000.
- Fallas, K.M. and Evenchick, C.A. (2002): Preliminary geology, Mount Merrill, Yukon Territory—British Columbia; *Geological Survey of Canada*, Open File 4264, scale 1:50 000.
- Fallas, K.M., Pigage, L.C. and MacNaughton, R.B. (2004): Geology, La Biche River southwest (95C/SW), Yukon Territory—British Columbia; *Geological Survey of Canada*, Open File 4664, scale 1:100 000.
- Ferri, F., Golding, M.L., Mortensen, J.K., Zonneveld, J-P. and Orchard, M.J. (2010): Toad Formation (Montney and Doig equivalent) in the northwestern Halfway River map area, British Columbia (NTS 094B/14); in *Geoscience Reports 2010, BC Ministry of Energy, Mines and Petroleum Resources*, pages 21–34.
- Ferri, F., Hickin, A. and Huntley, D. (2011): Besa River Formation, western Liard Basin, British Columbia; geochemistry and regional correlations; in *Geoscience Reports 2011, BC Ministry of Energy*, pages 1–18.
- Ferri, F., Rees, C., Nelson, J. and Legun, A. (1999): Geology and mineral deposits of the northern Kechika Trough between Gataga River and the 60th parallel; *BC Ministry of Forests, Mines and Lands*, Bulletin 107, 122 pages.
- Gabrielse, H. (1963): Geology, Rabbit River, British Columbia; *Geological Survey of Canada*, Preliminary Map 46-1962, scale 1:250 000.
- Gabrielse, H. (1967): Tectonic evolution of the northern Canadian Cordillera; *Canadian Journal of Earth Sciences*, Volume 4, pages 271–298.
- Huntley, D.H. and Hickin, A.S. (2010): Surficial deposits, landforms, glacial history and potential for granular aggregate and frac sand: Maxhamish Lake map sheet (NTS 94O), British Columbia; *Geological Survey of Canada*, Open File 6430, 17 pages.
- Huntley, D. H. and Hickin, A. S. (2011): Geo-Mapping for Energy and Minerals program (GEM-Energy): preliminary surficial geology, geomorphology, resource evaluation and geohazard assessment for the Maxhamish Lake map area (NTS 094O), northeastern British Columbia; in *Geoscience Reports 2011, BC Ministry of Energy*, pages 57–73.
- Huntley, D.H. and Sidwell, C.F. (2010): Application of the GEM surficial geology data model to resource evaluation and geohazard assessment for the Maxhamish Lake map area (NTS 94O), British Columbia; *Geological Survey of Canada*, Open File 6553, 12 pages.
- Huntley, D. H., Hickin, A. S. and Ferri, F. (2011): Provisional surficial geology, glacial history and paleogeographic reconstructions of the Toad River (NTS 094N) and Maxhamish Lake map areas (NTS 094O), British Columbia; in *Geoscience Reports 2011, BC Ministry of Energy*, pages 37–55.
- Jarvie, D.M. (1991): Total organic carbon (TOC) analysis; in *Source Migration Processes and Evaluation Techniques*, Merrill, R.K., Editor, *American Association of Petroleum Geologists*, Treatise of Petroleum Geology, pages 113–118.
- Jowett, D.M.S. and Schröder-Adams, C.J. (2005): Paleoenvironments and regional stratigraphic framework of the Middle–Upper Albian Lepine Formation in the Liard Basin, Northern Canada; *Bulletin of Canadian Petroleum Geology*, Volume 53, pages 25–50.
- Langford, F.F. and Blanc-Valleron, M.-M. (1990): Interpreting Rock-Eval pyrolysis data using graphs of pyrolyzable hydrocarbons vs. total organic carbon; *American Association of Petroleum Geologists Bulletin*, Volume 74, pages 799–804.
- Leckie, D.A., Kalkreuth, W.D. and Snowdon, L.R. (1988): Source rock potential and thermal maturity of Lower Cretaceous strata; Monkman Pass area, British Columbia; *American Association of Petroleum Geologists Bulletin*, Volume 72, Issue 7, pages 820–838.
- Leckie, D.A. and Potocki, D.J. (1998): Sedimentology and petrography of marine shelf sandstones of the Cretaceous, Scatter and Garbutt formations, Liard Basin, northern Canada; *Bulletin of Canadian Petroleum Geology*, Volume 46, Number 1, pages 30–50.
- Leckie, D.A., Potocki, D.J. and Visser, K. (1991): The Lower Cretaceous Chinkeh Formation: a frontier-type play in the Liard Basin of Western Canada; *American Association of Petroleum Geologists Bulletin*, Volume 75, Number 8, pages 1324–1352.
- Morrow, D.W., Potter, J., Richards, B. and Goodarzi, F. (1993): Paleozoic burial and organic maturation in the Liard Basin region, northern Canada; *Bulletin of Canadian Petroleum Geology*, Volume 41, Issue 1, pages 17–31.
- Mossop, G.D., Wallace-Dudley, K.E., Smith, G.G. and Harrison, J.C., Compilers (2004): Sedimentary basins of Canada; *Geological Survey of Canada*, Open File Map 4673, scale 1:5 000 000.
- Peters, K.E. (1986): Guidelines for evaluating petroleum source rock using programmed pyrolysis; *The American Association of Petroleum Geologists Bulletin*, Volume 70, Number 3, pages 318–329.



- Quinby-Hunt, M.S. and Wilde, P. (1994): Thermodynamic zonation in the black shale facies based on iron-manganese-vanadium content; *Chemical Geology*, Volume 113, Issue 3–4, pages 297–317.
- Richards, B.C., Barclay, J.E., Bryan, D., Hartling, A., Henderson, C.M., Hinds, R.C. and Trollope, F.H. (1994): Carboniferous strata of the Western Canada Sedimentary Basin; in Geological Atlas of the Western Canada Sedimentary Basin; Mossop, G.D. and Shetse, I., Compilers, *Canadian Society of Petroleum Geologists* and *Alberta Research Council*, Special Report 4, URL <[http://www.ags.gov.ab.ca/publications/wcsb\\_atlas/atlas.html](http://www.ags.gov.ab.ca/publications/wcsb_atlas/atlas.html)> [December 2010].
- Stott, D.F. (1982): Late Cretaceous Fort St. John Group and Upper Cretaceous Dunvegan Formation of the Foothills and Plains, Alberta, British Columbia, District of Mackenzie and Yukon Territory; *Geological Survey of Canada*, Bulletin 328, 124 pages.
- Stott, D.F. and Taylor, G.C. (1973): Tuchodi Lakes map area, British Columbia; *Geological Survey of Canada*, Memoir 373, 37 pages.
- Taylor, G.C. and Stott, D.F. (1999): Geology, Toad River, British Columbia; *Geological Survey of Canada*, Map 1955A, scale 1:250 000.
- Teichmuller, M. and Durand, B. (1983): Fluorescence microscopical rank studies on liptinites and vitrinites in peat and coals, and comparison with results of the rock-eval pyrolysis; *International Journal of Coal Geology*, Volume 2, Issue 3, pages 197–230.
- Tissot, B. and Welte, D.N. (1984): Petroleum Formation and Occurrence, 2nd edition; *Springer Verlag*, 699 pages.



# PROVISIONAL SURFICIAL GEOLOGY, GLACIAL HISTORY AND PALEO GEOGRAPHIC RECONSTRUCTIONS OF THE TOAD RIVER (NTS 094N) AND MAXHAMISH LAKE MAP AREAS (NTS 094O), BRITISH COLUMBIA

David H. Huntley<sup>1</sup>, Adrian S. Hickin<sup>2</sup> and Filippo Ferri<sup>2</sup>

---

## ABSTRACT

*The Geological Survey of Canada (GSC) and British Columbia Ministry of Energy and Mines (BC MEM) are collaborating to provide new insight into surficial and applied geology of northeastern British Columbia as part of the Geo-mapping for Energy and Minerals (GEM-Energy) Program Yukon Basins Project. Remote predictive digital terrain mapping and field-based reconnaissance studies are leading to a better understanding of the regional distribution of surficial deposits, permafrost, landslides and other geomorphic processes in the Toad River (NTS 094N) and Maxhamish Lake (NTS 094O) map areas. This work is improving our knowledge of the limits of glaciation, the range of subglacial processes, the patterns of ice flow, and the history of ice retreat and glacial lake formation during a dynamic period of climate change and geomorphic adjustment in the region. From an applied perspective, our work aims to encourage new investment in northern Canada by reducing the future risks for exploration, sustainable development and management of energy and mineral resources.*

Huntley, D. H., Hickin, A. S. and Ferri, F. (2011): Provisional surficial geology, glacial history and paleogeographic reconstructions of the Toad River (NTS 094N) and Maxhamish Lake map areas (NTS 094O), British Columbia; in Geoscience Reports 2011, *BC Ministry of Energy and Mines*, pages 37–56.

<sup>1</sup>Geological Survey of Canada, Pacific Division, Vancouver, British Columbia. [dhuntley@nrcan.gc.ca](mailto:dhuntley@nrcan.gc.ca)

<sup>2</sup>Geoscience and Natural Gas Development Branch, Oil and Gas Division, BC Ministry of Energy and Mines, Victoria, British Columbia

**Key Words:** GEM-Energy program; Yukon Basins project; Toad River map area (NTS 094N); Maxhamish Lake map area (NTS 094O); physiography; bedrock geology; surficial geology; stratigraphy; paleogeographic reconstruction

---

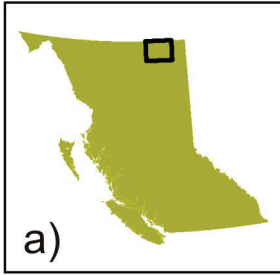
## INTRODUCTION

Northeastern British Columbia (Figure 1a) has seen an increase oil and gas land sale activity in recent years as vast organic-rich shale deposits become economically viable gas reservoirs (Adams 2009; Adams and Schwabe, 2009). Exploration is targeting mainly Middle Devonian to Lower Mississippian strata, specifically the Besa River Formation in Liard Basin and Muskwa/Otter Park and Exshaw formations in the Horn River Basin and the Cordova Embayment (Ferri et al., 2011a, 2011b). As these basins are developed, drilling activity and natural gas production are expected to expand, resulting in increased demands for quality infrastructure development (e.g., roads, well pads, campsites and pipelines) to ensure access to the land base and silica sand sources to facilitate hydrofracturing in gas wells (Huntley and Hickin, 2010, Hickin and Huntley, 2011).

An understanding of the extent and iceflow patterns of the Laurentide and Cordilleran ice sheets; the distribution of glaciofluvial and glaciolacustrine deposits, meltwater features and drainage directions; the distribution of colluvial deposits, landslides and permafrost; and the extent and nature of eolian deposits is critical to reduce exploration risks, to reduce the impact of geohazards upon infrastructure and to promote sustainable long-term investment and economic development in the eastern Liard Basin and Fold Belt (Liard Plateau and Tsoo Tablelands) and the Horn River Basin (Fort Nelson Lowlands and Etsho Plateau) shale gas producing regions of northeastern British Columbia (Figure 1b).

As part of the Geo-mapping for Energy and Minerals (GEM) program Yukon Basins project, the Geological Survey of Canada (GSC) and the British Columbia Ministry of Energy and Mines (MEM) Geoscience and Natural Gas Development Branch are collaborating to provide new insight into glacial and postglacial deposits and geomorphic

**Location of Study Area**



**Physiographic Regions**

- A Fort Nelson Lowland
- B Etsho Plateau
- C Maxhamish Escarpment
- D Tsoo Tablelands (Alberta Plateau)
- E Liard Plateau
- F Northern Rocky Mountains
- G Major Valleys

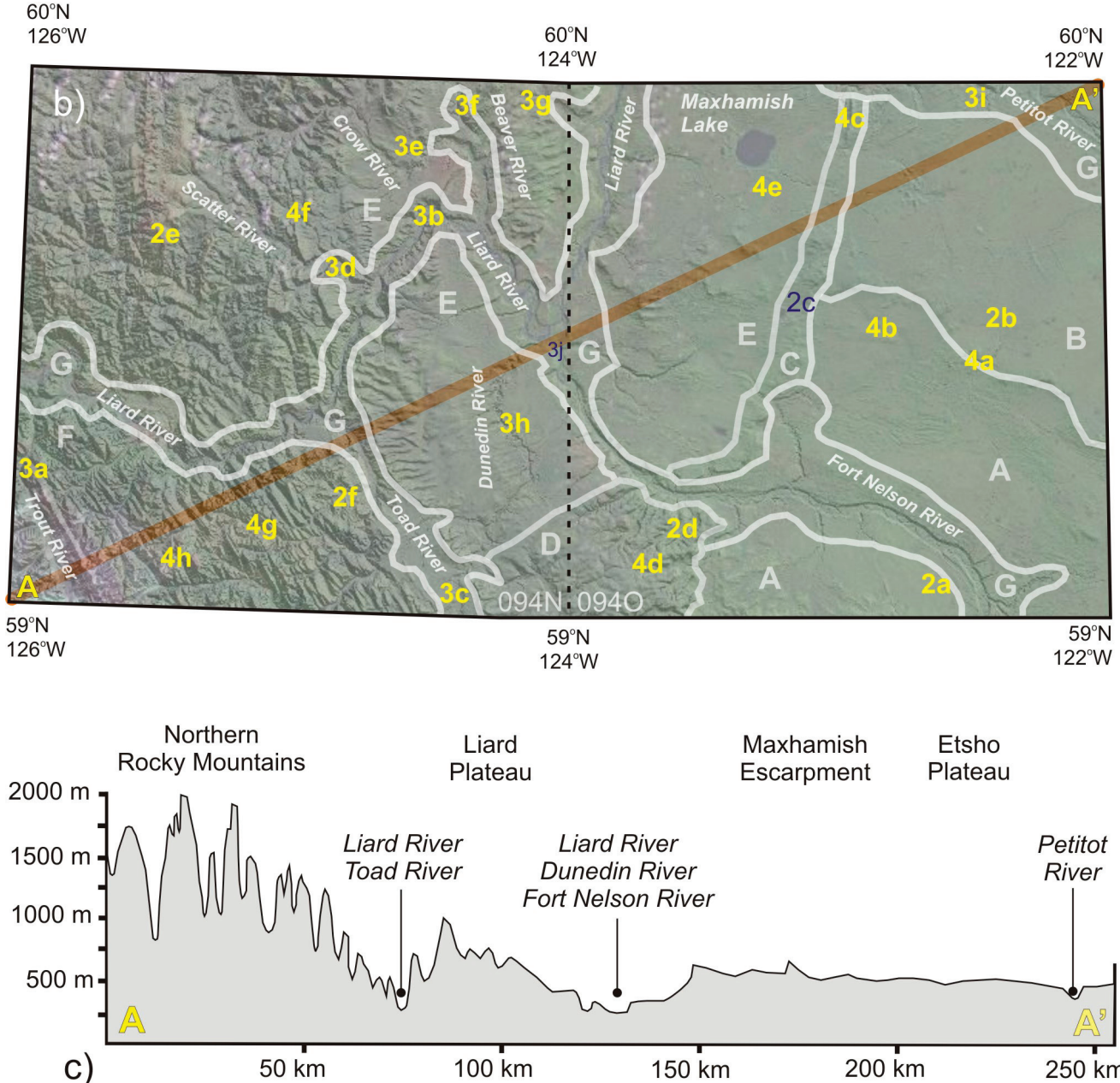


Figure 1. Toad River (NTS 094N) and Maxhamish Lake (NTS 094O) map areas are currently being investigated as part of the Geo-Mapping for Energy and Minerals (Energy) program Yukon Basins project: a) location of area of interest in northeastern British Columbia; b) major physiographic elements (after Bostock, 1970), rivers and line of section (A-A'); c) Line of section A-A' showing the range of topography, major physiographic elements and drainage features in the mapped area Location of photographs in Figures 2 to 4, shown as bold yellow numbers and letters (i.e., 2a-f, 3a-j, 4a-h).

processes in northeastern British Columbia (Figure 1a). Reconnaissance surficial geology mapping is focused on the Toad River (NTS 904N) and Maxhamish Lake (NTS 094O) map areas (Figures 1b and 1c). In this paper we present a regional overview of the bedrock and surficial geology, along with a geomorphic history interpreted from 16 sections representing the major physiographic elements and propose paleogeographic reconstructions for the map area from the last glacial maximum >18 C<sup>14</sup> ka BP (21.4 calendar ka BP) to the present.

## PHYSIOGRAPHY AND GEOLOGY OF THE STUDY AREA

The study area encompasses parts of a number of physiographic regions (Bostock, 1970). The northwestern limit of the Fort Nelson Lowland is generally below 530 m elevation (Figures 1b, 1c and 2a). The western Etsho Plateau lies between 600 to 740 m elevation (Figures 1b and 2b). The Maxhamish Escarpment (and Bovie Lake structure) range from 590 to 610 m elevation (Figures 1b, 1c and 2c). The Tsoo Tablelands, the northernmost part of the Alberta Plateau, reaches elevations up to 820 m (Figures 1b, 1c and 2d). The Liard Plateau rises from around 400 m west of the Maxhamish Escarpment to over 1200 m in the northwest of the map area (Figures 1b, 1c and 2e). In the Northern Rocky Mountains, southwest of the Liard and Toad rivers, some mountain peaks reach elevations over 2000 m (Figures 1b, 1c and 2f). The Liard, Toad, Scatter, Beaver, Crow, Dunedin, Petitot and Fort Nelson river valleys, with active flood plains at elevations generally below 320 m elevation, are incised into the landscape (Figures 1b, 1c and 3a to 3h).

The major landscape forms are controlled by bedrock characteristics and geological structures, and are modified by geomorphic processes over time. Lowland regions are underlain by shallowly dipping shale, siltstone and sandstone (Upper Cretaceous Kotaneelee Formation overlying Lower Cretaceous Fort St. John Group rocks) (Figures 4a, 4b). Folded and fault-bounded Lower Carboniferous (Mississippian) sandstone, natural gas-hosting sandstone (Mattson Formation) and limestone (Flett Formation), and Upper Cretaceous conglomerate, sandstone, carbonaceous shale and coal (Dunvegan and Wapiti formations) form escarpments, tablelands and plateaux (Figures 4c, 4d; Stott and Taylor 1968). West of the Bovie Lake structure, the Liard Basin is defined on the basis of thick Late Paleozoic and Cretaceous successions, and exploration targets the stratigraphically higher shale of the Exshaw Formation (Ferri et al., 2011a, 2011b). Folding and faulting, consistent with east to southeast crustal transpression, exposes Lower Mesozoic to Lower Paleozoic carbonate, shale and sandstone in the highest parts of the Liard Plateau (Figures 2e, 4e and 4f). South of the Liard River and west of Toad River, in the Northern Rocky Mountains (Figures 4e and

4f), Cretaceous and Triassic sedimentary rocks are folded and fault-bounded with Lower Paleozoic (Cambrian, Ordovician and Devonian) and Proterozoic carbonate and clastic sedimentary rocks (Ferri et al., 2011a, 2011b).

## SURFICIAL GEOLOGY OF THE STUDY AREA

Surficial earth materials and landforms were interpreted and mapped using 1:60,000 scale black-and-white stereo-pair air photos (e.g., 15BCB97010 series), free online Landsat 7 Pan-sharpened imagery and a Shuttle Radar Topography Mission 3-arc-second resolution DEM accessed through Global Mapper software, and base maps generated from CanVec shape files downloaded from the NRCAN GeoGratis website (<http://geogratis.cgdi.gc.ca/geogratis/> [URL 2011]; Huntley and Sidwell, 2010). Terrain polygons, landforms and other site symbols were digitized using commercially available computer software packages (Global Mapper, ArcMap and ArcGIS), edge-matched and rectified with published maps, reports and digital data (e.g., Bednarski, 2003a-c; Bednarski, 2005a, b; Clement et al., 2004).

Surficial deposits and landforms were described from more than 300 observation stations and waypoints digitally archived in the field and edited later in the office. Sixteen lithostratigraphic sections provide a sedimentary record of processes occurring in the major physiographic regions of the study area. Logged sections were located and measured with a handheld GPS unit and an altimeter during ground observation or logged remotely with the aid of oblique aerial and ground-level photographs (Figure 5). Surficial and stratigraphic units were distinguished from surrounding terrain on the basis of landform associations, earth material genesis, environment of deposition, sedimentology, morphology, texture, sorting, colour, thickness, degree of consolidation, physical limits, geological age, stratigraphic relationships and other distinguishing characteristics (Huntley and Hickin, 2010; Huntley and Hickin, 2011).

### *Etsho Plateau and Petitot River Valley*

In the Petitot River valley (Figure 6) up to 10 m of Laurentide till overlies glacially streamlined bedrock of the Fort St. John Group and, locally, advance-phase glaciolacustrine and glaciofluvial deposits preserved in buried paleochannels. Sub-till ice-thrust features in older glacial deposits suggest the Laurentide Ice Sheet overrode partly frozen sediments during its advance (cf. Boulton and van der Meer, J.J.M., 1999; Benediktsson et al., 2009). Till is unconformably overlain by 15 to 80 m of terraced deposits of glaciofluvial sand and gravel, colluvial diamictons and glaciolacustrine silt and clay graded to a glacial lake



Figure 2. Major physiographic regions of the study area (after Bostock, 1970): a) Fort Nelson Lowland; b) Etsho Plateau; c) Maxhamish Escarpment (Bovie Lake structure); d) Tsoo Tablelands (Alberta Plateau); e) Liard Plateau; f) Northern Rocky Mountains.

with a surface elevation of approximately 420 m. Multiple upward-fining sequences from diamicton to gravel to sand and silt are interpreted to represent changes in sediment supply and meltwater recharge related to periods of rapid lake drainage and impoundment controlled by retreating (and surging) ice lobes in the Petitot and Liard river valleys.

### ***Fort Nelson Lowland and Fort Nelson River Valley***

Laurentide till, 5-10 m thick, overlies glacially stream-lined Fort St. John Group and Dunvegan Formation rocks in the Fort Nelson River valley (Figure 7). Tributaries draining the Tsoo Tablelands are infilled with more than 30 m of glaciolacustrine clay, silt, sand and diamicton, deposited when the retreating Laurentide Ice Sheet in the Fort Nelson River valley impounded a glacial lake with a surface

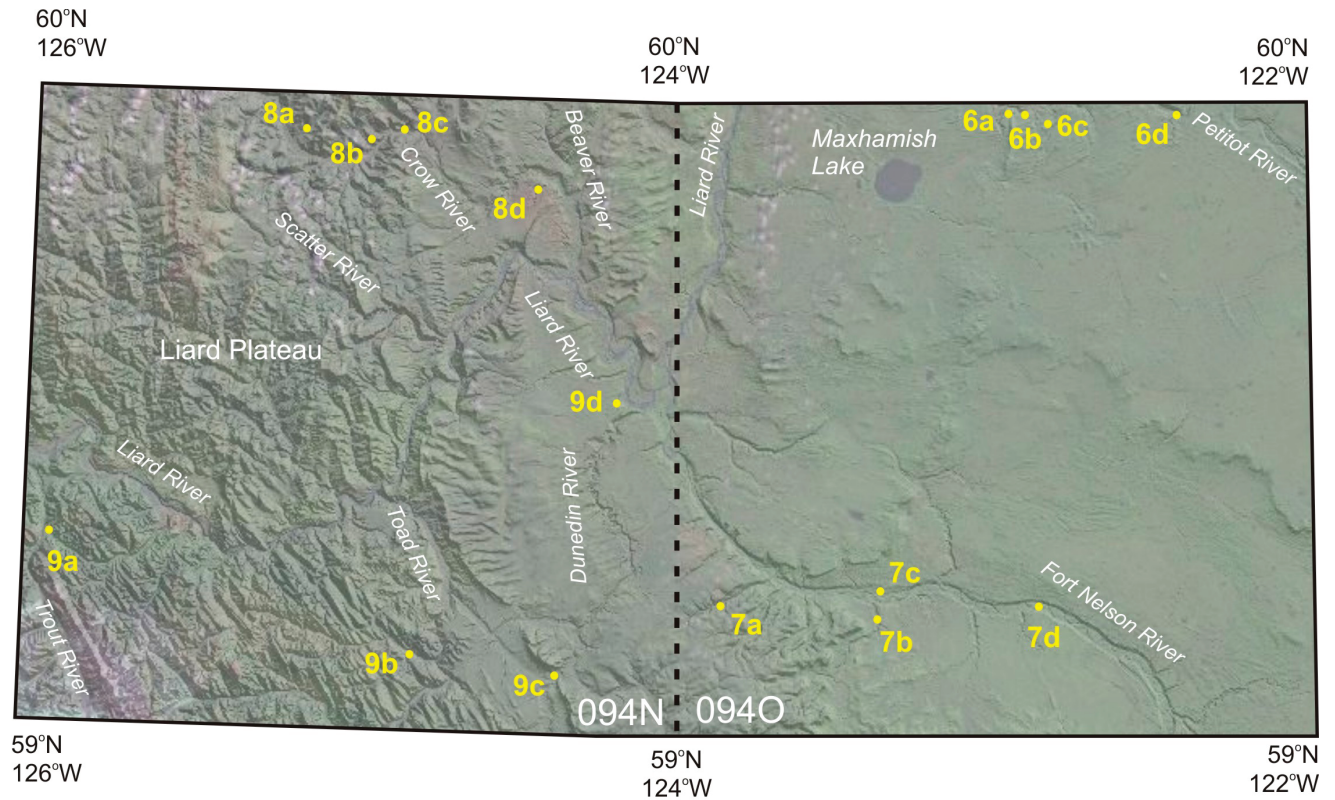


Figure 3. Major rivers in the study area: a) Trout River; b) Liard River; c) Toad River; d) Scatter River; e) Beaver River; f) Crow River; g) La Biche River; h) Dunedin River; i) Petitot River; and j) Fort Nelson River.



Figure 4. Geological overview of the study area: a) landslide involving till, siltstone and shale of the Fort St. John Group, Etsho Plateau; b) 3-5 m of Laurentide till overlying siltstone and shale of the Fort St. John Group, Fort Nelson Lowland; c) Carboniferous Flett Formation limestone with glacial striae indicating Laurentide iceflow towards 248°, Maxhamish Escarpment (Bovie Lake structure); d) Dunvegan sandstone and quartz-pebble conglomerate forming an escarpment of the Tsoo Tablelands; e) Till, glaciofluvial sediments and organic deposits blanket Upper Cretaceous clastic sedimentary rocks west of the Bovie Lake structure, in the vicinity of Maxhamish Lake, Liard Plateau; f) broad anticlinal-synclinal folds developed in Carboniferous to Triassic rocks, Liard Plateau; g) mid-Cretaceous and Triassic sequences, Cordilleran glaciers flowed southeast following the structural grain of the valleys, Northern Rocky Mountains; h) intensely folded and faulted Devonian, Ordovician, Cambrian and Proterozoic carbonate and clastic sedimentary rocks, Northern Rocky Mountains.





### Facies codes

Fm silt and clay, massive  
 Fl silt and clay, laminated  
 Fd silt and clay, with dropstones  
 Sm sand, massive  
 Sp sand, planar-bedded  
 Sr sand, ripple-bedded  
 St sand, trough-cross-bedded

Gm gravel, massive  
 Gp gravel, planar bedded  
 Gt gravel, trough-cross-bedded  
 Bm boulder, massive

Dmm diamicton, matrix-supported, massive  
 Dms diamicton, matrix-supported, stratified  
 Dcm diamicton, clast-supported, massive  
 Dcs diamicton, clast-supported, stratified

### Texture

d mixed fragments  
 b boulders  
 g gravel  
 s sand  
 z silt  
 c clay

### Lithostratigraphic units




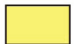








 Organic	 Glaciolacustrine	 Bedrock
 Alluvial	 Glaciofluvial	 Iceflow (Cordilleran)
 Eolian	 Laurentide till	 Iceflow (Laurentide)
 Colluvial	 Cordilleran till	 Paleocurrent

Figure 5. Location map and legend for facies codes, textures, lithostratigraphic units and paleoflow indicators appearing on graphic logs of sections in Figures 6 to 9. Holocene deposits include organic and alluvial units; eolian and colluvial deposits are Late Pleistocene to early Holocene in age; tills are late Pleistocene (Late Wisconsinan) deposits; bedrock in the map area ranges from Proterozoic to early Tertiary in age.

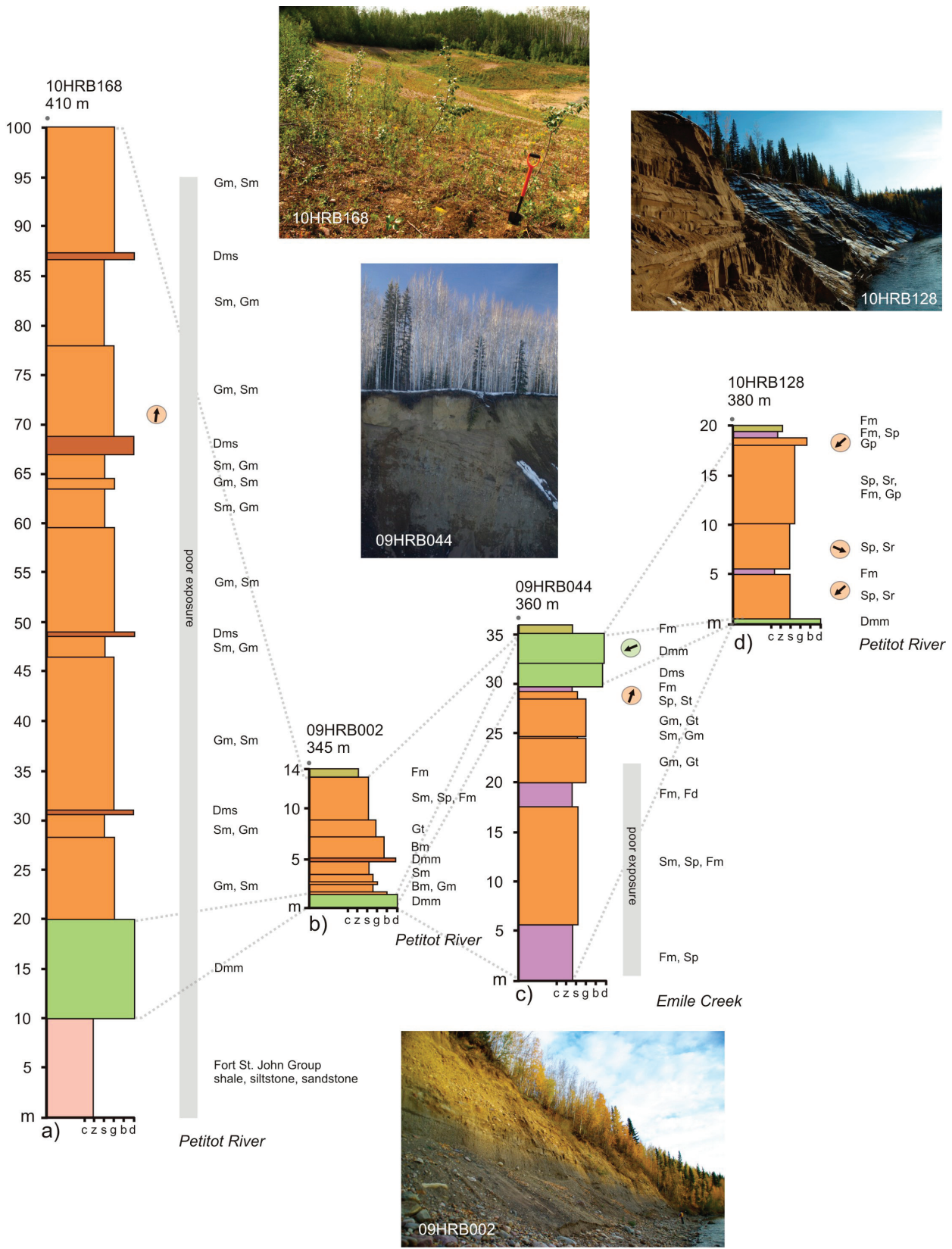


Figure 6. Graphic logs and station photographs for stratigraphic sections along the Petitot River and tributaries cutting across the Etsho Plateau. Logged profiles are measured from the top down, and each show the station identifier and surface elevation. Locations of logs a-d are shown in Figure 5.

ranging from 720 m to 540 m elevation. Multiple cycles of upward fining from diamicton to sand, silt and clay indicate that lakes periodically infilled then drained in response to retreating ice margins. Eolian-reworked glaciolacustrine sediments are deposited up to an elevation of 420 m in the Fort Nelson Lowland and parabolic dunes indicate katabatic winds flowed to the southeast. Glaciofluvial terraces graded to 300 m elevation, comprising sand and gravel 10-20 m thick, are confined to the spillway channel of the Fort Nelson River. Terrace and bedrock scarps are draped by a discontinuous veneer of colluvium resulting from debris slides, slumps and flows triggered by fluvial incision of the modern channel.

### ***Liard Plateau and Crow River Valley***

Sections along the Crow River valley record the transition from Cordilleran to Laurentide deposition and erosion (Figure 8). Cordilleran tills rest on glacially streamlined Paleozoic and Mesozoic bedrock: roches moutonnées and drumlins indicate a lobe of the Cordilleran Ice Sheet flowed southeast into the Crow River valley from the Liard River valley in southeast Yukon. Laurentide tills rest on the streamlined Toad Formation and were deposited by continental ice flowing northwest. Glaciofluvial outwash terraces contain clasts of predominantly Cordilleran provenance; although rare granitic erratics indicate some reworking of Laurentide tills and outwash at the terminal limit of continental ice. Multiple upward-fining cycles of boulder-rich gravel fining to sand, silt and clay indicate changes in sediment supply and meltwater discharge, and periodic drainage and refilling of a proglacial lake confined by retreating ice margins in the valleys of the Liard, Crow and Beaver rivers. Outwash and glacial lake deposits are graded to elevations from 620 m to 420 m. Loess and parabolic dunes mantle glaciolacustrine deposits, tills and bedrock, and indicate southeast katabatic wind flow from the remnants of Cordilleran Ice Sheet on the Liard Plateau.

### ***Northern Rocky Mountains, Toad, Dunedin and Liard River valleys***

Cordilleran and Laurentide conditions and the formation of an extensive retreat-phase glacial lake system in the major valleys are also recorded in logged sections of valleys draining the Northern Rocky Mountains and the southern Liard Plateau (Figure 9). Cirque basins are confined to the southwest of the map area and record the presence of a local accumulation centre in the Trout River watershed (cf. Mathews, 1980). Valley glaciers from this accumulation centre were confluent with the Liard lobe of the Cordilleran Ice Sheet. An upper limit to montane glaciation of 1800-2000 m elevation is inferred from the distribution of

Cordilleran tills and features in valleys south of the Liard Plateau. Glacial striae and streamlined bedrock on glaciated mountain summits below this limit indicate that Cordilleran ice flowed southeast, parallel to the structural grain of the Northern Rocky Mountains, and obliquely to west-flowing Laurentide ice. The zone of confluence between the two ice sheets is interpreted to lie along the axis of the Toad River valley. West of Toad River, basal surficial units in valleys contain clasts with Cordilleran provenances. On the Liard Plateau to the east, Laurentide tills were deposited over glacially streamlined clastic sedimentary rocks of the Kotaneelee Formation. Cordilleran and Laurentide tills are conformably overlain by outwash, colluvial and glaciolacustrine deposits that are a record of retreating ice sheet margins and inundation of valleys by proglacial lakes in the Liard River basin with stable surfaces at elevations of approximately 720 m, 640 m, 540 m and 420 m.

## **PALEOGEOGRAPHIC RECONSTRUCTIONS OF THE STUDY AREA**

Paleogeographic reconstructions presented here are based on a preliminary interpretation of earth surface materials, landforms and geomorphic processes observed in the Toad River and Maxhamish Lake map areas. The distinctive landscape of this area is largely a product of underlying bedrock and geological structures, with ornamentation by Late Wisconsinan ice sheets, ice fields and valley glaciers (equivalent to the Fraser Glaciation in British Columbia and the McConnell Glaciation in the Yukon). The landscape evolution model spans the period from the end of the last glacial maximum  $>18 \text{ C}^{14} \text{ ka}$  ( $>21.4 \text{ calendar ka}$ ) to the Present. The chronology presented is relative, but is constrained by radiocarbon dates on organic material and cosmogenic ages of glacial erratics in adjacent areas (e.g., Mathews, 1980; Rampton, 1987; Rutter et al., 1993; Lemmen et al., 1994; Duk-Rodkin and Lemmen, 2000; Smith, 2000, 2002; Bednarski and Smith, 2007; Bednarski, 2008; Hartman and Clague, 2008; Trommelen and Levson, 2008; Demchuk, 2010a, b).

### ***Glacial Maximum ( $>18 \text{ C}^{14} \text{ ka}$ [ $>21.4 \text{ calendar ka}$ ])***

As continental ice advanced into the region, the Tsoo Tablelands and the Maxhamish Escarpment formed barriers to westward meltwater drainage. Glacial lakes became impounded in paleovalleys east of the escarpment and were infilled with sand and gravel outwash (Figure 6c). The Laurentide and Cordilleran ice sheets subsequently overrode and deformed local ice sources, glacial lakes and advance-phase deposits. At the glacial maximum ( $>18 \text{ ka}$ ), the two ice sheets were confluent, and the Cordilleran Ice Sheet was

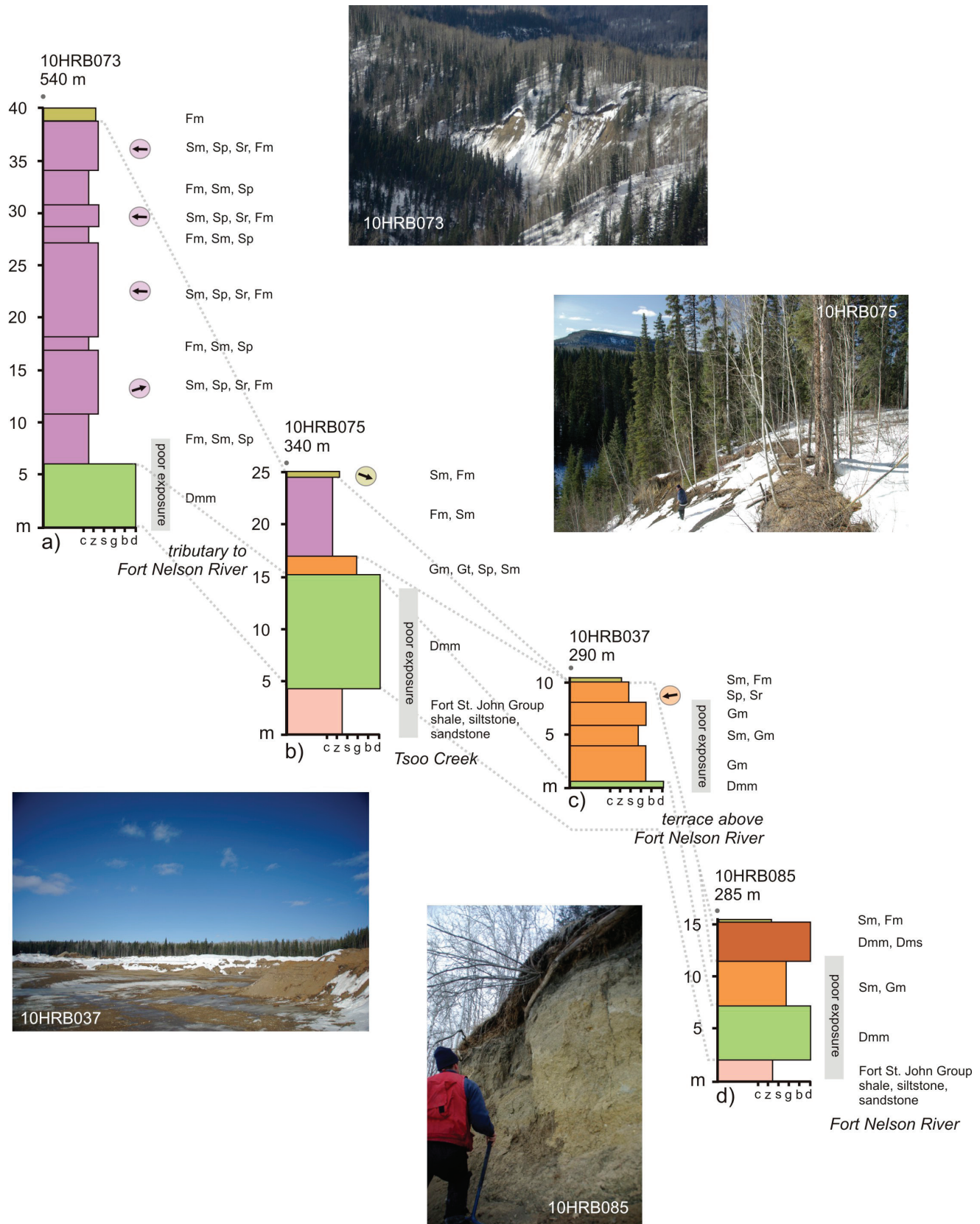


Figure 7. Graphic logs and station photographs for stratigraphic sections along the Fort Nelson River cutting across the Fort Nelson Lowland. Logged profiles are measured from the top down, and each show the station identifier and surface elevation. Locations of logs a-d are shown in Figure 5.

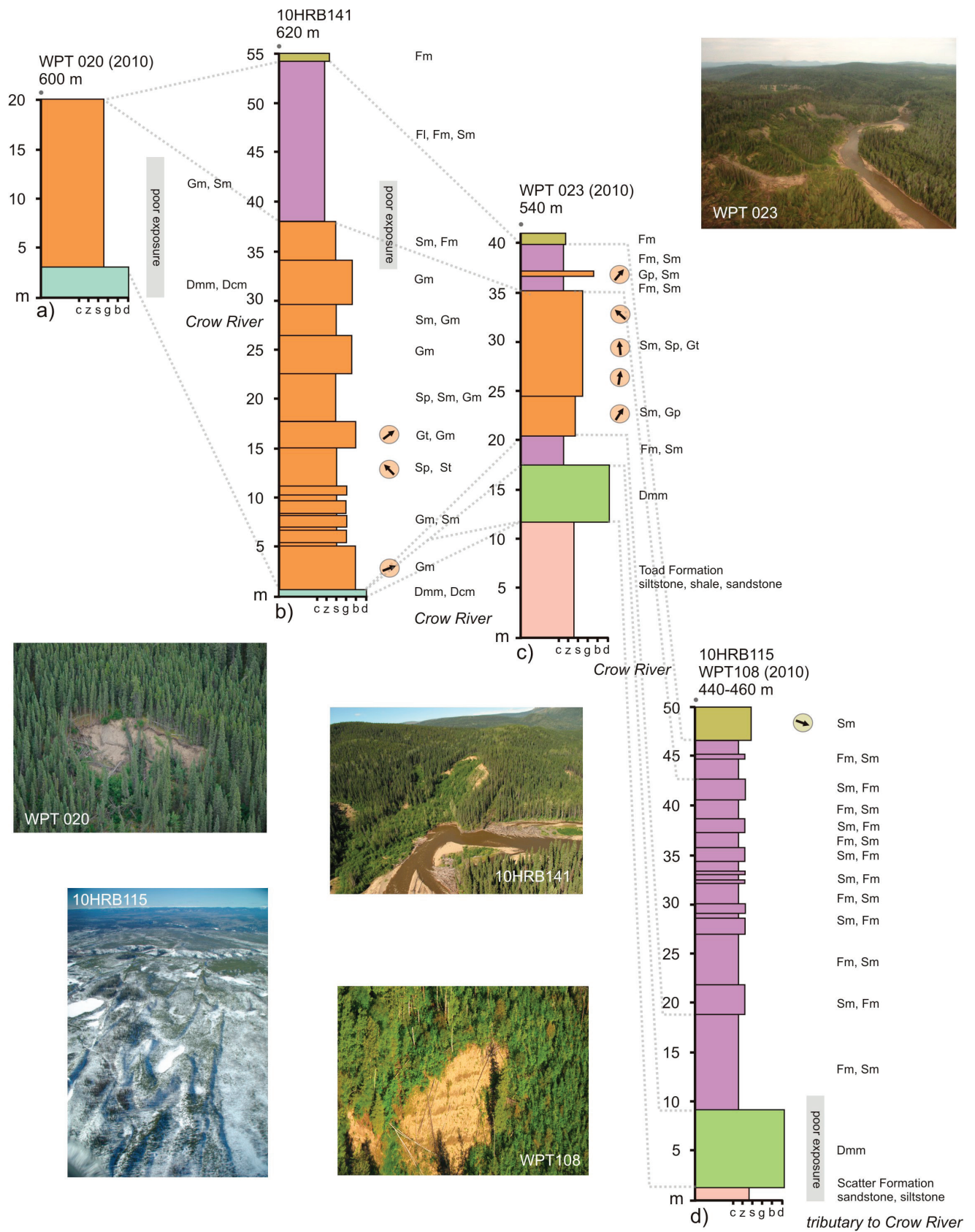


Figure 8. Graphic logs and station photographs for stratigraphic sections along the Crow River cutting across the northern Liard Plateau. Logged profiles are measured from the top down, and each show the station identifier and surface elevation. Locations of logs a-d are shown in Figure 5.

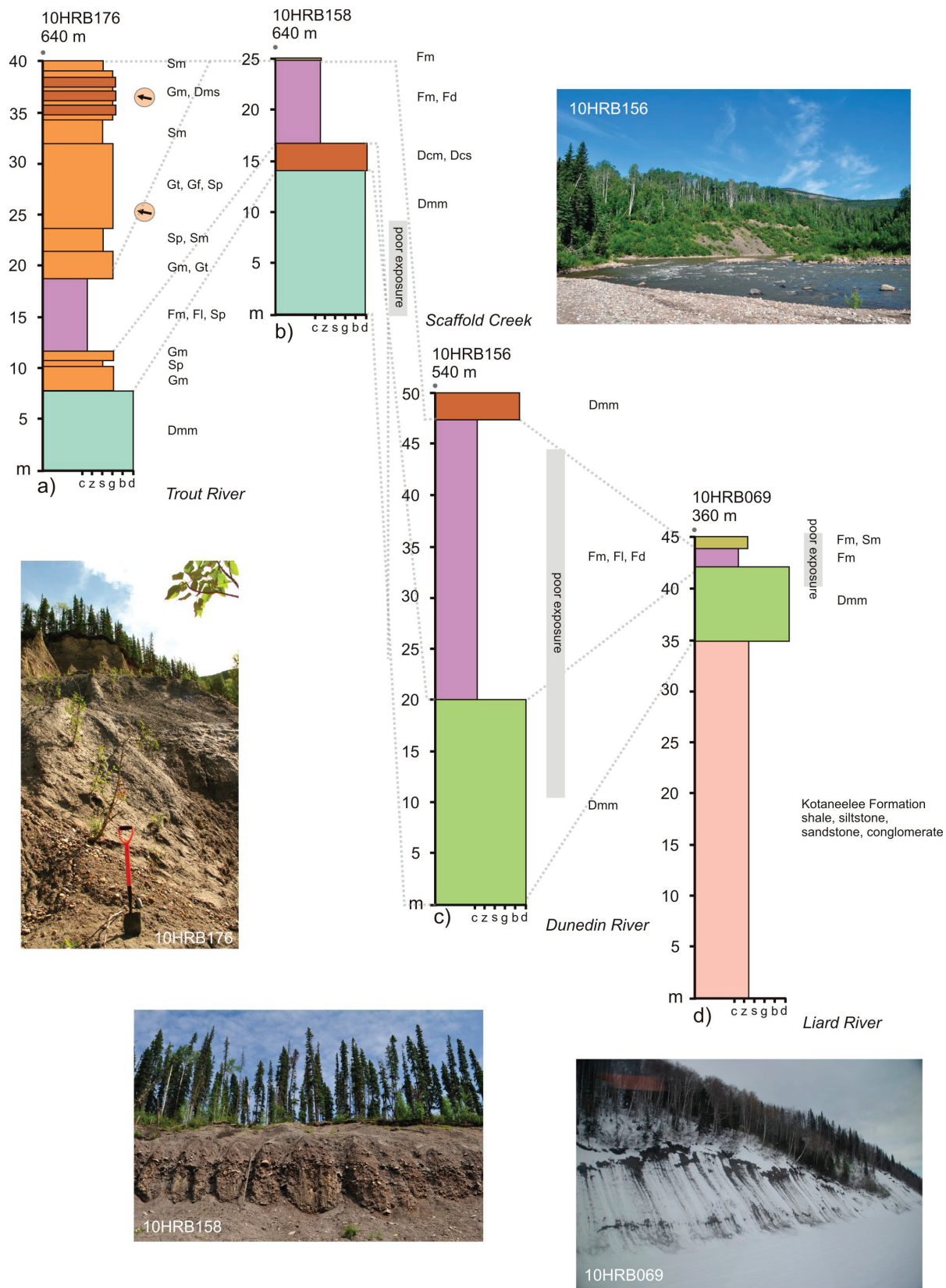


Figure 9. Graphic logs and station photographs for stratigraphic sections in tributaries to the Liard River in the Northern Rocky Mountains and southern Liard Plateau. Logged profiles are measured from the top down and each show the station identifier and surface elevation. Locations of logs a-d are shown in Figure 5.

deflected to the southeast by southwest flowing Laurentide ice (Figure 10). Topography and drainage patterns were greatly modified during the phase of maximum ice cover. Drift thicknesses in excess of 2-5 m are observed in major valleys and it is suspected that similar drift thicknesses blanket bedrock across the area (Figures 6 to 9). Laurentide tills have low clast contents (<20%) of proximally derived Cretaceous siliciclastic sedimentary rocks and distal exotic igneous and metamorphic clasts from the Canadian Shield exposed hundreds of kilometres to the northeast. Cordilleran tills have higher clast contents (>30%), and contain proximally derived Cretaceous siliciclastic sedimentary rocks and distal exotic igneous clasts from undefined montane sources in the west.

Bedrock had an important influence on the iceflow dynamics: the presence of weak siliciclastic bedrock would have resulted in deformable, lubricated conditions beneath Cordilleran and Laurentide ice (Mathews, 1974; Boulton, 1987; Fisher et al., 1995; Stokes and Clark, 2001; van der Meer et al., 2003). Glacially sculpted landforms up to several kilometres in length (drumlins, fluted till ridges and furrows) imply tills were deposited beneath active, wet-based ice sheets that were prone to fast-flowing and, or surging conditions (cf. Ross et al., 2009; Cofaigh, et al., 2010; Shaw et al., 2010). Drumlins in the western Liard Plateau indicate that Cordilleran ice flowed southeast toward the Liard and Toad River valleys, where it was confluent with glaciers flowing from cirques in the Northern Rocky Mountains. Continental ice (and subglacial meltwater) flowed from the northeast and southeast, and then continued westward into the Liard River basin and southwest over the Tsoo Tablelands towards the Northern Rocky Mountains (Figure 10). Drumlinized terrain is most pronounced south of the Petitot River and west of the Maxhamish Escarpment where ice flowed up-hill, and thick accumulations of till were deposited over soft bedrock and unconsolidated advance-phase sediments. Maxhamish Lake and numerous smaller basins were excavated by erosion and ice-thrusting when Laurentide ice and subglacial meltwater scoured and deformed older glacial deposits and weak bedrock (Figure 6c).

***Deglaciation (>18 C<sup>14</sup> ka [ >21.4 calendar ka] to 10 C<sup>14</sup> ka [ca. 12 calendar ka])***

Deglaciation began sometime after 18 ka, with retreating Laurentide and Cordilleran ice sheets, stagnant ice masses and landslide debris blocking and reordering regional drainage (Figures 3d, 11a to 11j). The mapped distribution of moraine ridges implies that ice margins receded to the northeast in the Petitot River valley and to the southeast in the Fort Nelson River valley (Huntley and Hickin, 2011). Some large end moraines are deformed and streamlined suggesting that receding lobes remained active during retreat and occasionally surged (Figures 11a to

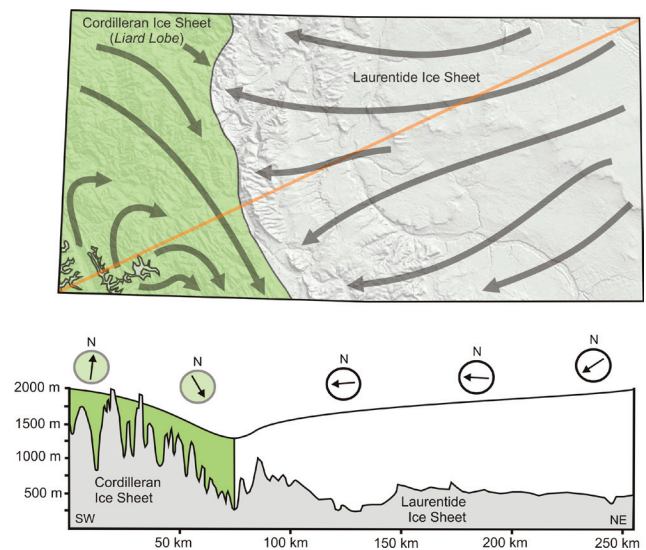


Figure 10. Greater than 18 C<sup>14</sup> ka before Present (>21.4 calendar ka BP), upper limit to the Cordilleran Ice Sheet approximately 1800 m, terminal limit to Laurentide Ice Sheet approximately 1250 m elevation.

11j). Minor moraine ridges drape drumlins in cross cutting patterns, and are interpreted as crevasse fillings and minor moraines deposited shortly after surging and drumlinization ended, or as ice retreated from the map area (Sharp, 1985; Bednarski 2008; Figure 3i).

Hummocky till associated with short segments of sub-aerial subglacial meltwater channels and eskers indicate that bodies of stagnant glacier ice remained in lowland areas on either side of the Maxhamish Escarpment and the Etsho Plateau. Eskers are composed of hummocky till and glaci-ofluvial gravelly sand, and likely exploited pre-existing crevasse patterns beneath the retreating ice sheet or stagnant ice bodies (Boulton et al., 2009; Utting et al., 2009). An extensive system of proglacial lakes was created in the Liard, Fort Nelson and Petitot river valleys, linked by spillways that drained meltwater into the Liard River valley and then northward into the Mackenzie River basin between 18 and 10 ka (Bednarski, 2008). In the map area, glaciolacustrine deposits and meltwater channel outlets incised into till and bedrock indicates that proglacial lakes had surface elevations of approximately 840 m, 720 m, 620 m, 540 m, 420 m, 380 m and <300 m throughout this interval (Figures 11a to 11k).

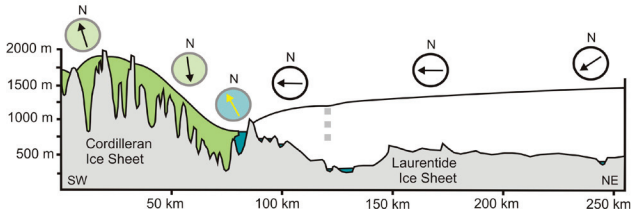
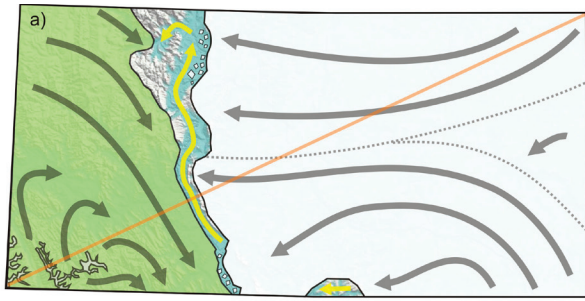


Figure 11 a) Greater 18 C<sup>14</sup> ka BP (21.4 calendar ka BP) to 13.5 C<sup>14</sup> ka BP (16.2 cal ka BP), early deglaciation, ice-marginal glacial lake still-stand elevation approximately 840 m.

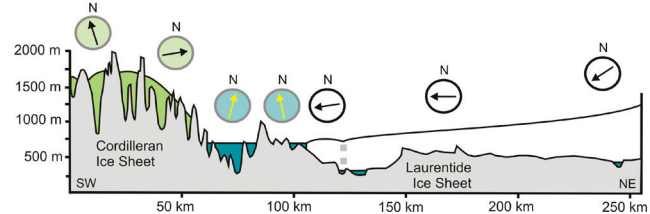
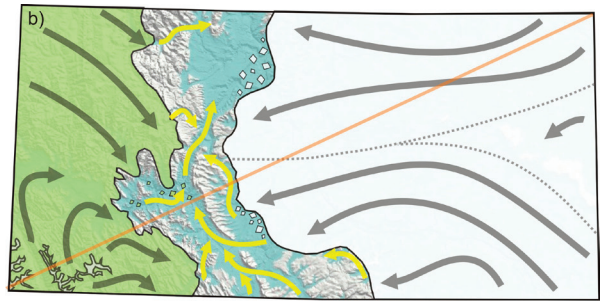


Figure 11 b) 13 C<sup>14</sup> ka BP (15.6 calendar ka BP) to 12.5 C<sup>14</sup> ka BP (15.2-14.4 calendar ka BP), Glacial Lake Liard still-stand elevation approximately 720 m.

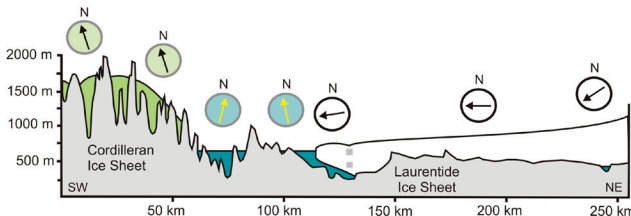
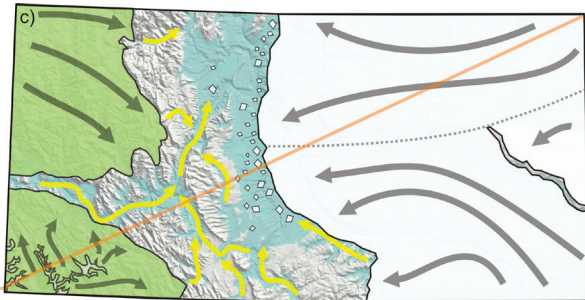


Figure 11 c) 12.5 C<sup>14</sup> ka BP (15.2-14.4 calendar ka BP) to 12 C<sup>14</sup> ka BP (14.1 calendar ka BP), Glacial Lake Liard still-stand elevation approximately 620 m.

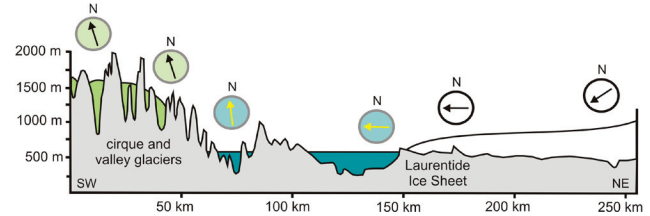
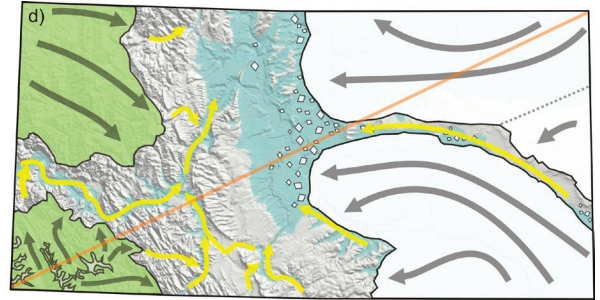


Figure 11 d) 12 C<sup>14</sup> ka BP (14.1 calendar ka BP) to 11.5 C<sup>14</sup> ka BP (13.45 calendar ka BP), Glacial Lake Liard still-stand elevation approximately 540 m.



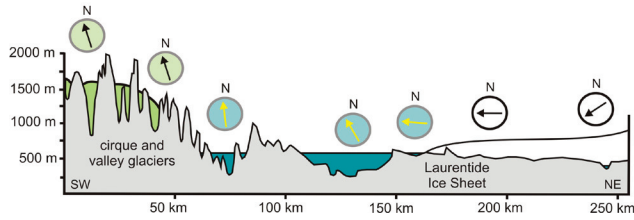
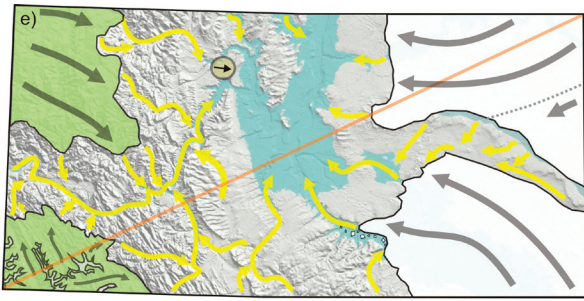


Figure 11e) 11.5 C<sup>14</sup> ka BP (13.45 calendar ka BP) to 11 C<sup>14</sup> ka BP (13 calendar ka BP), Glacial Lake Liard and Glacial Lake Fort Nelson still-stand elevation approximately 420 m.

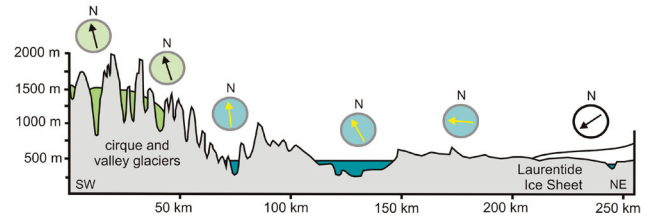
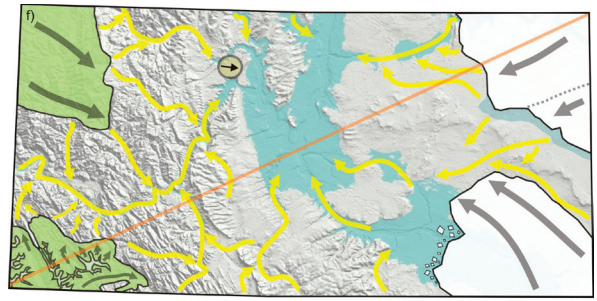


Figure 11f) 11.5 C<sup>14</sup> ka BP (13.45 calendar ka BP) to 11 C<sup>14</sup> ka BP (13 calendar ka BP), Glacial Lake Liard and Glacial Lake Fort Nelson still-stand elevation approximately 420 m.

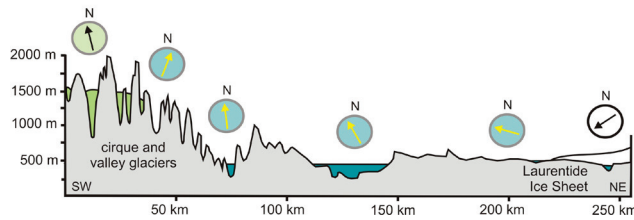
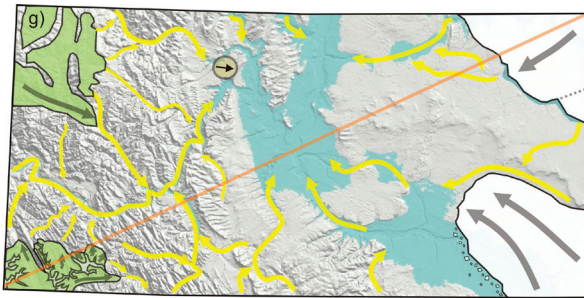


Figure 11g) 11.5 C<sup>14</sup> ka BP (13.45 calendar ka BP) to 11 C<sup>14</sup> ka BP (13 calendar ka BP), Glacial Lake Liard and Glacial Lake Fort Nelson still-stand elevation approximately 420 m.

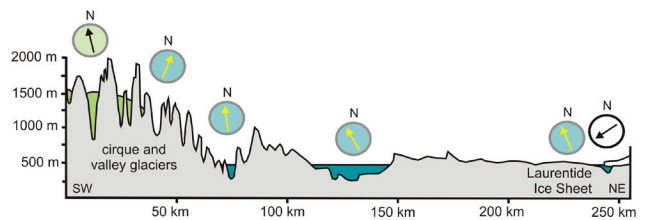
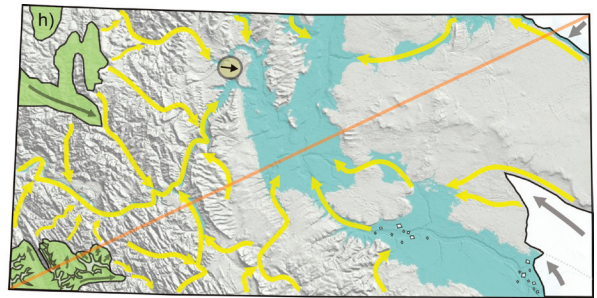


Figure 11h) 11.5 C<sup>14</sup> ka BP (13.45 calendar ka BP) to 11 C<sup>14</sup> ka BP (13 calendar ka BP), Glacial Lake Liard and Glacial Lake Fort Nelson still-stand elevation approximately 420 m;

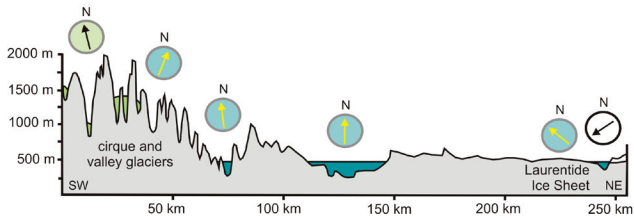
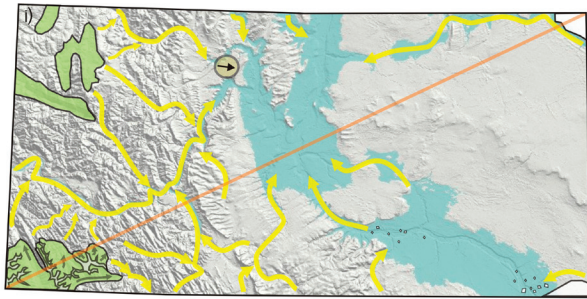


Figure 11i) 11.5  $C^{14}$  ka BP (13.45 calendar ka BP) to 11  $C^{14}$  ka BP (13 calendar ka BP), Glacial Lake Liard and Glacial Lake Fort Nelson still-stand elevation approximately 420 m

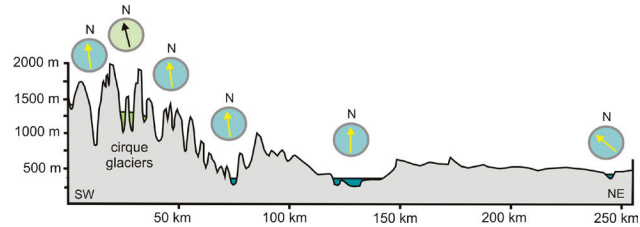
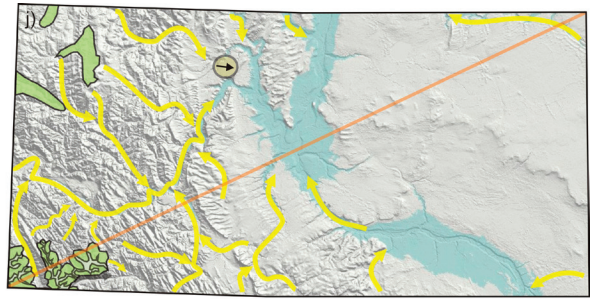


Figure 11j) 11  $C^{14}$  ka BP (13 calendar ka BP) to 10.5  $C^{14}$  ka BP (12.65 - 12.75 calendar ka BP), Glacial Lake Liard and Glacial Lake Fort Nelson still-stand elevation approximately 380 m.

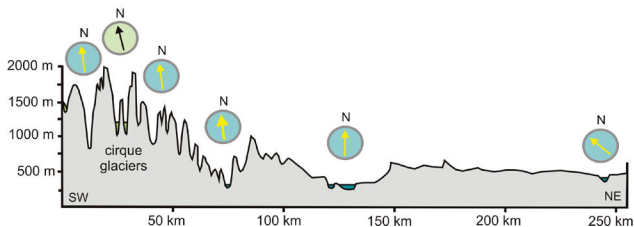
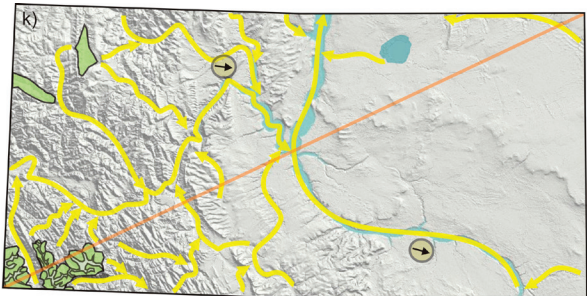


Figure 11k) 10.5  $C^{14}$  ka BP (12.65 - 12.75 calendar ka BP) to 10  $C^{14}$  ka BP (11.95 - 12.05 calendar ka BP), Liard and Fort Nelson spillways draining into Glacial Lake Mackenzie with a surface elevation less than 300 m.

### ***Post-glaciation (10 $C^{14}$ ka [ca. 12 calendar ka] to Present)***

After 10 ka, changes in regional base-level led to episodes of channel incision and aggradation, resulting in the formation of drift terraces along most stream and river valleys (Figure 12). In the early Holocene, pulses of fluvial terrace building followed initial valley incision by the Liard, Toad, Fort Nelson, Petitot and other major rivers. Most streams and rivers have alluvial terraces <5 m above active floodplains consisting of gravel overlain by silt and sand. Poorly drained clay-rich till on the plateaus and glaciolacustrine sediments in lowland areas are covered by extensive postglacial peat deposits and fens. Discontinuous permafrost is sporadically encountered in glaciolacustrine and some peat deposits. Charcoal, observed in dug pits on alluvial terraces, suggest forest fires may have contributed to periods of landslide activity on slopes and local fluvial aggradation. Landslides and colluviated deposits are common where bedrock outcrops form escarpments, and where shale or fine-grained glacial deposits are exposed along steep cutbanks. Stream networks draining lowland and plateau watersheds are disrupted by beaver activity, and to a lesser extent where roads, pipelines and other infrastructure cross streams, rivers and organic deposits (Huntley and Hickin, 2010; Huntley and Hickin, 2011).

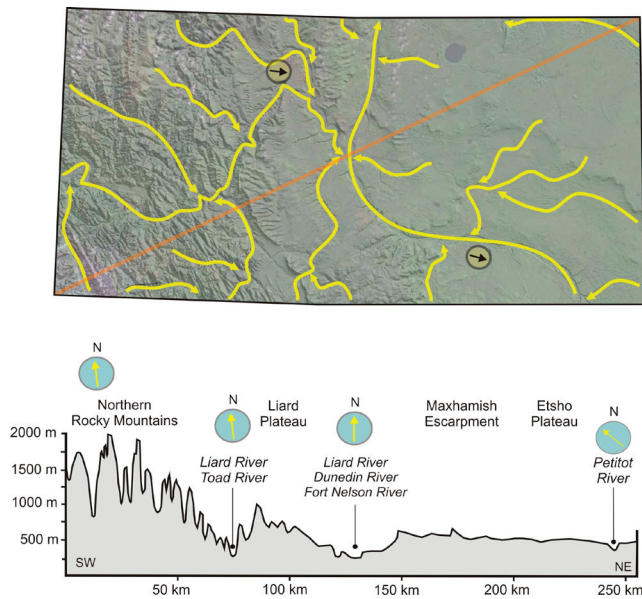


Figure 12. 10 C<sup>14</sup> ka BP (11.95 - 12.05 calendar ka BP) to Present; modern drainage network established.

## SUMMARY AND FURTHER RESEARCH

Knowledge of the extent and iceflow patterns of the Laurentide and Cordilleran ice sheets; the distribution of glaciofluvial and glaciolacustrine deposits, meltwater features and drainage directions; the distribution of colluvial deposits, landslides and permafrost; and the extent and nature of eolian deposits is critical to reduce the risks for exploration of energy, mineral and forest resources, sustainable long-term investment and economic development in northeastern British Columbia (Huntley and Hickin, 2010; Huntley and Hickin, 2011). The public geoscience data model created as part of the GEM-Energy Yukon Basins project is an important source of information for targeted exploration of granular aggregate, frac sand and groundwater resources; recognizing geological hazards that could influence surface engineering practices (e.g., road design, well pad locations, pipeline and power-line routing); understanding the long-term impacts of climate change on landscape evolution; land management decisions on energy and mineral resource development in the region; and e) innovative geoscience initiatives to encourage community engagement (e.g., Figure 13; Huntley, 2010).

New insights into the glacial history and paleogeography of the Toad River (NTS 094N) and Maxhamish Lake (NTS 094O) map areas (Figures 10 to 12) are provided by the regional-scale overview of the bedrock geology, surficial earth materials and landforms presented here (Figures 1 to 9). The distinctive landscape of northeastern B.C. is (in part) the product of the Late Wisconsinan Glaciation, beginning >18 C<sup>14</sup> ka (21.4 calendar ka) and terminating in this region at approximately 10 C<sup>14</sup> ka (ca. 12 calendar ka) before present. Topography and drainage patterns were greatly modified during the last glaciation. Underfit modern

ivers occupy Late Pleistocene glacial spillways that drained into the Liard River basin (Figure 3). Maxhamish Lake and numerous smaller basins were excavated when ice sheets and subglacial meltwater scoured older glacial deposits and weak bedrock (Figures 2 to 4). During deglaciation, and into the Holocene, changes in regional base-level led to episodes of channel incision and aggradation, resulting in the formation of terraces along most stream and river valleys (Figures 6 to 9). Forest fires may have been a key trigger for landslide activity on slopes. Watersheds are prone to disruption by beavers, and to a lesser extent, by humans.

Based on remote predictive mapping and field observations from 2003 to 2010, our landscape evolution model is geomorphologically robust, although the details and interpretations may change as new information is acquired. Results are pending for litho geochemistry and sedimentological analyses on glacial erratic boulders, potential frac sand sources and granular aggregates sampled in 2009 and 2010 (Hickin and Huntley, 2011). A future research focus should be to improve the age control of events and



Figure 13 Scatter River Fly Camp (2010): the original work in acrylic (by D.H. Huntley) is a 10x16 inch canvas that resides in a private collection. The painting depicts a joint BC Ministry of Energy and GSC summer field camp at the base of large trans-lacustrine bedrock slide involving failure of Paleozoic and Mesozoic clastic sedimentary rocks; successively lower terraces in the valley are related to the periodic blockage of the valley by landslides downstream (see also Figure 3d).

place the relative sequence of events presented here in regional chronolithostratigraphical context. Further, detailed investigation of bedrock and drift sections in the Liard, Toad and Dunedin river valleys; exposures in borrow pits and other anthropogenic sites; and at elevation is required to collect samples for detailed sedimentological analyses, organic material for radiocarbon dating, or to obtain optically stimulated luminescence dates and cosmogenic ages on sand (loess) dunes and large erratic boulders on mountain tops and ridges. Another focus could be the application of our digital surficial geology data model to other methods of drift exploration, including LiDAR, seismic shothole records, petrophysical logs, auger drilling, test pitting, ground-penetrating radar and airborne electromagnetic surveys (cf. Best et al., 2004; Levson et al., 2004; Smith et al., 2006; Hickin et al., 2008; Smith and Lesk-Winfield, 2009).

## ACKNOWLEDGMENTS

Our work in the region has benefitted from past collaboration with Travis Ferbey (BC Ministry of Forests, Mines and Lands) and Tania Demchuk (BC Ministry of Natural Resource Operations), Jan Bednarski (GSC-Pacific), Rod Smith (GSC-Calgary), Roger Paulen and Alain Plouffe (GSC-Ottawa). Derek Brown, Lauren Wilson and Lisa Fodor were able assistants during reconnaissance fieldwork in 2009 and 2010. Catherine Sidwell reviewed an early version of the manuscript. Thanks also to Deh Cho (Great Slave) Helicopters and the hamlet of Fort Liard, NWT for logistical support during the 2009 and 2010 field seasons.

## REFERENCES

- Adams, C. (2009): Summary of shale gas activity in Northeast British Columbia, 2008/09; *BC Ministry of Energy, Petroleum Geology Open File 2009-1*, page 17.
- Adams, C. and Schwabe, M. (2009): British Columbia oil and gas exploration activity report; in Activity Report 2007-2008, *BC Ministry of Energy*, pages 7-15.
- Bednarski, J.M. (2003a): Surficial geology of Fort Liard, Northwest Territories-British Columbia; *Geological Survey of Canada*, Open File 1760, scale 1:50 000.
- Bednarski, J.M. (2003b): Surficial geology of Lake Bovie, Northwest Territories-British Columbia; *Geological Survey of Canada*, Open File 1761, scale 1:50 000.
- Bednarski, J.M. (2003c): Surficial geology of Celibeta Lake, Northwest Territories-British Columbia; *Geological Survey of Canada*, Open File 1754, scale 1:50 000.
- Bednarski, J.M. (2005a): Surficial Geology of Etsine Creek, British Columbia; *Geological Survey of Canada*, Open File 4825, scale 1:50 000.
- Bednarski, J.M. (2005b): Surficial Geology of Gote Creek, British Columbia; *Geological Survey of Canada*, Open File 4846, scale 1:50 000.
- Bednarski, J.M. (2008): Landform assemblages produced by the Laurentide Ice Sheet in northeastern British Columbia and adjacent Northwest Territories – constraints on glacial lakes and patterns of ice retreat; *Canadian Journal of Earth Sciences*, Volume 45, pages 593-610.
- Bednarski, J.M. and Smith, I.R. (2007): Laurentide and montane glaciation along the Rocky Mountain Foothills of northeastern British Columbia; *Canadian Journal of Earth Sciences*, Volume 44, pages 445-457.
- Benediktsson, Í.Ö., Ingólfsson, Ó, Schomacker, A. and Kjær, K. (2009): Formation of submarginal and proglacial end moraines: implications of ice-flow mechanisms during the 1963-64 surge of Brúarjökull, Iceland; *Boreas*, Volume 38, pages 440-457.
- Best, M.E., Levson, V. and McConnell, D. (2004): Sand and gravel mapping in northeast British Columbia using airborne electromagnetic surveying methods; in Summary of Activities, *BC Ministry of Energy*, pages 1-6.
- Bostock, H.S. (1970): Physiographic regions of Canada; *Geological Survey of Canada*, Map 1254A, scale 1:5 000 000.
- Boulton, G.S. (1987): A theory of drumlin formation by subglacial deformation; in Drumlins: A Symposium, Menzies, J. and Rose, J. Editors, *Balkema*, pages 25-80.
- Boulton, G.S., Hagdorn, M., Maillot, P.B., and Zatzepin, S. 2009. Drainage beneath ice sheets: groundwater-channel coupling, and the origin of esker systems from former ice sheets. *Quaternary Science Reviews*, Vol. 28, pp. 621-638
- Boulton, G.S. and van der Meer, J.J.M. (1999): The sedimentary and structural evolution of a recent push moraine complex: Holmströmbreen, Spitsbergen; *Quaternary Science Reviews*, Volume 18, pages 339-371.
- Cofaigh, C.Ó., Evans, J.A. and Smith, I.R. (2010) Large-scale reorganization and sedimentation of terrestrial ice streams during late Wisconsinan Laurentide Ice Sheet deglaciation; *Geological Society of America Bulletin*, Volume 122, pages 743-756.
- Clement, C., Kowall, R. Huntley, D and Dalziel, R. (2004): Ecosystem units of the Sahtaneh area; *Slocan Forest Products* (Fort Nelson), 39 pages and appendices.
- Demchuk, T.E. (2010a): Surficial Geology of the Komie Creek area (NTS 94P/05); *British Columbia Ministry of Energy, Mines and Petroleum Resources*, Open File 2010-08; *Geological Survey of Canada Open File 6568*, scale 1:50 000.
- Demchuk, T.E. (2010b): Surficial geology of the Komie Creek map area and an investigation of an ice-contact glaciofluvial delta, northeast British Columbia (NTS 94P/05); *unpublished M.Sc. thesis*, University of Victoria, 266 pages.
- Duk-Rodkin, A. and Lemmen, D.S. (2000): Glacial history of the Mackenzie region; in The Physical Environment of the Mackenzie Valley, Northwest Territories: A Base Line for the Assessment of Environmental Change. Dyke, L.D. and Brooks, G.R., Editors, *Geological Survey of Canada*, Bulletin 547, pages 11-20.

- Ferri, F., Hickin, A. and Huntley, D. (2011a): Bedded massive sulphide horizons (SEDEX) in upper Besa River Formation, western Liard Basin, British Columbia. in Geological Fieldwork 2010, *BC Ministry of Forests, Mines and Lands*, Paper 2011-1, pages 13-29.
- Ferri, F., Hickin, A.S. and Huntley, D.H. (2011b): Besa River Formation, western Liard Basin, British Columbia (NTS 094N): Geochemistry and regional correlations; *Geoscience Reports 2011*, BC Ministry of Energy and Mines, pages 1-18.
- Fisher, D.A., Reech, N. and Langley, K. (1995): Objective reconstruction of Late Wisconsinan Laurentide Ice Sheet and the significance of deformable beds; *Géographie physique et Quaternaire*, Volume 39, pages 229-238.
- Hartman, G.M.D. and Clague, J.J. (2008): Quaternary stratigraphy and glacial history of the Peace River valley, northeast British Columbia; *Canadian Journal of Earth Sciences*, Volume 45, pages 549-564.
- Hickin, A.S. Kerr, B., Turner, D.G. and Barchyn, T.E. (2008): Mapping Quaternary paleovalleys and drift thickness using petrophysical logs, northeast British Columbia, Fontas map sheet, NTS 094I; *Canadian Journal of Earth Sciences*, Volume 45, pages 577-591.
- Hickin, A.S. and Huntley, D.H. (2011): Attrition Experiments for the Beneficiation of Northeast BC Unconsolidated Sand Sources for Hydraulic Fracture Sand; *Geoscience Reports 2011*, BC Ministry of Energy, pages 75-85.
- Huntley, D.H. (2010): GEOART: Application to Geo-mapping for Energy and Minerals (GEM-Energy) Program and Geoscience Outreach; *Geological Survey of Canada*, Open File 6543, 12 pages.
- Huntley, D.H. and Hickin, A.S. (2010): Surficial deposits, landforms, glacial history and potential for granular aggregate and frac sand: Maxhamish Lake Map Area (NTS 940), British Columbia; *Geological Survey of Canada*, Open File 6430, 17 pages.
- Huntley, D.H. and Hickin, A.S. 2011. Geo-Mapping for Energy and Minerals program (GEM-Energy): preliminary surficial geology, geomorphology, resource evaluation and geohazard assessment for the Maxhamish Lake map area (NTS 094O), northeastern British Columbia; *Geoscience Reports 2011*, BC Ministry of Energy, pages 57-73.
- Huntley, D.H. and Sidwell, C.F. (2010): Application of the GEM surficial geology data model to resource evaluation and geohazard assessment for the Maxhamish Lake map area (NTS 094O), British Columbia; *Geological Survey of Canada*, Open File 6553, 22 pages.
- Lemmen, D.S., Duk-Rodkin, A. and Bednarski, J.M. (1994): Late glacial drainage systems along the northwestern margin of the Laurentide Ice Sheet; *Quaternary Science Reviews*, Volume 13, pages 341-354.
- Levson, V.M., Ferbey, T., Kerr, B., Johnsen, T., Bednarski, J., Smith, I.R., Blackwell, J. and Jonnes, S. (2004): Quaternary geology and aggregate mapping in northeast British Columbia: application for oil and gas exploration; in Summary of Activities, *BC Ministry of Energy, Geoscience and Natural Gas Development Branch*, pages 29-40.
- Mathews, W.H. (1974): Surface profiles of the Laurentide Ice Sheet in its marginal areas; *Journal of Glaciology*, Volume 13, pages 37-43.
- Mathews, W.H. (1980): Retreat of the last ice sheets in northeastern British Columbia and adjacent Alberta; *Geological Survey of Canada*, Bulletin 331, 22 pages.
- Rampton, V.N. (1987): Late Wisconsinan deglaciation and Holocene river evolution near Fort Nelson, northeastern British Columbia; *Canadian Journal of Earth Sciences*, Volume 24, pages 188-191.
- Ross, M., Campbell, J.E., Parent, M. and Adams, R.S. (2009): Paleo-ice streams and the subglacial landscape mosaic of the North American mid-continental prairies. *Boreas*, Volume 38, pages 421-439.
- Rutter, N.W., Hawes, R.J. and Catto, N.R. (1993): Surficial Geology, southern Mackenzie River valley, District of Mackenzie, Northwest Territories; *Geological Survey of Canada*, GSC A-Series Map 1683A, scale 1:500 000.
- Sharp, M. (1985) Crevasse-fill ridges – a landform type characteristic of surging glaciers? *Geografiska Annaler*, Volume 67A, pages 213-220.
- Shaw, J., Sharpe, D., and Harris, J., (2009): A flowline map of glaciated Canada based on remote sensing data; *Canadian Journal of Earth Sciences*, Volume 47, pages 89-101.
- Smith, I.R. (2000): Preliminary report on surficial geology investigations of La Biche River map area, southeast Yukon Territory; *Geological Survey of Canada*, Current Research 2000-B3, 9 pages.
- Smith, I.R. (2002): Surficial geology, Mount Martin (95C/1), Yukon Territory – Northwest Territories – British Columbia; *Geological Survey of Canada*, Open File 4260, 1 map, scale 1:50 000.
- Smith, I.R. and Lesk-Winfield, K. (2009): An integrated assessment of potential granular aggregate resources in Northwest Territories; *Geological Survey of Canada*, Open File 6058, 1 DVD-ROM.
- Smith, I.R. Lesk-Winfield, K., Huntley, D.H., Sidwell, C.F., Liu, Y and MacDonald, L.E. (2006): Potential granular aggregate occurrences, Camsell Bend (NTS 095J), Northwest Territories; *Geological Survey of Canada*, Open File 5315, scale 1:250 000.
- Stokes, C.R. and Clark, C.D. (2001): Palaeo-ice streams; *Quaternary Science Reviews*, Volume 20, pages 1437-1457.
- Stott, D.F. and Taylor, G.C. (1968): Geology of Maxhamish Lake; *Geological Survey of Canada*, Map 2-1968, scale 1:250 000.
- Trommelen, M. and Levson, V.M. (2008): Quaternary stratigraphy of the Prophet River, northeastern British Columbia; *Canadian Journal of Earth Sciences*, Volume 45, pages 565-575.
- Utting, D.J., Ward, B.C. and Little, E.C. (2009): Genesis of hummocks in glaciofluvial corridors near the Keewatin Ice divide; *Boreas*, Volume 38, pages 471-481.
- van der Meer, J.J.M., Menzies, J. and Rose, J. (2003): Subglacial till: the deforming glacier bed. *Quaternary Science Reviews*, Volume 22, pages 1659-1685.



# GEO-MAPPING FOR ENERGY AND MINERALS PROGRAM (GEM-ENERGY): PRELIMINARY SURFICIAL GEOLOGY, GEOMORPHOL- OGY, RESOURCE EVALUATION AND GEOHAZARD ASSESSMENT FOR THE MAXHAMISH LAKE MAP AREA (NTS 094O), NORTHEASTERN BRITISH COLUMBIA

David H. Huntley<sup>1</sup> and Adrian S. Hickin<sup>2</sup>

---

## ABSTRACT

*As part of the Geo-mapping for Energy and Minerals program (GEM-Energy) Yukon Basins project, the Geological Survey of Canada (GSC) and British Columbia Ministry of Energy and Mines (BC MEM) are collaborating to produce digital surficial geology and landform maps and geodatabases of terrain, landforms and geomorphic processes in the Maxhamish Lake map area (NTS 094O), British Columbia. Our work is providing reliable geoscience information on surficial earth materials, geohazards and resource potential for granular aggregate, frac sand and groundwater to government agencies, industry, communities and the public access. In this paper we present the provisional distribution of surficial deposits and landforms; and describe the sedimentology, surface morphology and facies associations of major terrain units and landforms. This terrain inventory is evaluated to better define the regional potential for granular aggregate and frac sand resources in the map area; identify key geohazards that could impact surface infrastructure (e.g., road design, well pad locations, pipeline routing); and provide baseline information useful for future land management decisions on resource development in northeastern British Columbia. The intent of our work is to attract new investment and reduce risks for exploration and development of natural resources in northern British Columbia.*

Huntley, D. and Hickin, A. (2011): Geo-Mapping for Energy and Minerals program (GEM-Energy): preliminary surficial geology, geomorphology, resource evaluation and geohazard assessment for the Maxhamish Lake map area (NTS 094O), northeastern British Columbia; in Geoscience Reports 2011, *BC Ministry of Energy and Mines*, pages 57–74.

<sup>1</sup>Geological Survey of Canada, Pacific Division, Vancouver, British Columbia. [dhuntley@nrcan.gc.ca](mailto:dhuntley@nrcan.gc.ca)

<sup>2</sup>Geoscience and Natural Gas Development Branch, Oil and Gas Division, BC Ministry of Energy and Mines, Victoria, British Columbia

**Key Words:** Geo-Mapping for Energy and Minerals program, Yukon and Liard Basin project, Maxhamish Lake, NTS 094O, surficial geology, data model, granular aggregate, frac sand, geohazards

---

## INTRODUCTION

Sustainable economic investment in exploration and development of energy and mineral resources in northeastern British Columbia requires quality infrastructure development (roads and pipelines) to ensure access to the land base and reliable silica sand sources to facilitate hydrofracturing in gas wells. To help address these needs, the Geological Survey of Canada (GSC) and British Columbia Ministry of Energy and Mines (BC MEM) are currently compiling regional-scale information on surficial deposits and landform processes in northeastern British Columbia as part of the Geo-Mapping for Energy and Minerals (GEM) program, Yukon Basins project (Huntley, 2010a-c; Huntley and Hickin, 2010; Huntley and Sidwell, 2010; Hickin and Huntley, 2011; Huntley et al., 2011).

Current research builds on the knowledge of other regional studies and surficial mapping projects (e.g., Mathews, 1980; Rampton, 1987; Rutter et al., 1993; Lemmen et al., 1994; Fisher et al., 1995; Duk-Rodkin and Lemmen, 2000; Bednarski and Smith, 2007; Bednarski, 2008; Hartman and Clague, 2008; Hickin et al., 2008; Trommelen and Levson, 2008; Demchuck, 2010a, b). The terrain model presented here conforms to the science language for the data management component of the GSC GEM geological map flow process (cf. Deblonde et al., 2011; Huntley and Sidwell, 2010). Remote predictive terrain classification and digital mapping combined with benchmarking field-based studies have led to a better understanding of the regional distribution of surficial deposits, permafrost, landslides and other geomorphic processes. Our work is also improving our knowledge of the limits of glaciation, the range of

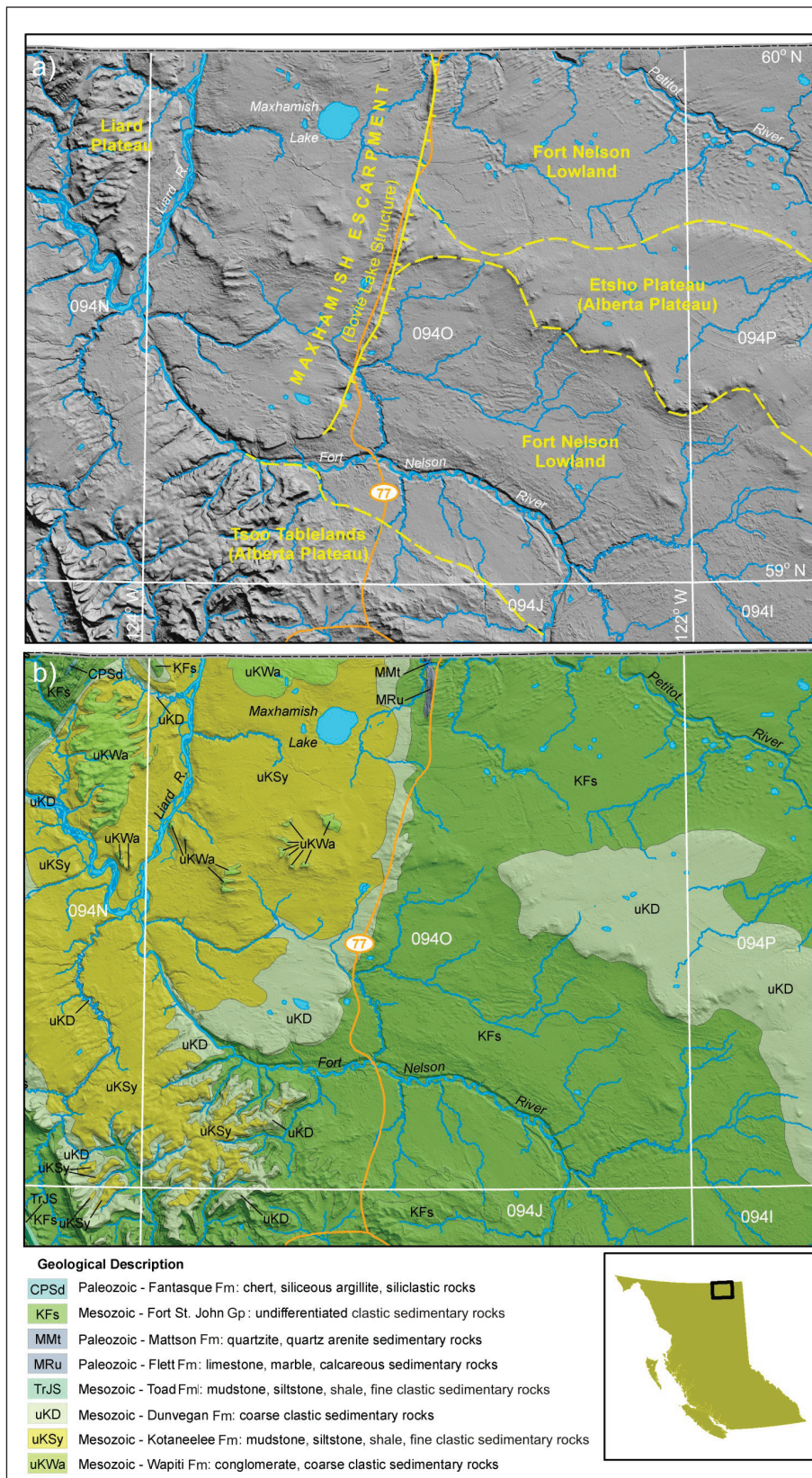


Figure 1. Limits of the Maxhamish Lake map area (NTS 094O), northeastern British Columbia: a) major physiographic regions and hydrology (after Bostock, 1970); b) bedrock geology modified from Stott and Taylor (1968); figure drafted by Mike Fournier (formerly of the BC Ministry of Energy and Mines).



subglacial processes, the patterns of ice flow, and the history of ice retreat and glacial lake formation during a dynamic period of climate change and geomorphic adjustment. This new geoscience information is critical for a preliminary evaluation of the potential for granular aggregate, possible frac sand sources and baseline assessment of geohazards in the study area (Figure 1).

## LOCATION, PHYSIOGRAPHY AND GEOLOGY

This paper focuses on the surficial geology units and landforms mapped and classified on the Maxhamish Lake map sheet (NTS 0940), an area of approximately 12,624 km<sup>2</sup> in northeastern British Columbia (Figures 1 and 2). The Maxhamish Lake map area encompasses the north-western limits of the Fort Nelson Lowland, generally lying below 530 m elevation; the western Etsho Plateau, between 600 to 740 m elevation; the Maxhamish Escarpment (and Bovie Lake structure) ranging from 590 to 610 m elevation; the Tsoo Tablelands, the northernmost part of the Alberta Plateau, reaching elevations up to 820 m; and the Liard, Fort Nelson and Petitot rivers, with active flood plains at elevations below 280 m elevation (Bostock, 1970; Figure 1a).

Lowland regions are underlain by shallow dipping shale, siltstone and sandstone (Upper Cretaceous Kotanelee Formation overlying Lower Cretaceous Fort St. John Group rocks). Folded and fault-bounded Mississippian sandstone, shale (Mattson Formation) and limestone (Flett Formation), and Upper Cretaceous conglomerate, sandstone, carbonaceous shale and coal (Dunvegan and Wapiti formations) form escarpments, tablelands and plateaus (Figure 1b; Stott and Taylor 1968). Exploration is targeting gas-bearing Middle Devonian to lower Mississippian strata in the Liard and Horn River basins (Ferri et al., 2011a, 2011b). Much of the map area is covered in glacial drift dating to the Late Pleistocene (Late Wisconsinan, >25 to 10 ka) and non-glacial Holocene (10 ka to present) deposits (Huntley and Hickin, 2010).

## APPROACH TO SURFICIAL GEOLOGY MAPPING

Remote predictive mapping of surficial earth materials and landforms was based on interpretation of 1:60 000 scale black-and-white stereo-pair aerial photographs (15BCB97010 series), Landsat 7 satellite imagery and digital elevation models from the Shuttle Radar Topography Mission (free online data sources downloaded using Global Mapper software). The base map was generated from NRCAN CanVec shape files (<http://geogratis.cgdi.gc.ca/geogratis/> [URL 2011]; Huntley and Sidwell, 2010). Terrain polygons and on-site symbols were digitized

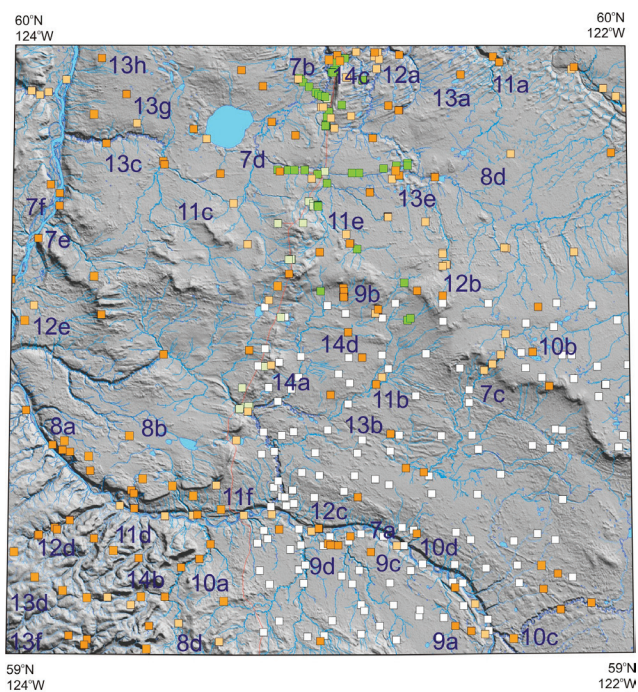
using commercially available computer software packages (Global Mapper, ArcMap and ArcGIS) and edge-matched with published maps, reports and digital data (Bednarski, 2003a-c; Bednarski, 2005a-b; Clement et al., 2004).

Reconnaissance fieldwork was undertaken in 2009 and



Figure 2. Maxhamish Lakescape (2003): original is 5x7 inches, acrylic on cotton, private collection; this artwork by D.H. Huntley depicts the major physiographic elements of the map area described in the text (see also Huntley, 2010a, b). In the foreground, a beaver-dammed meltwater channel incises morainal deposits with a forest cover of trembling aspen and white spruce. Mid-ground, the painting is transected by fen and peatlands. This terrain gives way to the tablelands, upland plateau and foothills to thrust-and-folded mountains.

2010 to verify the interpreted aerial photographs and satellite imagery with surficial geology polygons and to check characteristics that could not be determined from air photos, satellite images and digital elevation models. Earth materials were defined on the basis of landform associations, texture, sorting, colour, sedimentary structures, degree of consolidation, and stratigraphic contact relationships at approximately 300 field stations and remote observations from helicopters and trucks (Figure 3). Approximately 6% of polygons have been ground-checked, which is a survey-intensity level appropriate for regional-scale reconnaissance terrain mapping (Resource Inventory Committee, 1996).



**FIELD STATION LEGEND**

- 2010 (Huntley and Hickin)    ■ 2008 (Hickin)    □ 2004 (Huntley)
- 2009 (Huntley and Hickin)    ■ 2007 (Ferbey)

Figure 3. Location of benchmarking field observations (2003 to 2010) in the Maxhamish Lake map area; also showing locations of photographs in Figures 7 to 14.

## DISTRIBUTION OF SURFICIAL GEOLOGY UNITS AND LANDFORMS

The landscape is a composite of different earth materials and landforms that must be spatially represented in terms that will be meaningful to professionals and non geoscientists. Figure 4a depicts the provisional distribution, extent and location of bedrock, earth materials and landforms of the Maxhamish Lake map area. Terrain codes and symbols used in Figure 4b are derived from mapping conventions used by the Geological Survey of Canada and by terrain analysts in British Columbia and the Yukon (Resource Inventory Committee, 1996; Howes and Kenk, 1997; Bednarski, 2003a-c; Bednarski, 2005a-b; Clement et al., 2004). The surficial geology data model conforms to the science language for the data management component of the GSC GEM geological map flow process (cf. Deblonde et al., 2011).

Map units are distinguishable from surrounding terrain on the basis of earth material genesis, environment of deposition, sedimentology, morphology, thickness, physical limits, geological age and other distinguishing characteristics. Map unit (terrain) polygons are delimited so that their positions represent a particular characteristic of the landscape (Figure 4a). Map units in Figure 4b are presented chronostratigraphically and include alluvial sediments, organic deposits, colluvium, eolian deposits, glaciofluvial deposits,

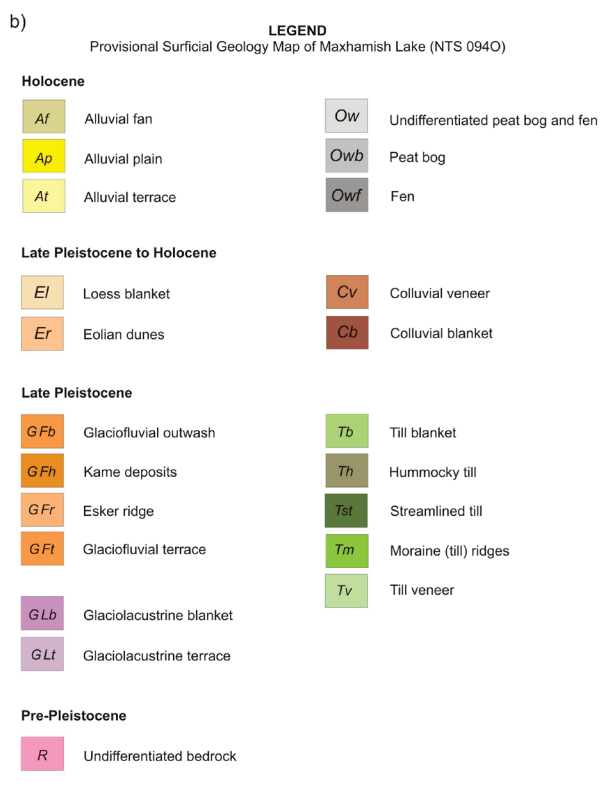


Figure 4. a) Provisional surficial geology of the Maxhamish Lake map area (NTS 940); b) map legend.

glaciolacustrine sediments, till deposits and bedrock. The distribution of landforms is depicted on Figure 5a, with the working legend shown in Figure 5b.

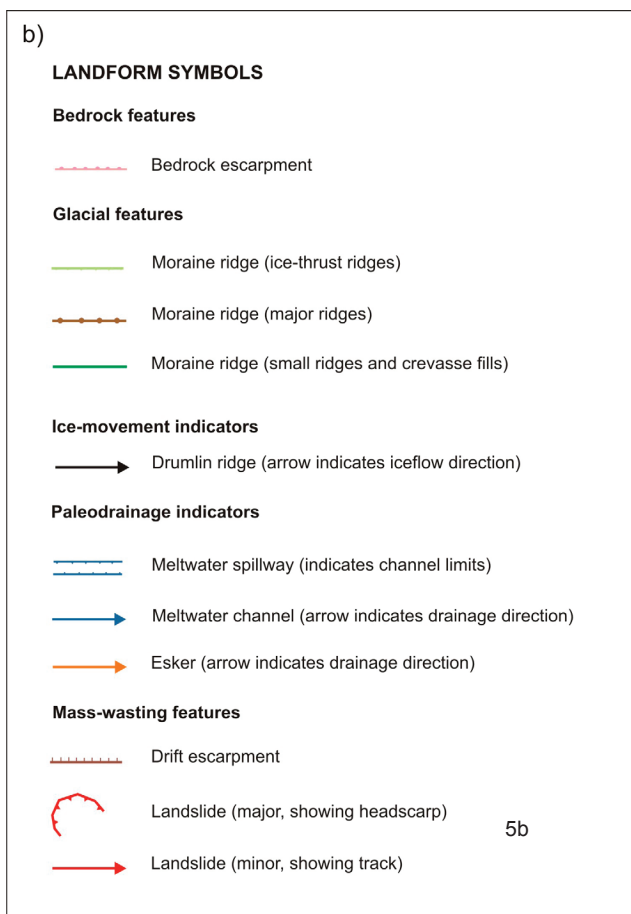
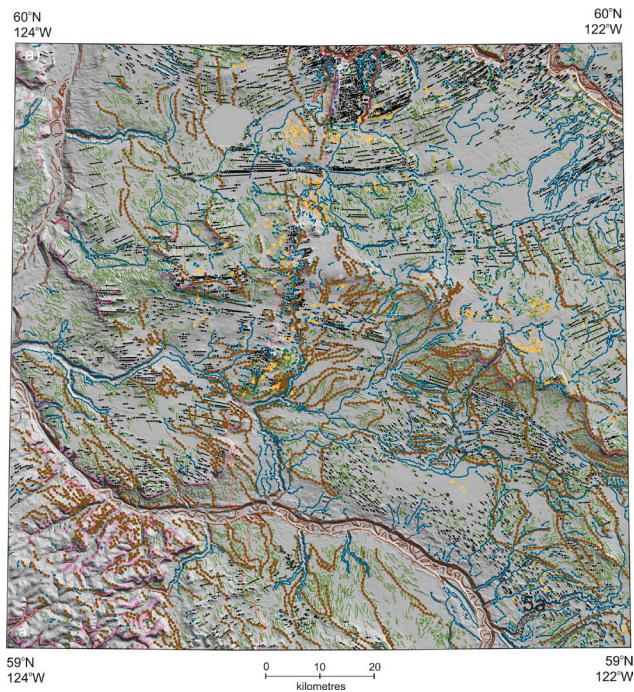


Figure 5. a) Provisional geomorphology of the Maxhamish Lake map area (NTS 940); b) map legend.

## SURFICIAL EARTH MATERIALS AND LANDFORM INVENTORY

The number of units mapped ( $n=2700$  terrain polygons) is graphically summarized in Figure 6a. Polygons most frequently contain tills as dominant terrain units ( $n=1085$ ) and organic deposits ( $n=515$ ). Glaciolacustrine deposits ( $n=272$ ), alluvial sediments ( $n=290$ ), and colluvium ( $n=240$ ) are less frequent. Terrain polygons mapped with glaciofluvial sediments ( $n=193$ ), bedrock ( $n=55$ ) and eolian deposits ( $n=50$ ) are least common (Figure 6a).

The areal extent ( $\text{km}^2$ ) of surficial units is shown in Figure 6b. The most extensive surficial units are tills (covering  $5965.36 \text{ km}^2$  or 47.25% of the map area) and organic deposits (covering  $4269.48 \text{ km}^2$  or 33.68 % of the map area). Glaciolacustrine deposits ( $881.80 \text{ km}^2$  or 6.98%), alluvial sediments ( $726.43 \text{ km}^2$  or 5.73%), and colluvium ( $552.74 \text{ km}^2$  or 4.38%) cover much of the remaining map area. Glaciofluvial ( $117.71 \text{ km}^2$  or 0.94%), bedrock ( $48.21 \text{ km}^2$  or 0.38%) and eolian deposits ( $82.05 \text{ km}^2$  or 0.66%) are the least areally extensive (Figure 6b).

Figure 6c shows that the dominant landforms in the map area are minor moraine ridges ( $n=10185$ ), drumlins ( $n=4016$ ) and meltwater channels ( $n=1188$ ). Less common are major moraine ridges ( $n=1211$ ), drift escarpments ( $n=698$ ), eskers ( $n=332$ ), meltwater spillways ( $n=174$ ), ice-thrust ridges ( $n=153$ ) and bedrock escarpments ( $n=183$ ).

### *Holocene earth materials and landforms*

Alluvial deposits include boulders, gravel, sand, and silt transported and deposited by modern rivers, streams and creeks (Figures 7a to 7f). Deposits are confined to deltas and fans (Af), terraces in river valleys (At), bedrock channels, point bars and floodplains (Ap): all of which are subject to periodic flooding. Generally, alluvial deposits are well sorted and stratified, greater than 2 m thick, and may contain interbedded debris flows and buried organic material (e.g., trees, driftwood, charcoal and anthropogenic material). Alluvial sediments are a potential source of aggregate: however, gravel extraction and other land-use activities (e.g., road construction, pipeline crossings and logging) which adversely affect stream courses or conditions, and have impacts on fish and wildlife resources.

Organic deposits include undifferentiated muskeg (Ow), peat bogs (Owb) and fens (Owf) formed by the accumulation of organic matter in poorly drained depressions or level areas (Figures 8a to 8d). Typically, they are treeless or with scattered black spruce and tamarack. Lichens commonly account for greater than 50% of the vegetated surface. In vertical profile, organic deposits comprise sedge and woody sedge overlain by Sphagnum peat. In 2003, discontinuous permafrost was observed sporadically at depths

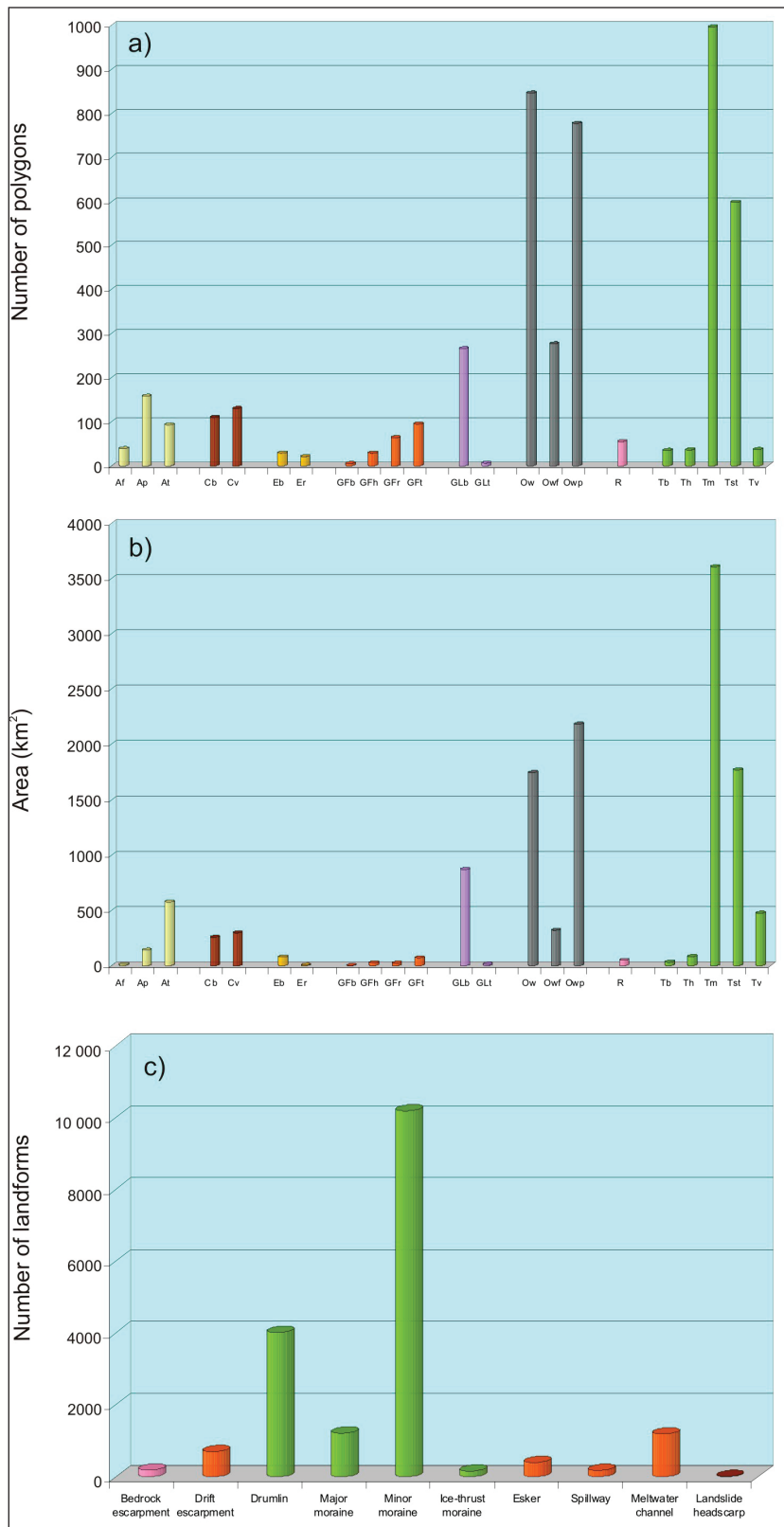


Figure 6. Summary statistics for surficial map units and landforms: a) number of polygons per map unit; b) areal extent of map units (km<sup>2</sup>); and c) number of landforms. Note colours are generalized in relation to the map legend (see Figures 4 and 5).



Figure 7. Alluvial deposits: a) underfit Fort Nelson River occupying northwest-trending meltwater spillway (At.Ap); b) alluvial and glaciofluvial terraces, and flood plain along the Petitot River (GFt.At, Ap); c) alluvial channels incising moraine deposits below the Etsho Plateau (At.Ap); d) beaver-dammed stream occupying the meltwater channel on the Fort Nelson Lowland (Ap.Owf); e) Liard River looking south to confluence with Fort Nelson River; f) Alluvial terrace (At), in-channel bar on the Liard River comprising massive, planar and cross-bedded silt, sand and rare gravel.

of less than 1 m throughout the map area, especially where peat overlies unconsolidated glacial lake sediments. Peat in wet depressions is thawed to depths greater than 1 m.

### ***Late Pleistocene to Holocene earth materials and landforms***

Eolian (loess) deposits include discontinuous veneers and blankets (El) and parabolic dunes (Er) of silt and sand

derived from the deflation of glacial lake sediments, outwash, tills and alluvial sediments, then transported and deposited by wind action (Figures 9a to 9d). Loess deposits are generally less than a metre in thickness, display cross-, ripple- or massive bedding and contain little to no ground ice. Quartz-rich eolian deposits may be potential frac sand sources.

Colluvial deposits are a product of the weathering and down-slope movement of earth materials by gravitational processes (mass wasting). Massive to stratified,

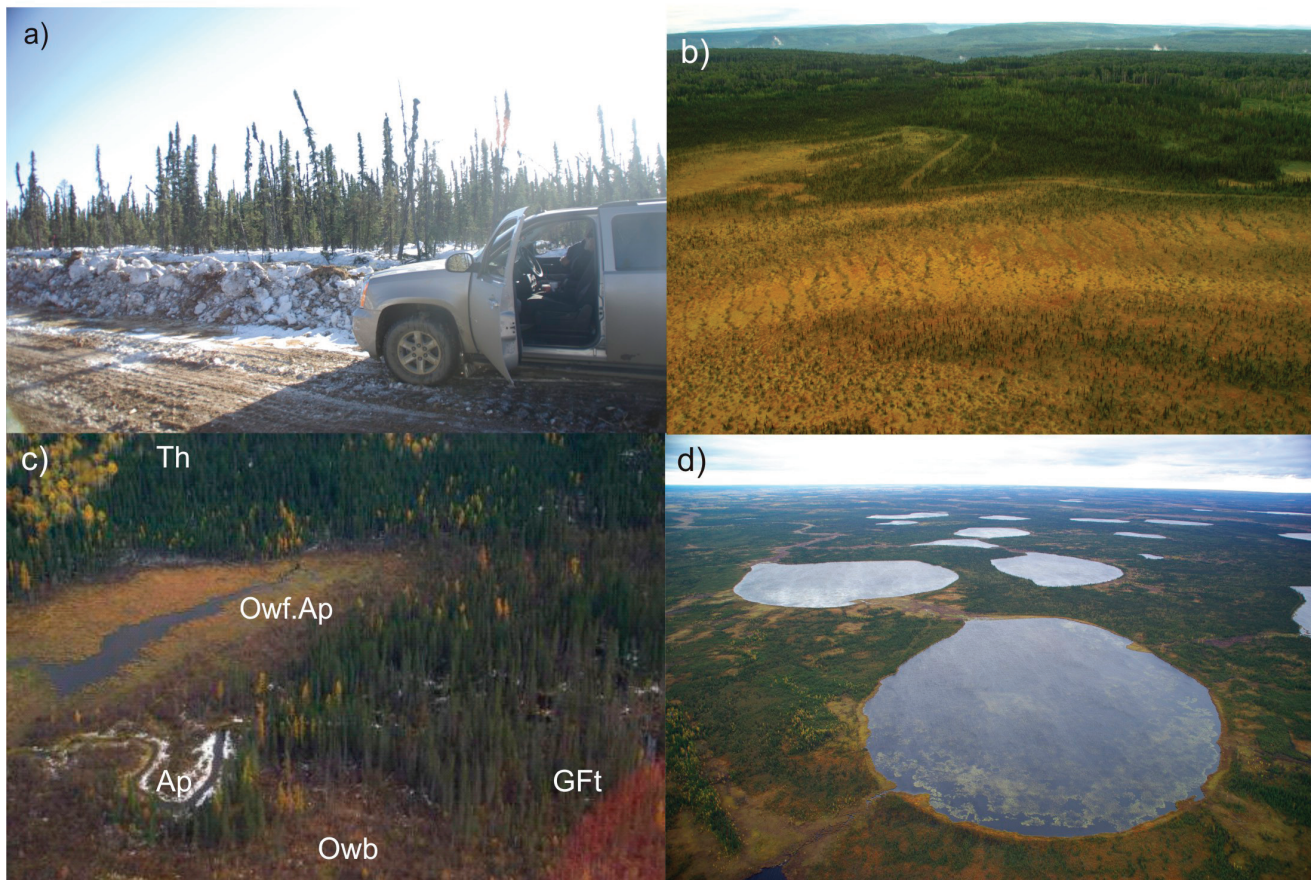


Figure 8. Organic deposits: a) hummocky bogs with sphagnum and forest peat (Owb) are formed in wet environments, usually treeless or with a cover of black spruce and ericaceous herbs; b) ribbed fen peat (Owf) are derived from sedges and shrubs in a relatively open environment with a mineral-rich water table that persists seasonally near the surface; c) fenland developed over alluvial plain (Ap) in response to beaver-damming of the meltwater channel, d) undifferentiated organic deposits (Ow) with thermokarst lakes indicate the presence of sporadically discontinuous permafrost.

clast-supported diamictons form a veneer (Cv) or blanket (Cb) on bedrock and debris-covered slopes. Mass wasting processes include retrogressive rotational slides in glaciolacustrine sediments and outwash in lowland valleys; rock falls, topples, rock slides and debris flows occur where shale, sandstone and carbonate strata is exposed at or close to the surface (Figures 10a to 10d). Earth materials on slopes above 10-15° with greater than 5 m relief are prone to remobilization by landslides and debris flows. In areas underlain by glaciolacustrine deposits with discontinuous permafrost, debris slides and flows occur on slopes less than 5°. Slope instability could present major problems for construction in some areas (e.g., the south flank of the Etsho Plateau, Fort Nelson and Petitot river valleys).

### ***Late Pleistocene earth materials and landforms***

Glaciofluvial deposits include boulders, cobbles, pebble-gravel, sand, silt and diamicton deposited by rivers and streams flowing from, or in contact with glacial ice. Glaciofluvial deposits are generally massive to stratified and

greater than 2 m thick (GFb). Landforms include kames and hummocky outwash deposits (GFh), esker ridges (GFr), terraces (GFt), spillways, meltwater channels and fan deltas (Figures 11a to 11e). Evidence for ice collapse including slumping, kettles and irregular topography is also observed (GFh). Glaciofluvial sediments are a potential source of granular aggregate when material is gravel rich. Eskers and fan-deltas should be evaluated as frac sand sources if they are quartz rich. Gravel deposits buried beneath till and other glacial sediments are potential groundwater aquifers.

Glaciolacustrine deposits (Figures 12a to 12e) include massive or rhythmically interbedded silt and clay, with subordinate sand, gravel and diamicton. Sediments are deposited by subaqueous gravity flows and thermal melting of ice, and reworked by wave action in lakes adjacent to glaciers and along shorelines. Glacial lake deposits are generally thicker than 1 m, blanketing other deposits (GLb) and occasionally forming terraces (GLt). Slump structures, irregular topography and kettles indicative of collapse from the melting of buried ice may be locally present. Where permafrost is, or was present, glaciolacustrine deposits may be subject to thermokarst processes and slopes less

than 5° are potentially unstable and prone to landslides and debris flows.

Till deposits comprise massive, matrix-supported diamictites deposited directly by lodgement, basal meltout, glacial deformation and in situ melting from stagnant ice. Tills are sand, silt and clay-rich with low clast contents (<20%) and contain sub-rounded granitic erratic boulders with sources on the Canadian Shield. The till is interpreted to be deposited by the Laurentide Ice Sheet (Figures 13a to 13h). Generally, till is compact and moderately or well drained. Landforms include till blankets (Tb), veneers and boulder lags (Tv), streamlined crag-and-tails, drumlins and

fluted ridges (Tst), major and minor till ridges (Tm) and hummocky ground moraine with kettle depressions (Th). Polygons mapped with till as the dominant terrain unit are suitable for infrastructure placement (e.g., well pads, building sites, all-season roads).

### *Pre-Quaternary earth materials and landforms*

Bedrock includes outcrops of Paleozoic to Mesozoic sedimentary rocks (R), exposed in steep cliffs along the Liard, Fort Nelson and Petitot rivers, the Maxhamish



Figure 9. Eolian deposits: a) loess field (EI) formed by eolian re-working of outwash (GFt) and glacial lake sediments (Ow.GLb); b) eolian veneer of silty fine sand (Ev) overlying glaciofluvial pebbly sand (GFf); c) fine to medium-grained quartz and feldspar-rich eolian sand exposed in parabolic dune (Er); d) parabolic dunes (Er) formed over organic (Ow) and glacial lake deposits (GLb), paleowind direction to southeast (indicated by SE on the photo).

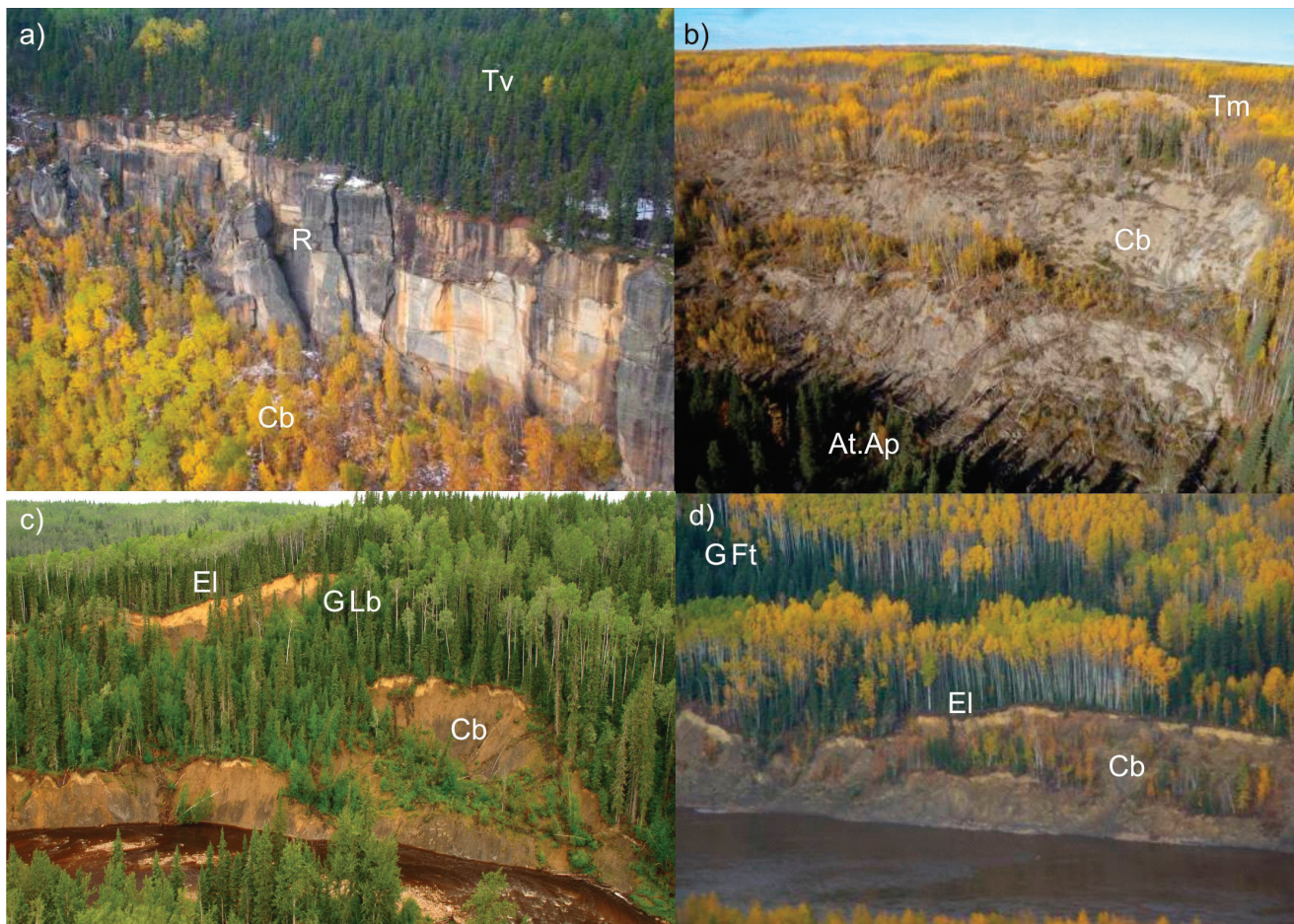


Figure 10. Colluvial deposits: a) Tsoo Tablelands, conglomerate and sandstone escarpment (Dunvegan Formation, indicated by R) prone to toppling, rock slides and failure along debuttinging fractures subparallel to the escarpment face (Cb); b) Etsho Plateau, complex retrogressive, rotational-translational bedrock-debris slide (Cb) incorporating shale, sandstone and siltstone (Fort St. John Group) and Quaternary glacial deposits, landslide triggered by postglacial incision of plateau escarpment; c) rotational debris slide (Cb) triggered by cutbank erosion along a tributary to the Fort Nelson River, failure is confined to glaciolacustrine deposits (GLb) draped with a discontinuous loess cover (EI); d) rotational debris slide (Cb) triggered by cutbank erosion along the Fort Nelson River, failure is confined to glaciofluvial terraces (GFt) draped with a discontinuous loess cover (EI).

Escarpment and the Tsoo Tablelands (Figures 14a to 14b). South of the Petitot River, limestone exposed along the Maxhamish Escarpment and clastic sedimentary rocks in the Fort Nelson Lowland are quarried as a source of crushed granular aggregate (Figures 14c to 14d).

## AGGREGATE AND FRAC SAND RESOURCE EVALUATION

Important objectives of current research for the GEM-Energy program are the regional mapping and assessment of the nature and genesis of known surficial deposits, and the recognition and description of new and/or potential granular aggregate and frac sand deposits (Huntley and Hickin, 2010; Huntley and Sidwell, 2010). With the new geoscience data presented above, a further evaluation of the regional potential for granular aggregate and frac sand is now possible.

Glacial paleodrainage features are potential exploration targets for granular aggregate, frac sand and mineral resources. Proven aggregate sources observed in the map area include: a) borrow pits in till and outwash along the highway and all-season access roads (Figure 14c); b) crushed limestone (Flett Formation) quarried at the northern end of the Maxhamish Escarpment (Figure 14d); and c) glaciofluvial terraces with access via cutlines, winter trails and access roads along the Fort Nelson and Petitot Rivers and their tributaries (Figure 11f). There are no known frac sand sources in the map area.

The most favourable granular aggregate targets identified are bedrock escarpments (n=183), eskers (n=392), drift terraces (n=698), meltwater channels (n=1188), and spillways (n=174) graded to glacial lake surface elevations at approximately 610 m and 420 m (Figures 5 and 6). Glaciofluvial deposits visited during the 2009 and 2010 field seasons were assessed as having low to moderate potential as granular aggregate sources (Huntley and Hickin, 2010).



Although volumetrically favourable, most surface features in the Fort Nelson Lowland are constructed of silt-rich sands with only a minor pebble and cobble fraction (< 20%; Figure 7f); sand and gravel beds (up to 5 m thick) were also observed underlying > 3 m of clay-rich till in the Petitot River valley (Figure 12a). These sites need to be further evaluated for their frac sand potential.

Deeply incised valleys and lower colluvial slopes on

escarpments in the Tsoo Tablelands are potential sources of sandstone and conglomerate (Dunvegan Formation) for crushed aggregate (Figure 14a). Flat-lying terrain underlain by thick deposits of till, glaciolacustrine sediments and extensive bogs and fens covers some 88% of the map area (Figure 4a) and may obscure other deposits. Possible surface frac sand targets include eolian deposits and sand-rich glaciofluvial features in the Fort Nelson River valley

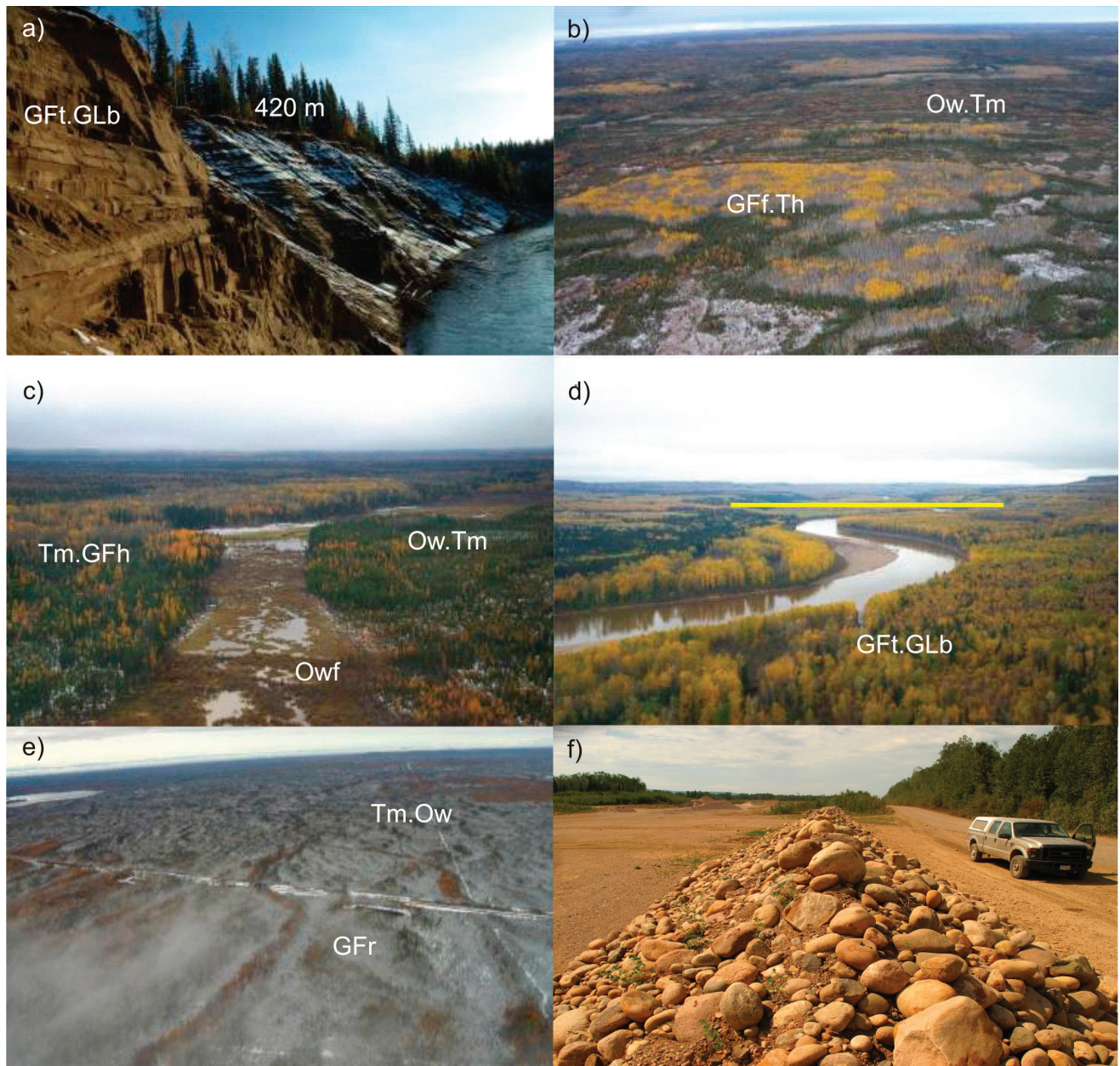


Figure 11. Glaciofluvial deposits: a) terraced retreat-phase glaciodeltaic outwash (GFt) graded to a glacial lake surface elevation of approximately 420 m, in the Petitot River valley; b) hummocky ice-contact kame-delta constructed of pebbly sand (GFh) and meltout diamictons (Th), Fort Nelson Lowland; c) organic-filled meltwater tunnel channel (Owf) incised into fine-grained till ridges (Tm) and sandy ice-contact glaciofluvial deposits (GFh); d) Fort Nelson River occupies a broad meltwater channel (yellow bar=channel width); e) sinuous esker ridge (GFr) composed of pebbly sand and diamicton, formed in association with crevasse fill ridges and minor (recessional) moraines (Tm); f) anthropogenic accumulation of granitic and metamorphic cobbles and boulders extracted from a gravel deposit in a glaciofluvial terrace (GFt) formed along the north flank of the Fort Nelson spillway.



Figure 12. Glaciolacustrine deposits: a) advance phase glaciolacustrine sand, silt and clay (GLb), truncated, deformed and overlain by streamlined lodgement till (Tst), Petitot River valley; b) organic, eolian-reworked till and glaciolacustrine terrain (Ow.GLb) approximately 610 m elevation, associated with proglacial lakes confined to flanks of the Etsho Plateau and the Maxhamish Escarpment; c) glaciolacustrine plain with end moraines (GLb.Tm), incised by the Fort Nelson River, ice-lobe margins and meltwater features were graded to a proglacial lake surface elevation ca. 420 m in the Liard, Fort Nelson and Petitot river valleys; d) colluviated glaciolacustrine deposits (>50 m thick) confined to valleys draining Tsoo Tablelands to the southeast, graded to approximately 640 m elevation; e) silty clay glaciolacustrine deposits (GLb) exposed below 420 m elevation along the Liard River.



Figure 13. Till deposits: a) glacially streamlined till (Tst) indicating paleoiceflow to the southwest, Petitot River; b) ice-marginal moraine ridges (Tm), Fort Nelson Lowland; c) trembling aspen and white spruce and jack pine stand on loess veneer (El) draped over the till ridge (Tm); d) observation pit exposing >1 m of massive, matrix-supported diamicton interpreted as Laurentide till, Tsou Tablelands; e) Laurentide till, massive matrix-supported diamicton with a silty clay matrix and clast content <8%, Fort Nelson Lowland; f) granitic erratic with a Canadian Shield provenance recovered from till, Tsou Tablelands; g) crevasse fills, minor moraine ridges (Tm) and hummocky till (Th) west of the Maxhamish Escarpment; h) glacially streamlined till plain (Tst) terminating at an end moraine complex (Tm) in the vicinity of Maxhamish Lake.

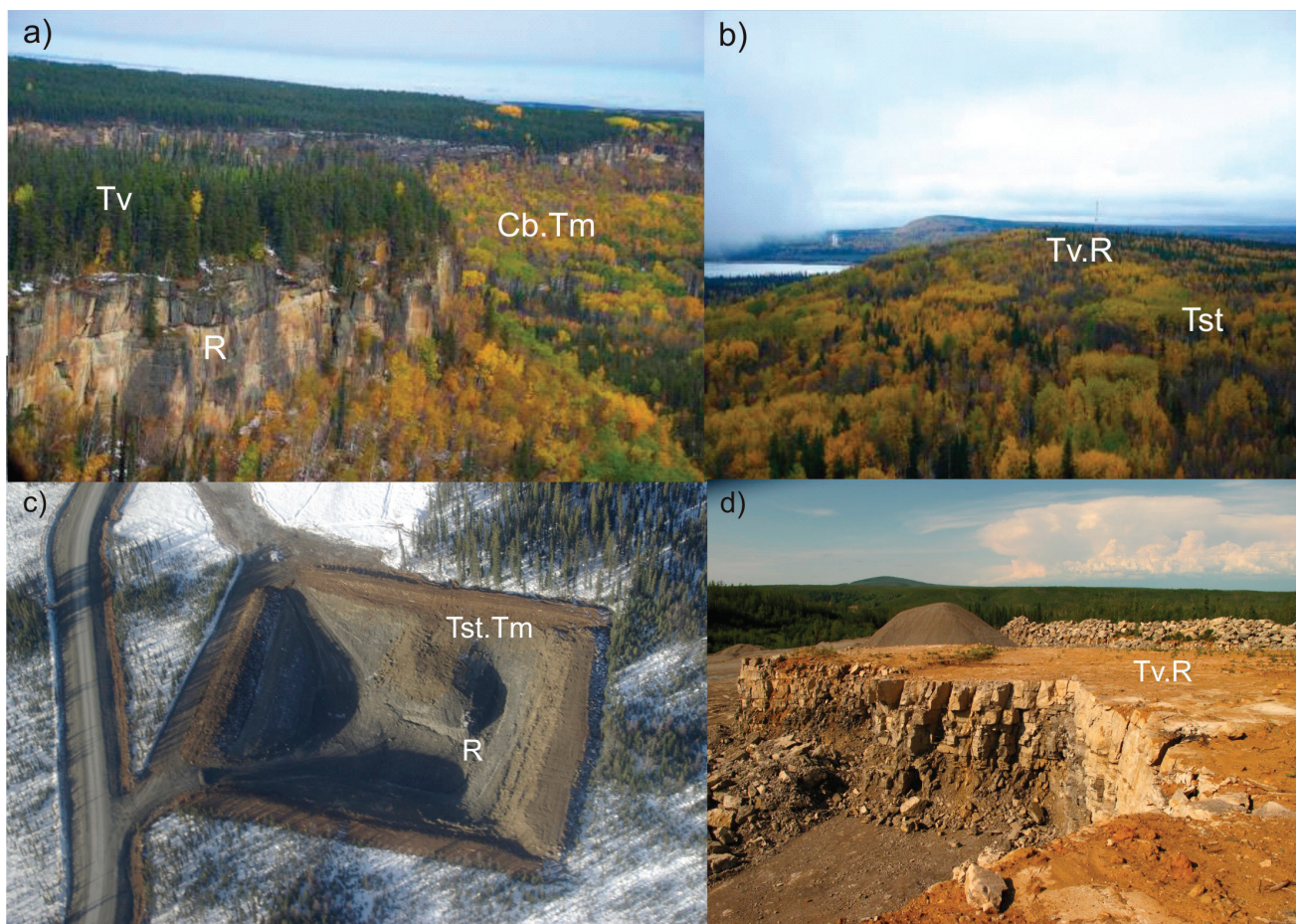


Figure 14. Bedrock: a) exposed conglomerate and sandstone (R, Dunvegan Formation) forming an escarpment of the Tsoo Tablelands; b) till veneer (Tv.R) overlying glacially streamlined conglomerate, sandstone and shale (R, Dunvegan Formation); c) borrow pit exposing 3-5 m of drumlinized Laurentide till (Tst) overlying siltstone and shale of the Cretaceous Fort St. John Group; d) crushed aggregate quarry exploiting Carboniferous Flett Formation limestone, bedrock at this site is glacially striated, indicating Laurentide iceflow towards 248o.

(Figures 4a and 9a-d). However, the low frequency of occurrence and limited areal extent of bedrock (48.21 km<sup>2</sup> or 0.38% of the map area), glaciofluvial (117.71 km<sup>2</sup> or 0.94%) and eolian deposits (82.04 km<sup>2</sup> or 0.65%) suggests that there is limited economic potential for surface sources of granular aggregate and frac sand in the Maxhamish Lake map area. Sedimentological analyses and attrition experiments indicate that sand deposits in their natural state have limited potential as regional sources of frac sand (Hickin and Huntley, 2011).

## GEOHAZARD ASSESSMENT

With resource exploration, drilling activities, natural gas production and other land uses (e.g., forest harvesting, hunting and tourism) expected to increase and expand in the map area over the coming years, it is anticipated that there will be demand for quality infrastructure development (e.g., all-season access roads, well pads, campsites, power lines and pipelines) to ensure secure access to the land base. An understanding of the spatial distribution and range of

geohazards is essential for regional development of energy and mineral resources.

Mass wasting processes in the Maxhamish Lake map area include soil creep, debris flows, rock fall and landslides involving rock and surficial deposits. Colluviated glacial sediment and bedrock on the slopes of stream and river valleys, escarpments and upland plateaux covers approximately 552.74 km<sup>2</sup> (or 4.38%) of the map area (Figures 4a and 6). Terrain identified with colluvium has either failed in the past or is expected to fail in the future, especially if disturbed by natural processes or anthropogenic activity (e.g., wildfires, construction or logging). The best management practice is to recognize locations where landslides and colluvium occur and to avoid infrastructure development where geohazards are present. In the case of existing infrastructure located within zones of potential geohazards they should be protected from risk of damage (e.g., pipe ruptures or damage to access roads). Continual visual inspection and instrumental monitoring of unstable and potentially unstable terrain and geohazards is recommended.

Approximately 726.43 km<sup>2</sup> (or 5.73%) of the map area is at some risk from fluvial geohazards. Existing and new infrastructure will be prone to damage by alluvial processes at stream and river crossings. Management plans must focus on measures to reduce risks for infrastructure associated with ice break-up, floods, flow diversions, channel bank erosion and deposition at stream and river crossings, and beaver activity in tributary drainage basins. Periodic visual inspection and monitoring of terrain at risk from fluvial geohazards is recommended. Mitigation measures along aggrading channel reaches must accommodate often rapid natural changes in sedimentation rates and patterns. In addition, land-use management practices must reduce the risk of hazards associated with the release of sediments during construction at stream crossings. An appropriate mitigation plan for sediment control and channel erosion in the post construction phase is also essential to reduce risk over time.

Organic deposits are generally seen as an obstacle to year-round development in northern Canada. Wetland bog and fen peat deposits cover approximately 4249.48 km<sup>2</sup> (or 33.68%) of the map area. Organic deposits also insulate underlying permafrost. In 2003, undifferentiated organic deposits and peat bogs containing sporadic discontinuous permafrost blanketed till and glaciolacustrine deposits covering approximately 1603.45 km<sup>2</sup> (or 12.68% of the map area) on the Etsho Plateau and the Fort Nelson Lowland (Clement et al., 2004). Relict thermokarst lakes on the plateau and lowland (Figure 8d) indicate melting permafrost, localized land subsidence and an increase in groundwater levels over time. If organic deposits are disturbed and/or removed during development, melting of sporadic discontinuous permafrost may result in localized ground subsidence, thermokarst erosion, debris slides and thaw-flows. In addition, large areas of fen can be inundated following drainage damming by beaver activities.

Drumlins, flutes and moraine ridges composed of silt- and clay rich tills (Figure 13e) typically rise above the surface of wetlands and comprise compact, moderately well-drained substrate suitable for the placement of well pads, building sites, road bases and other infrastructure development. Surficial geology and geomorphology maps (Figures 4 and 5) can be applied to best locate infrastructure, leading to less environmental impact and lower costs of installation and geotechnical modification over time.

South of the Petitot River valley, streamlined till, moraines and organic deposits locally overlie advance-phase glaciolacustrine silt and clay and glaciofluvial sand and gravel (Smith and Lesk-Winfield, 2009; Huntley and Hickin, 2010; Huntley and Hickin, 2011). Variations in deposit thicknesses suggest unconsolidated glacial sediments are infilling a sub-surface basin or buried palaeochannel system. Buried sand and gravel could be potential sources of granular aggregate, groundwater and shallow natural gas hazards (cf. Smith et al., 2006; Smith and Lesk-Winfield, 2009).

Eolian deposits and parabolic dunes cover only 0.65% of the map area and support rare ecosystems (Clement et al., 2004). Dune fields mapped along the Fort Nelson River valley and localized accumulations of loess over the Tsoo Tablelands and the Etsho Plateau are environmentally sensitive areas with little potential for economic development.

## SUMMARY

Surficial geology maps (Figures 4 and 5) and related databases (Figures 3 and 6a to 6c) for the Maxhamish Lake map area (NTS 0940) provide essential baseline geoscience data relevant for a range of potential end-users including resource explorationists, geotechnical engineers, land-use managers, terrestrial ecologists, archaeologists, geoscientists and communities in the region.

In the map area, approximately corresponding to the region underlain by the parts of the gas-producing Horn River and Liard basins, key surface exploration targets for granular aggregate are glaciofluvial landforms: eskers, terraces, meltwater channels and spillways (Figures 11a to 11f). On-site and laboratory-based assessments indicate that most glaciofluvial deposits in the map area have low to, at best, moderate potential as granular aggregate sources (Hickin and Huntley, 2011). Eolian deposits derived from glaciofluvial and glaciolacustrine sediment may be a viable source for frac sand. Unfortunately, these deposits and landforms have a limited geographic extent: approximately 0.66% of the map area and support rare ecosystems (Figures 9a to 9d). Polygons mapped with silt- and clay-rich till as the dominant terrain unit (streamlined till and moraine ridges) are suitable for well pads, building sites, road bases and other infrastructure development.

Geohazards in the map area include mass-wasting of glacial sediment and bedrock on the slopes of stream and river valleys, escarpments and upland plateaus (affecting approximately 4.38% of the map area); flooding, erosion, deposition and beaver activity in valleys (impacting 5.73%); and undifferentiated organic deposits and peat bogs containing sporadic discontinuous permafrost blanketing till and glaciolacustrine deposits (12.68% of the mapped area) on the Liard and Etsho plateaus and the Fort Nelson Lowland (Figure 4a).

Project outputs include GSC Open File Reports and digital maps (available on CD-ROM) which can be used in mineral and energy resource evaluations, environmental assessments and for drift geochemical exploration. Reports and maps are available as free downloads from the GSC bookstore website (<http://gsc.nrcan.gc.ca/bookstore/>). Surficial geology maps (e.g., Figures 4 and 5), released as part of the GEM-Energy Yukon and Liard Basin project, will be valuable tools to help identify, classify and evaluate in more detail the potential for granular aggregate, frac sand

sources, groundwater and geohazards, especially if combined with other methods of exploration. Examples of other useful geoscience data types include LiDAR, seismic shot-hole records, petrophysical logs, auger drilling, test-pitting, ground-penetrating radar and airborne electromagnetic surveys (e.g., Best et al., 2004; Levson et al., 2004; Smith et al., 2006, Hickin et al., 2008; Smith and Lesk-Winfield, 2009).

Collaboration between the GSC, the BC Ministry of Energy and Mines, and other agencies is ongoing. Collectively, our work is providing descriptive information and quantitative data about surficial sediments, their distribution and providing insight into their geologic history, the nature of geohazards and resource potential. Further, site-specific field studies in the Maxhamish Lake map area (NTS 0940) are required to better define the regional resource potential for granular aggregate and frac sands, and to evaluate the impact of climate change and land use on the distribution of unstable terrain and discontinuous permafrost.

## ACKNOWLEDGMENTS

The authors are indebted to past collaboration with Travis Ferbey (BC Ministry of Forests, Mines and Lands) and Tania Demchuk (BC Ministry of Natural Resource Operations), Rod Smith (GSC-Calgary), Jan Bednarski (GSC-Pacific), Alain Plouffe (GSC-Ottawa) and Roger Paulen (GSC-Ottawa) during fieldwork in the region. The manuscript was critically reviewed by Alain Plouffe. Derek Brown, Catherine Sidwell, Lauren Wilson and Lisa Fodor were able assistants during reconnaissance fieldwork in 2009 and 2010. Mike Fournier drafted Figure 1. The authors also thank Deh Cho (Great Slave) Helicopters and the Hamlet of Fort Liard, NWT, for logistical support during the 2009 and 2010 field seasons.

## REFERENCES

- Bednarski, J.M. (2003a): Surficial geology of Fort Liard, Northwest Territories-British Columbia; *Geological Survey of Canada*, Open File 1760, scale 1:50 000.
- Bednarski, J.M. (2003b): Surficial geology of Lake Bovie, Northwest Territories-British Columbia; *Geological Survey of Canada*, Open File 1761, scale 1:50 000.
- Bednarski, J.M. (2003c): Surficial geology of Celibeta Lake, Northwest Territories-British Columbia; *Geological Survey of Canada*, Open File 1754, scale 1:50 000.
- Bednarski, J.M. (2005a): Surficial Geology of Etsine Creek, British Columbia; *Geological Survey of Canada*, Open File 4825, scale 1:50 000.
- Bednarski, J.M. (2005b): Surficial Geology of Gote Creek, British Columbia; *Geological Survey of Canada*, Open File 4846, scale 1:50 000.
- Bednarski, J.M. (2008): Landform assemblages produced by the Laurentide Ice Sheet in northeastern British Columbia and adjacent Northwest Territories – constraints on glacial lakes and patterns of ice retreat; *Canadian Journal of Earth Sciences*, Volume 45, pages 593-610.
- Bednarski, J.M. and Smith, I.R. (2007): Laurentide and montane glaciation along the Rocky Mountain Foothills of northeastern British Columbia; *Canadian Journal of Earth Sciences*, Volume 44, pages 445-457.
- Best, M.E., Levson, V. and McConnell, D. (2004): Sand and gravel mapping in northeast British Columbia using airborne electromagnetic surveying methods; in Summary of Activities, *BC Ministry of Energy, Mines and Petroleum Resources*, pages 1-6.
- Bostock, H.S. (1970): Physiographic regions of Canada; *Geological Survey of Canada*, Map 1254A, scale 1:5 000 000.
- Clement, C., Kowall, R. Huntley, D and Dalziel, R. (2004): Ecosystem units of the Sahtaneh area; *Slocan Forest Products* (Fort Nelson), 39 pages and appendices.
- Deblonde, C., Paradis, S., Kerr, D., Davenport, P., Moore, A. and Boisvert, E. (2011): Science language for a common GSC data model for Surficial Geology maps; *Geological Survey of Canada*, Technical Note (in preparation).
- Demchuk, T.E. (2010a): Surficial Geology of the Komie Creek area (NTS 94P/05); *British Columbia Ministry of Energy, Mines and Petroleum Resources*, Open File 2010-08; Geological Survey of Canada Open File 6568, scale 1:50 000.
- Demchuk, T.E. (2010b): Surficial geology of the Komie Creek map area and an investigation of an ice-contact glaciofluvial delta, northeast British Columbia (NTS 94P/05); *unpublished M.Sc. thesis*, University of Victoria, 266 pages.
- Duk-Rodkin, A. and Lemmen, D.S. (2000): Glacial history of the Mackenzie region; in The Physical Environment of the Mackenzie Valley, Northwest Territories: A Base Line for the Assessment of Environmental Change. Dyke, L.D. and Brooks, G.R., Editors, *Geological Survey of Canada*, Bulletin 547, pages 11-20.

- Ferri, F., Hickin, A. and Huntley, D. (2011a): Bedded massive sulphide horizons (SEDEX) in upper Besa River Formation, western Liard Basin, British Columbia. *in Geological Fieldwork 2010, BC Ministry of Forests, Mines and Lands, Paper 2011-1*, pages 13-29.
- Ferri, F., Hickin, A. S. and Huntley, D. H. (2011b): Besa River Formation, western Liard Basin, British Columbia (NTS 094N): geochemistry and regional correlations; *in Geoscience Reports 2011, BC Ministry of Energy and Mines*, pages 1-18.
- Fisher, D.A., Reech, N. and Langley, K. (1995): Objective reconstruction of Late Wisconsinan Laurentide Ice Sheet and the significance of deformable beds; *Géographie physique et Quaternaire*, Volume 39, pages 229-238.
- Hartman, G.M.D. and Clague, J.J. (2008): Quaternary stratigraphy and glacial history of the Peace River valley, northeast British Columbia; *Canadian Journal of Earth Sciences*, Volume 45, pages 549-564.
- Hickin, A.S. Kerr, B., Turner, D.G. and Barchyn, T.E. (2008): Mapping Quaternary paleovalleys and drift thickness using petrophysical logs, northeast British Columbia, Fontas map sheet, NTS 094I; *Canadian Journal of Earth Sciences*, Volume 45, pages 577-591.
- Hickin, A.S. and Huntley, D.H. (2011): Attrition Experiments for the Beneficiation of Northeast BC Unconsolidated Sand Sources for Hydraulic Fracture Sand; *Geoscience Reports 2011*, BC Ministry of Energy and Mines, pages 75-85.
- Howes, D.E. and Kenk, E. (1997): Terrain classification system for British Columbia (revised edition): a system for the classification of surficial materials, landforms and geological processes of British Columbia; *BC Ministry of Environment, Manual 10*, 90 pages.
- Huntley, D.H. (2010a): GEOART: application to Geo-mapping for Energy and Minerals (GEM-Energy) program and geoscience outreach; *Geological Survey of Canada, Open File 6543*, 12 pages.
- Huntley, D.H. (2010b): GEOART: Application to geoscience outreach and education; *Geological Society of America, Abstracts and Proceedings of the 2010 GSA Annual Meeting, GSC Contribution 20100128*, 1 page.
- Huntley, D.H. (2010c): Geo-mapping for Energy and Minerals in Canada's North: digital and applied geological mapping of natural resources; *Geological Society of America, Abstracts and Proceedings of the 2010 GSA Annual Meeting, GSC Contribution 20100131*, 1 page.
- Huntley, D.H. and Hickin, A.S. (2010): Surficial deposits, landforms, glacial history and potential for granular aggregate and frac sand: Maxhamish Lake map area (NTS 094O), British Columbia; *Geological Survey of Canada, Open File 6430*, 17 pages.
- Huntley, D.H., Hickin, A.S. and Ferri, F. (2011): Provisional surficial geology, glacial history and paleogeographic reconstructions of the Toad River (NTS 94N) and Maxhamish Lake map areas (NTS 94O), British Columbia; *Geoscience Reports 2011*, BC Ministry of Energy, pages 37-55.
- Huntley, D.H. and Sidwell, C.F. (2010): Application of the GEM surficial geology data model to resource evaluation and geo-hazard assessment for the Maxhamish Lake map area (NTS 094O), British Columbia; *Geological Survey of Canada, Open File 6553*, 22 pages.
- Lemmen, D.S., Duk-Rodkin, A. and Bednarski, J.M. (1994): Late glacial drainage systems along the northwestern margin of the Laurentide Ice Sheet; *Quaternary Science Reviews*, Volume 13, pages 341-354.
- Levson, V.M., Ferbey, T., Kerr, B., Johnsen, T., Bednarski, J., Smith, I.R., Blackwell, J. and Jonnes, S. (2004): Quaternary geology and aggregate mapping in northeast British Columbia: application for oil and gas exploration; *in Summary of Activities, BC Ministry of Energy, Geoscience and Natural Gas Development Branch*, pages 29-40.
- Mathews, W.H. (1980): Retreat of the last ice sheets in northeastern British Columbia and adjacent Alberta; *Geological Survey of Canada, Bulletin 331*, 22 pages.
- Rampton, V.N. (1987): Late Wisconsin deglaciation and Holocene river evolution near Fort Nelson, northeastern British Columbia; *Canadian Journal of Earth Sciences*, Volume 24, pages 188-191.
- Resource Inventory Committee (1996): Terrain stability mapping in British Columbia: a review and suggested methods for landslide hazard and risk mapping; *Resource Inventory Committee Publications*, URL [www.publications.gov.bc.ca](http://www.publications.gov.bc.ca) [January 2011].
- Rutter, N.W., Hawes, R.J. and Catto, N.R. (1993): Surficial Geology, southern Mackenzie River valley, District of Mackenzie, Northwest Territories; *Geological Survey of Canada, GSC A-Series Map 1683A*, scale 1:500 000.
- Smith, I.R. and Lesk-Winfield, K. (2009): An integrated assessment of potential granular aggregate resources in Northwest Territories; *Geological Survey of Canada, Open File 6058*, 1 DVD-ROM.
- Smith, I.R. Lesk-Winfield, K., Huntley, D.H., Sidwell, C.F., Liu, Y and MacDonald, L.E. (2006): Potential granular aggregate occurrences, Camsell Bend (NTS 095J), Northwest Territories; *Geological Survey of Canada, Open File 5315*, scale 1:250 000.
- Stott, D.F. and Taylor, G.C. (1968): Geology of Maxhamish Lake; *Geological Survey of Canada, Map 2-1968*, scale 1:250 000.
- Trommelen, M. and Levson, V.M. (2008): Quaternary stratigraphy of the Prophet River, northeastern British Columbia; *Canadian Journal of Earth Sciences*, Volume 45, pages 565-575.





# ATTRITION EXPERIMENTS FOR THE BENEFICIATION OF UNCONSOLIDATED SAND SOURCES OF POTENTIAL HYDRAULIC FRACTURE SAND, NORTHEASTERN BRITISH COLUMBIA

*Adrian S. Hickin<sup>1</sup> and David H. Huntley<sup>2</sup>*

---

## ABSTRACT

*Sand for use as a hydraulic fracture proppant is critical in the development of shale gas. The cost of transporting proppants from distant suppliers has prompted the evaluation of local sand sources to meet or subsidize demand in northeastern British Columbia. Several sand deposits have been identified as potential proppant sources; however, in their natural state, these sand deposits do not meet industry standards. Several experiments are presented in this paper that focus on washing, sizing and attrition to improve the quality of a promising aeolian sand deposit. These beneficiation methods were selected because they are the least expensive processing steps for improving silica sand proppants.*

*Results suggest attrition will reduce the content of deleterious sand grains; however, success was limited and attrition alone is insufficient to elevate the SiO<sub>2</sub> content to industry standards. Other physical, physiochemical or chemical treatments will be required. The most substantial improvement in the silica content was achieved early in the experiments (i.e., in the first 5 minutes), after which results were negligible. A short period of attrition is a beneficial processing step, but prolonged attrition will be of little advantage. Prolonged attrition may, in fact, be detrimental to the quality of the proppant because grain breakage may result in an abundance of undesirable angular grains. Aggressive milling tended to produce the greatest increase in SiO<sub>2</sub> and greatest decrease in Al<sub>2</sub>O<sub>3</sub> and Fe<sub>2</sub>O<sub>3</sub>.*

Hickin, A.S. and Huntley, D.H. (2011): Attrition experiments for the beneficiation of unconsolidated sand sources of potential hydraulic fracture sand, northeastern British Columbia; *in Geoscience Reports 2011, BC Ministry of Energy and Mines*, pages 75–85.

<sup>1</sup>Geoscience and Natural Gas Development Branch, Oil and Gas Division, BC Ministry of Energy and Mines, Victoria, British Columbia. [adrian.hickin@gov.bc.ca](mailto:adrian.hickin@gov.bc.ca)

<sup>2</sup>Geological Survey of Canada, Pacific Division, Vancouver, British Columbia.

**Key Words:** frac sand, proppant, attrition, beneficiation, silica sand

---

## INTRODUCTION

The demand for hydraulic fracture proppants ('frac sand') in northeastern British Columbia will increase as shale gas resources development in this area continues. The BC Ministry of Energy and Mines, with its partner, the Geological Survey of Canada (through the Geo-mapping for Energy and Minerals [GEM] Program), is currently investigating surface sand and bedrock deposits to attract industry evaluation of the commercial potential of northeastern British Columbia frac sand sources (Hickin et al., 2010; Huntley and Hickin, 2010; Huntley and Sidwell, 2010; Huntley and Hickin, 2011; Huntley et al., 2011).

Hickin et al. (2010) identified a number of unconsolidated and bedrock sand sources in northeastern British Columbia that may hold some potential for use as a frac sand source. They indicated, however, that without processing or

beneficiation, none of these deposits would meet industry standards in their natural state. To be used as a proppant, sand must meet very stringent requirements, which are outlined in several industry standards, such as API RP 56 (American Petroleum Institute, 1995a), API RP 60 (American Petroleum Institute, 1995b) and International Organization for Standards (ISO) report number ISO 13503-2 (International Organization for Standards, 2006). If sand sources from northeastern British Columbia are to be considered as viable exploration targets, it is necessary to evaluate the processing and cost required to upgrade these deposits to meet industry standards.

Northeastern British Columbia sand sources might be considered economic for use as a proppant if the cost of beneficiation is less than the cost of transporting the products from established sources. Most frac sand in North America is produced from the Middle to Late Ordovician St. Peter

sandstone of the northeastern United States (also known by the industrial names of ‘Ottawa’ or ‘White’ sand), the Cambrian Hickory Member or Riley Formation (‘Brown’ or ‘Brady’ sand) or more recently, the Middle Ordovician Black Island Member in Saskatchewan (Dumont, 2007; Zdunczyk, 2007). To supply the British Columbia market, the product must be moved substantial distances from the mine to the well site. In addition to the cost associated with transportation, current frac sand production may not be able to keep pace with growing North American markets. The increased demand on the current supply may result in escalating costs. Processing sources from northeastern British Columbia may partially alleviate this supply gap if raw sand can be satisfactorily processed and/or blended with traditional products.

Beneficiation is the process of separating ore from gangue. It is achieved through physical or chemical processing (Taxiarchaou et al., 1997; Dumont, 2007; Sundararajan et al., 2009). Silica sand requires the washing and separation of quartz sand grains from other mineral grains (e.g., feldspar and mica) and lithic fragments. The cost of beneficiation increases as processing becomes more elaborate or intensive. Simple washing, screening and attrition scrubbing are the least expensive methods. Chemical separation and treatment would add significant cost and

regulation to processing. This study explores rudimentary beneficiation to elevate silica content through washing, sieving and attrition (through light milling), thereby providing the industry some sense of the processing requirement. The experimental method and design described in this report is not intended to be a substitute or alternative to established industrial processing (e.g., attrition scrubbing, other physical and chemical treatment). The most comparable industrial-scale process to that presented here is attrition scrubbing, where the action of one high-speed slurry flow impacts on another. The equipment involved in attrition scrubbing generally consists of two opposed impellers mounted on a shaft in a cell (cf. Freeman et al., 1993). In the experiments presented here, attrition is achieved by lightly milling the sample slurry with small stainless steel balls.

## METHOD

Three experiments were conducted on splits from a homogenized sample from the Fontas Eolian Sand Dune Field located along Dazo Creek, a tributary of the Fontas River (Hickin et al., 2010; Figure 1). A Fontas dune sample was selected because Hickin et al. (2010) reported this deposit as having relatively high potential as a frac sand source.

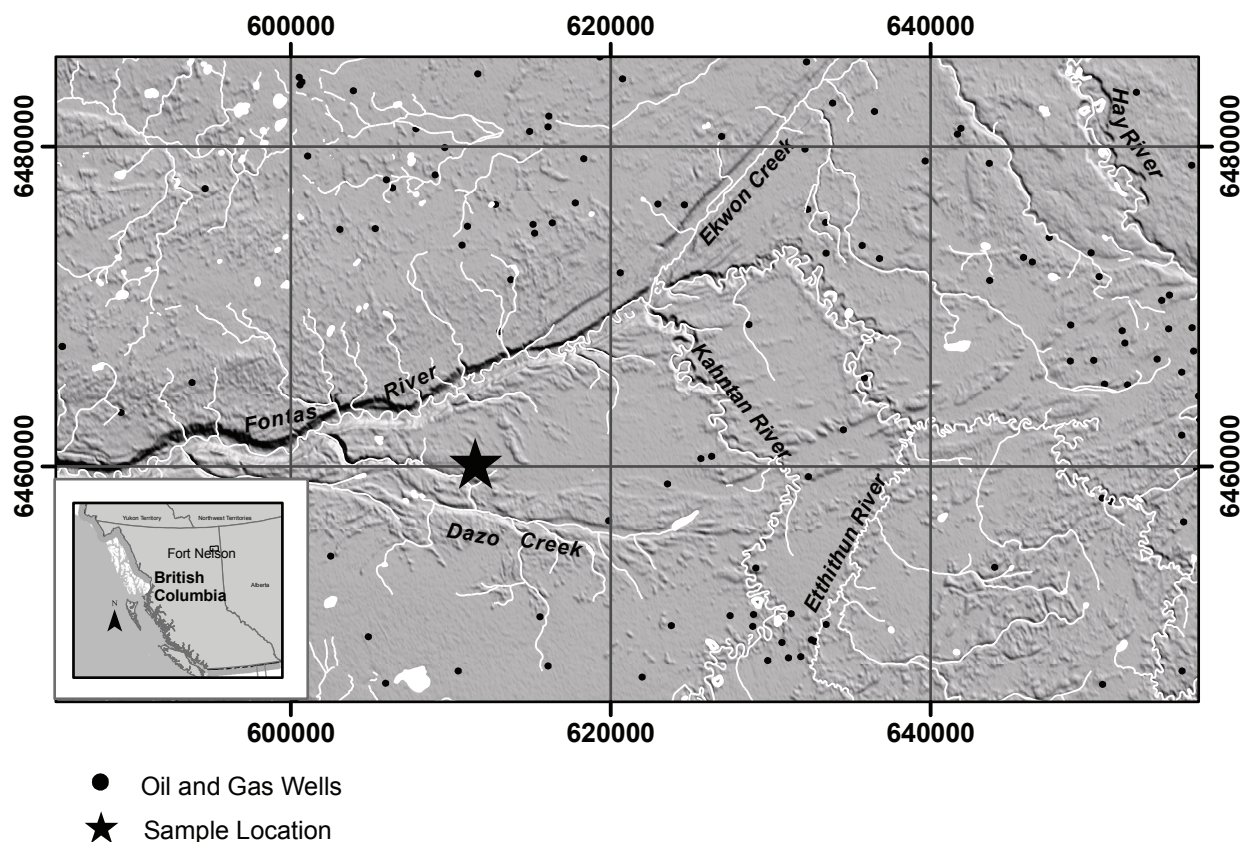


Figure 1. The sample used in the experiments is from the Fontas Dune Field located along Dazo Creek in northeastern British Columbia.

The sample is dominantly fine sand (Figure 2); therefore, a high proportion of material is in the 70/140 size fraction (<0.21 to >0.105 mm). Samples were initially washed using standard ASTM-approved sieves to remove buoyant organic material, silt and clay, preserving the sand-sized fraction (<2.0 to >0.063 mm; Wentworth, 1922). Although the majority of grains in this sample are quartz, there are also grains of other silicate minerals (e.g., feldspar) and lithic fragments of local Cretaceous rock (e.g., siltstone, chert and ironstone; Figure 3a).

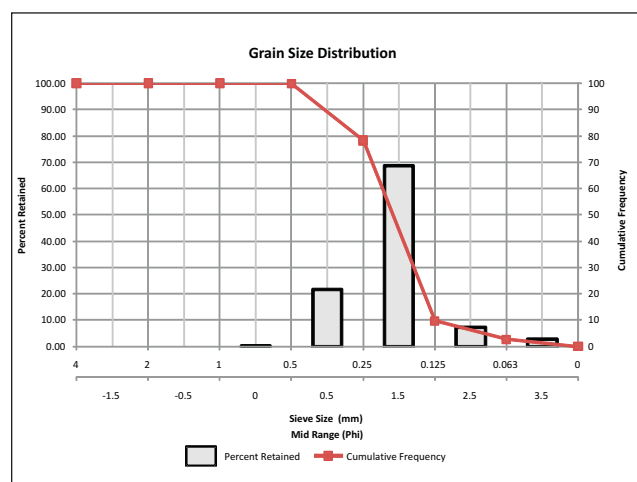


Figure 2. The original unwashed sample from the Fontas Dune Field consists mainly of fine-grained sand.

The equipment used in these experiments is listed and shown in Figure 4. In general, a given number of small steel balls, each 10 mm in diameter and weighing 3.6 g, were used to mill a predetermined weight of dry sample and water. The sample, water and steel balls were placed in a 250 mL plastic bottle and mounted in a table shaker to agitate the mixture for a predetermined period. The processed sample was then screened in standard ASTM-approved sieves to the desired size fraction, then dried in an oven and weighed to determine weight percent loss. This loss is assumed to be the result of the removal of grain coatings and the breakdown of sand grains into silt- and clay-sized material, which was washed out of the sample after agitation. The washed and processed samples were sent to Acme Laboratories (Vancouver, BC) for major oxides analysis. Total abundances of the major oxides and several minor elements were reported on a 0.2 g sample milled to <200 mesh (<0.074 mm). Samples were fused and analyzed by inductively coupled plasma–emission spectrometry (ICP-ES) following a lithium metaborate/tetraborate fusion and dilute nitric digestion. Loss on ignition (LOI) was determined from the weight difference after ignition at 1000°C. Oxide analysis was normalized to the major oxides to account for the organic content assumed to be equivalent to the material lost on ignition.

## Quality Control

Two blind duplicates were prepared and submitted to the laboratory. The laboratory also randomly duplicated one sample. The analytical data for these samples were used to establish precision error. The standard error was determined for three duplicate pairs for the three most abundant oxides (i.e., SiO<sub>2</sub>, Al<sub>2</sub>O<sub>3</sub> and Fe<sub>2</sub>O<sub>3</sub>). The percent error of each pair of analyses was determined by taking the standard error of all three pairs and dividing it by the mean of each pair and reported as a percent. The three percent errors were then averaged for a mean percent error for each of the abundant oxides.

## Experiment 1

This experiment was designed to determine the effects of the duration of attrition on a raw sand sample. Bottles were prepared with 50 g of raw sample, 50 g of water and ten steel balls. The mixture was agitated for 2, 5, 10 and 20 minutes. The processed samples (after agitation) in part 1 of the experiment were washed and screened to the complete sand fraction (<2.0 to >0.063 mm) and in part 2, were washed and screened to 70/140 mesh (<0.21 to >0.105 mm). Samples were then dried, weighed and sent for analysis.

## Experiment 2

This experiment was designed to determine the effects of the duration of attrition on a prescreened (before processing) 70/140 mesh (<0.21 to >0.105 mm) split of the raw sand sample. Bottles were prepared with 50 g of 70/140 mesh sample, 50 g of water and ten steel balls. The mixture was agitated for 2, 5, 15 and 20 minutes. Sets of samples were washed and screened to 70/140 mesh (<0.21 to >0.105 mm), then dried, weighed and sent for analysis.

## Experiment 3

This experiment was designed to determine the effects of increasingly more aggressive attrition on a raw sand sample over several periods of time. Bottles were prepared with 20 g of raw sample, 20 g of water and 10, 15 and 20 steel balls. The mixture was agitated for 2, 5, 10 and 20 minutes. Samples were washed and screened to the complete sand fraction (<2.0 to >0.063 mm), then dried, weighed and sent for analysis.

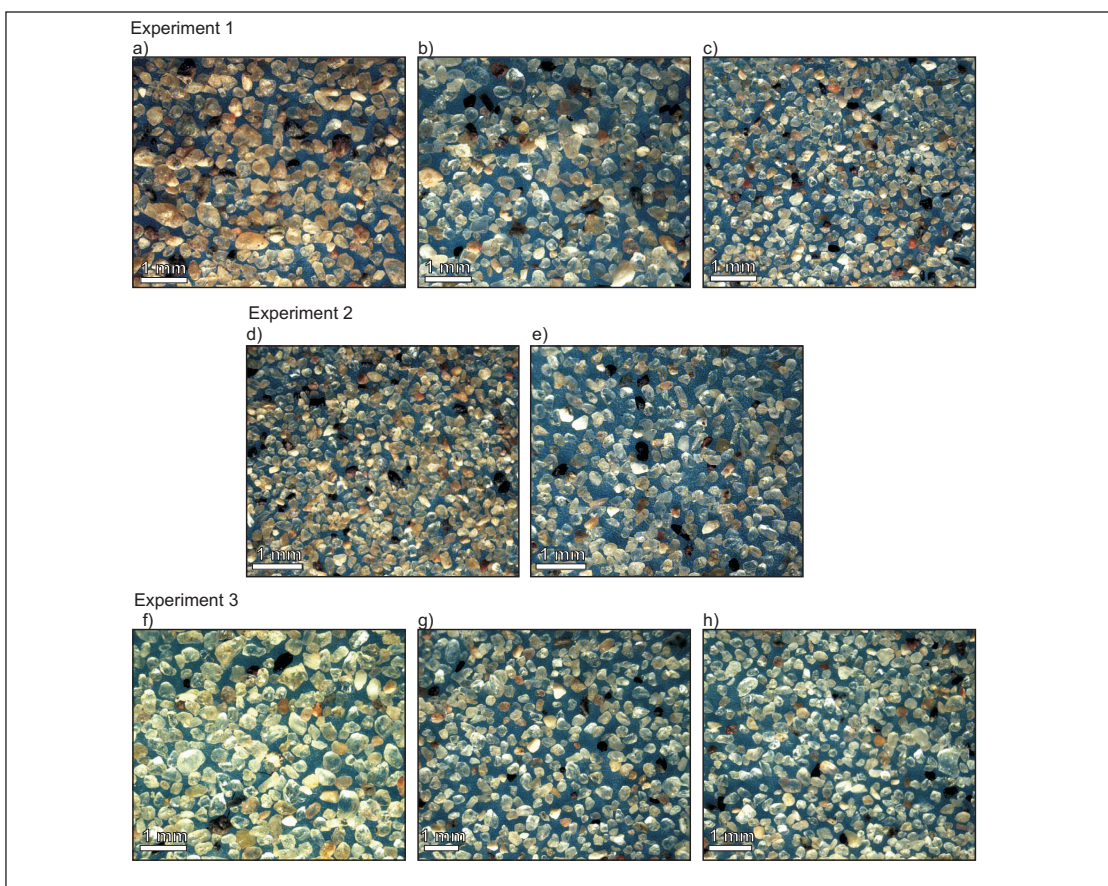


Figure 3. Photograph of sand grains before and after the experiments: a) Unprocessed, washed sand-sized fraction; b) Sand-sized fraction from experiment 1, part 1, after 20 minutes; c) 70/140 mesh-sized fraction from experiment 1, part 2, after 20 minutes; d) Unprocessed, washed 70/140 mesh size fraction used in experiment 2; e) 70/140 mesh-sized fraction from experiment 2, after 20 minutes; f) Sand-sized fraction from experiment 3, after 20 minutes of attrition using 10 steel balls; g) Sand-sized fraction from experiment 3, after 20 minutes of attrition using 15 steel balls; h) Sand-sized fraction from experiment 3, after 20 minutes of attrition using 20 steel balls.



Figure 4. Equipment used in the experiments consisted of a) 250 ml plastic bottles; b) 10 mm, 3.6 g stainless steel balls; c) table shaker; d) scale; e) sieves.

## RESULTS

All analyses are provided in Table 1. In each experiment, the results of the three main oxides ( $\text{SiO}_2$ ,  $\text{Al}_2\text{O}_3$  and  $\text{Fe}_2\text{O}_3$ ) are explored.

### *Quality Control*

The three duplicate analyses offer some measure of variability (Table 2). The quantification of the error gives some assurances that the changes reported in each experiment are significant. Correlation of  $\text{SiO}_2$  and  $\text{Fe}_2\text{O}_3$  in the duplicate pairs is poor, with  $R^2$  values of 0.3289 and 0.0004, respectively (Figure 5). Correlation of  $\text{Al}_2\text{O}_3$  is very good, with an  $R^2$  value of 0.9573. Error bars for each analysis are determined from an average percent error calculated for a standard error and are 0.6663%, 3.04% and 14.33% for  $\text{SiO}_2$ ,  $\text{Al}_2\text{O}_3$  and  $\text{Fe}_2\text{O}_3$ , respectively (Table 3).

TABLE 1. NORMALIZED MAJOR OXIDE GEOCHEMISTRY

Sample	SiO <sub>2</sub>	Al <sub>2</sub> O <sub>3</sub>	Fe <sub>2</sub> O <sub>3</sub>	MgO	CaO	Na <sub>2</sub> O	K <sub>2</sub> O	TiO <sub>2</sub>	P <sub>2</sub> O <sub>5</sub>	MnO	Cr <sub>2</sub> O <sub>3</sub>
	%	%	%	%	%	%	%	%	%	%	%
*D.L.	0.01	0.01	0.04	0.01	0.01	0.01	0.01	0.01	0.01	0.01	0.002
1	90.21	4.57	2.26	0.31	0.52	0.78	1.01	0.20	0.10	0.03	0.005
2	87.71	4.76	4.13	0.38	0.65	0.82	0.99	0.36	0.13	0.05	0.009
3	91.15	4.19	1.93	0.26	0.45	0.75	0.97	0.18	0.09	0.02	0.004
4	89.46	4.71	2.63	0.33	0.60	0.82	1.02	0.26	0.11	0.03	0.017
5	91.22	4.09	1.96	0.25	0.47	0.74	0.96	0.19	0.09	0.02	0.006
6	89.56	4.54	2.72	0.32	0.60	0.82	1.02	0.26	0.11	0.03	0.017
7	91.57	3.93	1.84	0.23	0.44	0.74	0.98	0.17	0.08	0.02	0.004
8	90.12	4.35	2.46	0.29	0.57	0.82	1.01	0.23	0.10	0.03	0.016
9	91.47	3.94	1.89	0.23	0.45	0.76	0.97	0.18	0.08	0.02	0.004
10	90.11	4.31	2.55	0.28	0.56	0.84	1.01	0.22	0.09	0.03	0.006
11	91.73	3.77	1.86	0.22	0.44	0.75	0.95	0.17	0.08	0.02	0.014
12	89.31	4.59	2.91	0.33	0.61	0.80	0.98	0.31	0.12	0.03	0.008
13	89.42	4.57	2.79	0.32	0.61	0.82	1.01	0.30	0.11	0.03	0.016
14	90.01	4.28	2.61	0.30	0.59	0.80	0.97	0.29	0.11	0.03	0.004
15	89.76	4.34	2.78	0.31	0.59	0.80	0.94	0.33	0.10	0.03	0.018
16	90.98	4.13	2.18	0.24	0.45	0.76	0.97	0.17	0.08	0.02	0.003
17	91.35	3.97	2.00	0.22	0.45	0.76	0.96	0.17	0.08	0.02	0.019
18	91.59	3.82	1.99	0.21	0.43	0.75	0.96	0.15	0.07	0.02	0.003
19	91.94	3.70	1.79	0.20	0.42	0.75	0.95	0.14	0.07	0.02	0.019
20	90.85	4.08	2.32	0.24	0.46	0.76	0.97	0.19	0.09	0.02	0.003
21	91.56	3.87	1.99	0.21	0.43	0.75	0.95	0.15	0.07	0.02	0.004
22	91.68	3.82	1.88	0.20	0.44	0.76	0.95	0.16	0.07	0.02	0.017
23	92.11	3.59	1.83	0.18	0.41	0.73	0.91	0.14	0.07	0.02	0.003
24	91.35	3.98	2.00	0.23	0.44	0.75	0.97	0.16	0.08	0.02	0.017
25	91.62	3.86	1.92	0.21	0.42	0.76	0.96	0.15	0.07	0.02	0.004
26	91.73	3.77	1.86	0.21	0.43	0.74	0.97	0.17	0.07	0.02	0.017
27	92.38	3.46	1.76	0.17	0.39	0.71	0.91	0.13	0.06	0.02	0.003

\*Detection Limit

### Experiment 1

Experiment 1 was designed to examine the changes in composition during progressively longer periods of agitation and therefore attrition. Both parts of this experiment were conducted on the raw sand-sized fraction. In part 1, the processed samples were washed to the sand-sized fraction and in part 2, the processed sample was washed to 70/140 mesh size fraction.

In part 1, there was a 4% mass loss in the raw sand-sized fraction over 20 minutes (Figures 3b and 6). During this period, the SiO<sub>2</sub> content increased from 90.21 to 91.73%, a difference of 1.52%. After 20 minutes, the Al<sub>2</sub>O<sub>3</sub> content was reduced from 4.57 to 3.77%, a change of 0.80%, and the Fe<sub>2</sub>O<sub>3</sub> content was reduced from 2.26 to

1.86%, a change of 0.40%. The largest change in the oxide composition happened within the first minute of the experiment. For example, 61.8% of the total increase in SiO<sub>2</sub> content occurred within 1 minute.

In part 2, the 70/140 mesh fraction was separated from the attrition-processed sample. The unprocessed sample experienced a 60.0% loss of mass, indicating that 40% of the sand sample consists of grains in the 70/140 size fraction (Figure 7). When processed, the sample initially lost an additional 4.2% of its mass after 1 minute. Interestingly, the percent mass loss decreased at 5 minutes to a level similar to the unprocessed sample. After 5 minutes, the percent loss fell to below the unprocessed level, indicating the 70/140 size fraction was gaining mass, likely from crushing larger grains. This is consistent with the abundance of angular grains in the sample after 20 minutes (Figure 3c). The SiO<sub>2</sub>

TABLE 2. NORMALIZED MAJOR OXIDE GEOCHEMISTRY OF DUPLICATE SAMPLES FOR QUALITY CONTROL

Sample	SiO <sub>2</sub>	Al <sub>2</sub> O <sub>3</sub>	Fe <sub>2</sub> O <sub>3</sub>	MgO	CaO	Na <sub>2</sub> O	K <sub>2</sub> O	TiO <sub>2</sub>	P <sub>2</sub> O <sub>5</sub>	MnO	Cr <sub>2</sub> O <sub>3</sub>
	%	%	%	%	%	%	%	%	%	%	%
*D.L.	0.01	0.01	0.04	0.01	0.01	0.01	0.01	0.01	0.01	0.01	0.002
3	91.15	4.19	1.93	0.26	0.45	0.75	0.97	0.18	0.09	0.02	0.004
3 Duplicate	90.66	4.29	2.10	0.29	0.56	0.78	1.00	0.19	0.09	0.02	0.015
11	91.73	3.77	1.86	0.22	0.44	0.75	0.95	0.17	0.08	0.02	0.014
11 Duplicate	91.21	3.92	2.14	0.23	0.47	0.77	0.95	0.20	0.08	0.02	0.018
9	91.47	3.94	1.89	0.23	0.45	0.76	0.97	0.18	0.08	0.02	0.004
9 Duplicate	91.71	3.92	1.78	0.22	0.43	0.76	0.93	0.16	0.07	0.02	0.003

\* Detection Limit

TABLE 3. SUMMARY OF DUPLICATE ANALYSIS FOR CONSTRUCTING AVERAGE % ERROR BARS

Oxide	Duplicate Sample	Sample 1	Sample 2	mean	% Error	Standard Error	Average % Error
SiO <sub>2</sub>	3	91.15	90.66	90.91	0.669	0.608	0.666
	11	91.73	91.21	91.47	0.665		
	9	91.47	91.71	91.59	0.664		
Al <sub>2</sub> O <sub>3</sub>	3	4.19	4.29	4.24	2.87	0.122	3.04
	11	3.77	3.92	3.85	3.16		
	9	3.94	3.92	3.93	3.09		
Fe <sub>2</sub> O <sub>3</sub>	3	1.93	2.10	2.02	13.85	0.279	14.33
	11	1.86	2.14	2.00	13.95		
	9	1.89	1.78	1.84	15.20		

content increased from 87.71% in the unprocessed sample to 90.11%, a change of 2.40%. The majority of the increase (72.9% of the total change) occurred within the first 2 minutes. The Al<sub>2</sub>O<sub>3</sub> was reduced from 4.76 to 4.31%, a meagre reduction of only 0.45%. Much of this change occurred between 2 and 10 minutes. The maximum Fe<sub>2</sub>O<sub>3</sub> reduction was from 4.13 to 2.46% (a change of 1.67%) after 10 minutes. This indicates that approximately 40.4% of the Fe<sub>2</sub>O<sub>3</sub> in the unprocessed sample was removed in the experiment, 89.8% of which occurred during the first two minutes.

### Experiment 2

Experiment 2 was designed to examine the changes in composition if the 70/140 mesh size fraction was separated from the raw sand sample before processing and was milled over progressively longer periods of time. The sample experienced 7.8% mass loss over 20 minutes (Figure 8). The SiO<sub>2</sub> content increased from 87.71% in the unprocessed

sample to 90.01% at 15 minutes and dropped to 89.76% after 20 minutes, showing a maximum change of 2.30%. The apparent decline in SiO<sub>2</sub> content from 15 minutes to 20 minutes is within the acceptable margin of error, so is not considered significant. The majority of the increase (53.5% of the total change) occurred in the first minute. The Al<sub>2</sub>O<sub>3</sub> values dropped from 4.76% to a low at 4.28% (15 minutes), a change of only 0.48%. Initially, there was a relatively rapid drop in Al<sub>2</sub>O<sub>3</sub> (35% total reduction), but the majority (60.4% total reduction) of loss occurred between 5 and 15 minutes. The Fe<sub>2</sub>O<sub>3</sub> content decreased from 4.13% to a low of 2.61%, with the most significant drop (80.9% of the total reduction) occurring in the first 2 minutes.

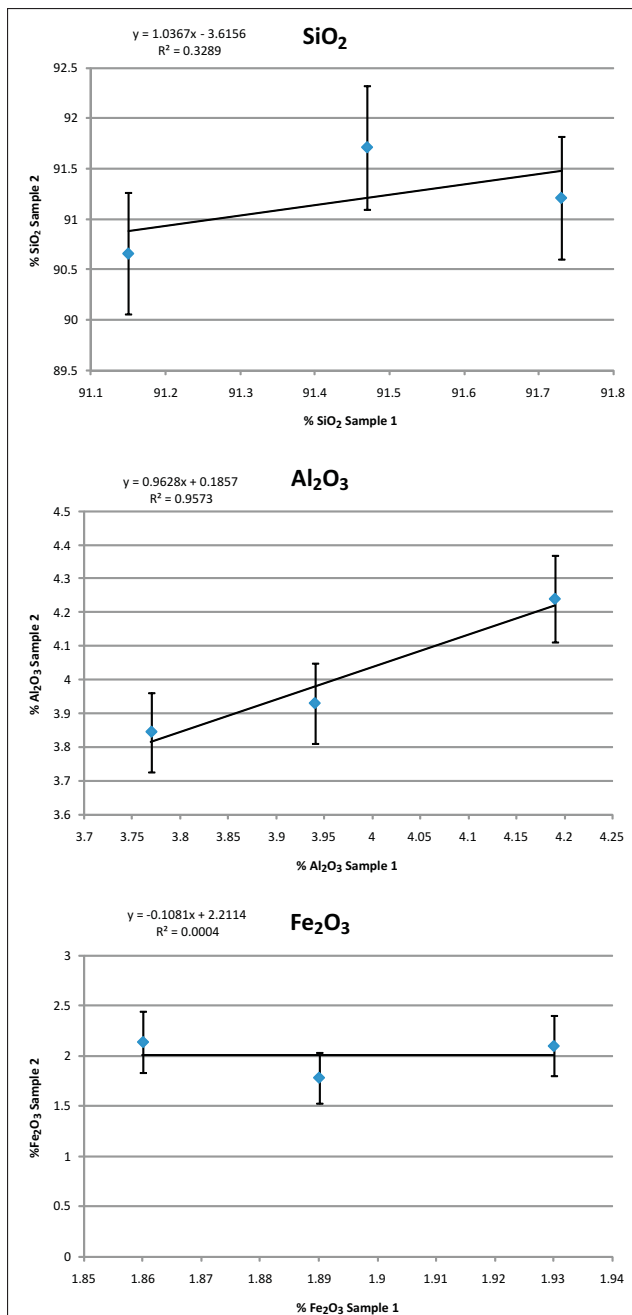


Figure 5. Three duplicate samples were used to assess variation expected in SiO<sub>2</sub>, Al<sub>2</sub>O<sub>3</sub> and Fe<sub>2</sub>O<sub>3</sub>, the three dominant major oxides.

### Experiment 3

Experiment 3 was designed to evaluate progressively more aggressive attrition. After 20 minutes, the 10, 15 and 20 ball experiments lost 4.5%, 4.0% and 6.5% of their mass, respectively (Figure 9). The shape of the percent loss curves suggest that the 10 and 20 ball experiments would continue to lose mass if attrition were continued. The 15 ball experiment, however, shows the curve flattening, indicating that only minor loss would be expected if the experiment was

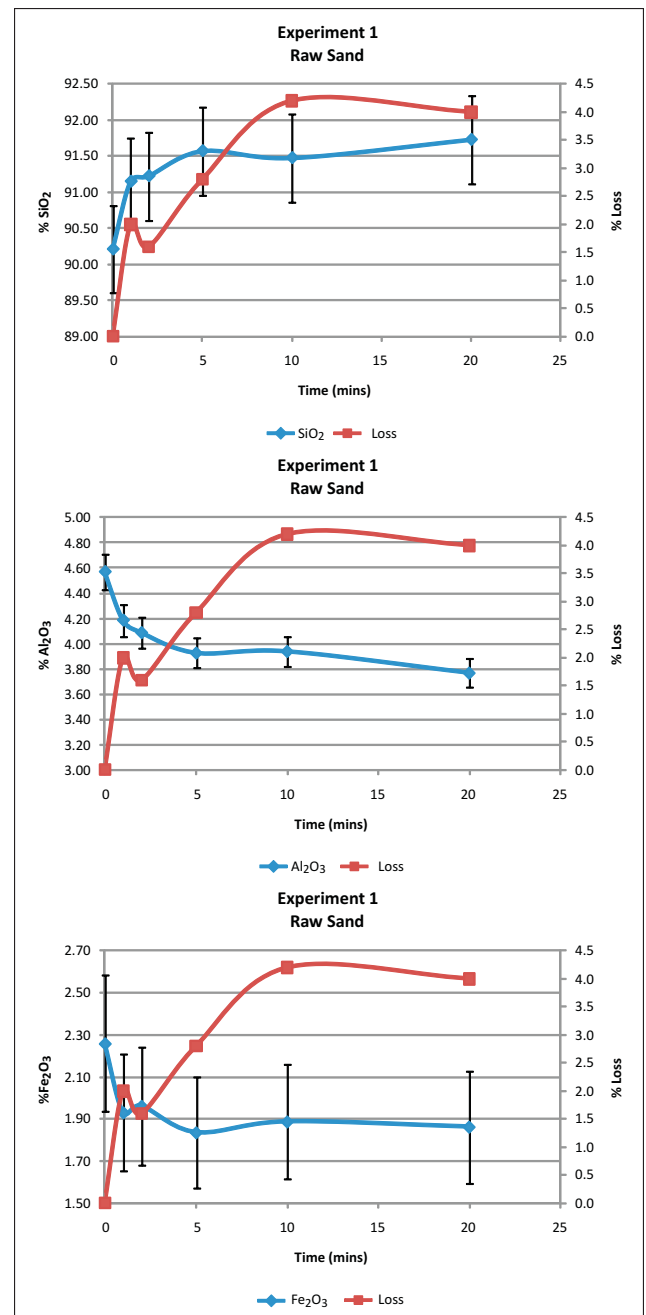


Figure 6. Chart of the percentage mass lost and the SiO<sub>2</sub>, Al<sub>2</sub>O<sub>3</sub> and Fe<sub>2</sub>O<sub>3</sub> analysis versus time from experiment 1, part 1.

continued. The 10 ball experiment showed the SiO<sub>2</sub> content increased by 1.73% from 90.21 to 91.94%. The 15 ball experiment showed only slightly better results, with the SiO<sub>2</sub> content increasing from 90.21 to 92.11%, a change of 1.9%. The 20 ball experiment showed the SiO<sub>2</sub> content increasing from 90.21 to 92.38%, a change of 2.17%. All the curves show a rapid increase in SiO<sub>2</sub> in the early part of the experiment before flattening.

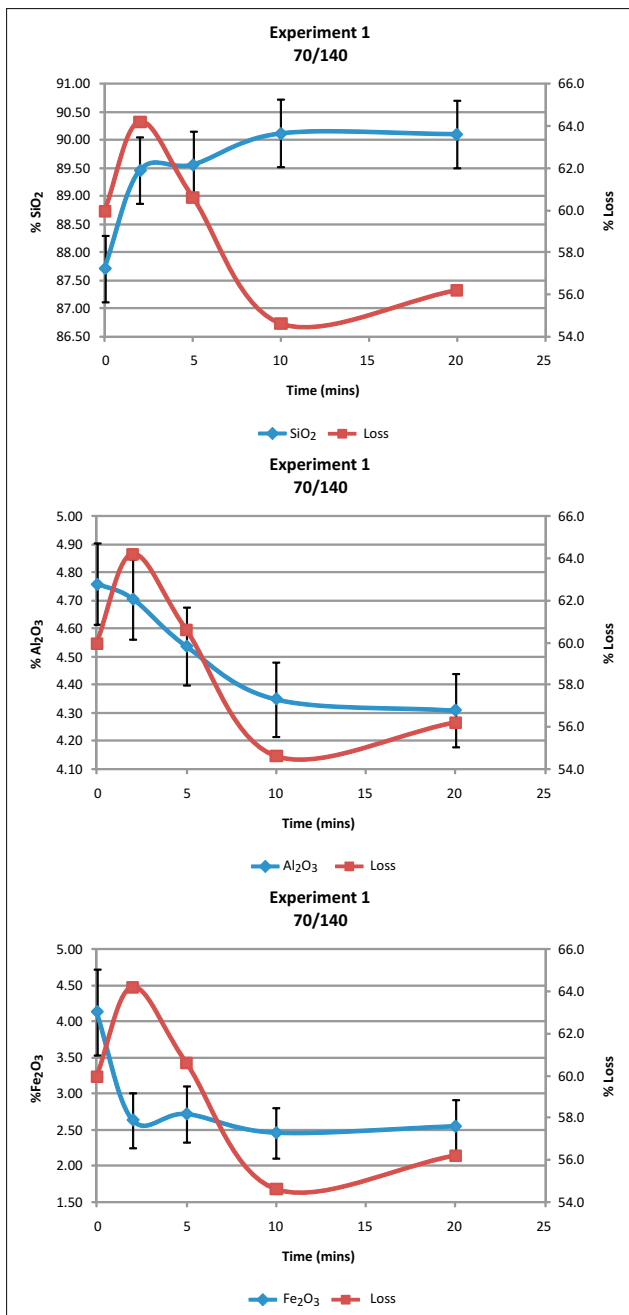


Figure 7. Chart of the percentage mass lost and the SiO<sub>2</sub>, Al<sub>2</sub>O<sub>3</sub> and Fe<sub>2</sub>O<sub>3</sub> analysis versus time from experiment 1, part 2.

## DISCUSSION

The duplicate samples used in the quality-control portion of this experiment show that the precision of the SiO<sub>2</sub> and the Fe<sub>2</sub>O<sub>3</sub> data is relatively poor; therefore, there is a large margin of error associated with the precision of the analyses (indicated by the error bars in Figure 5). There must be a relatively large change in the proportion of these two oxides to consider the change significant. The experiments do show a significant change from the initial measurement to the final measurement, but much of the variability in the later time values are within acceptable error.

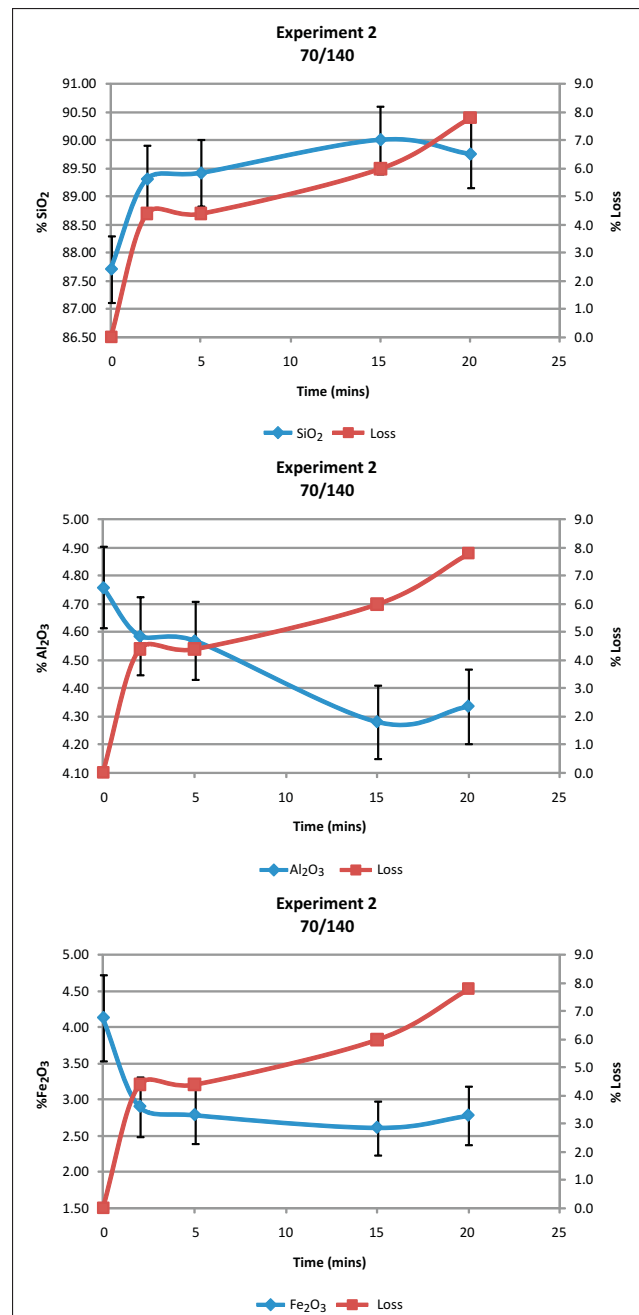


Figure 8. Chart of the percentage mass lost and the SiO<sub>2</sub>, Al<sub>2</sub>O<sub>3</sub> and Fe<sub>2</sub>O<sub>3</sub> analysis versus time from experiment 2.

Experiment 1, part 1 shows approximately 4% mass loss over 20 minutes, indicating grains were breaking down; however, SiO<sub>2</sub> increased to a maximum of 91.73%, 1.52% more than the unprocessed sample (Figure 6). The reduction of Al<sub>2</sub>O<sub>3</sub> and Fe<sub>2</sub>O<sub>3</sub> indicate that grains of undesirable minerals and lithic fragments (e.g., feldspar, mica, clay) were partially removed, but a substantial proportion remained. Most of the SiO<sub>2</sub> increase and Al<sub>2</sub>O<sub>3</sub> and Fe<sub>2</sub>O<sub>3</sub> decrease occurred in early stages of the experiment, so it is unlikely that increasing the duration of attrition would improve the SiO<sub>2</sub> content of the sample under these experimental conditions.



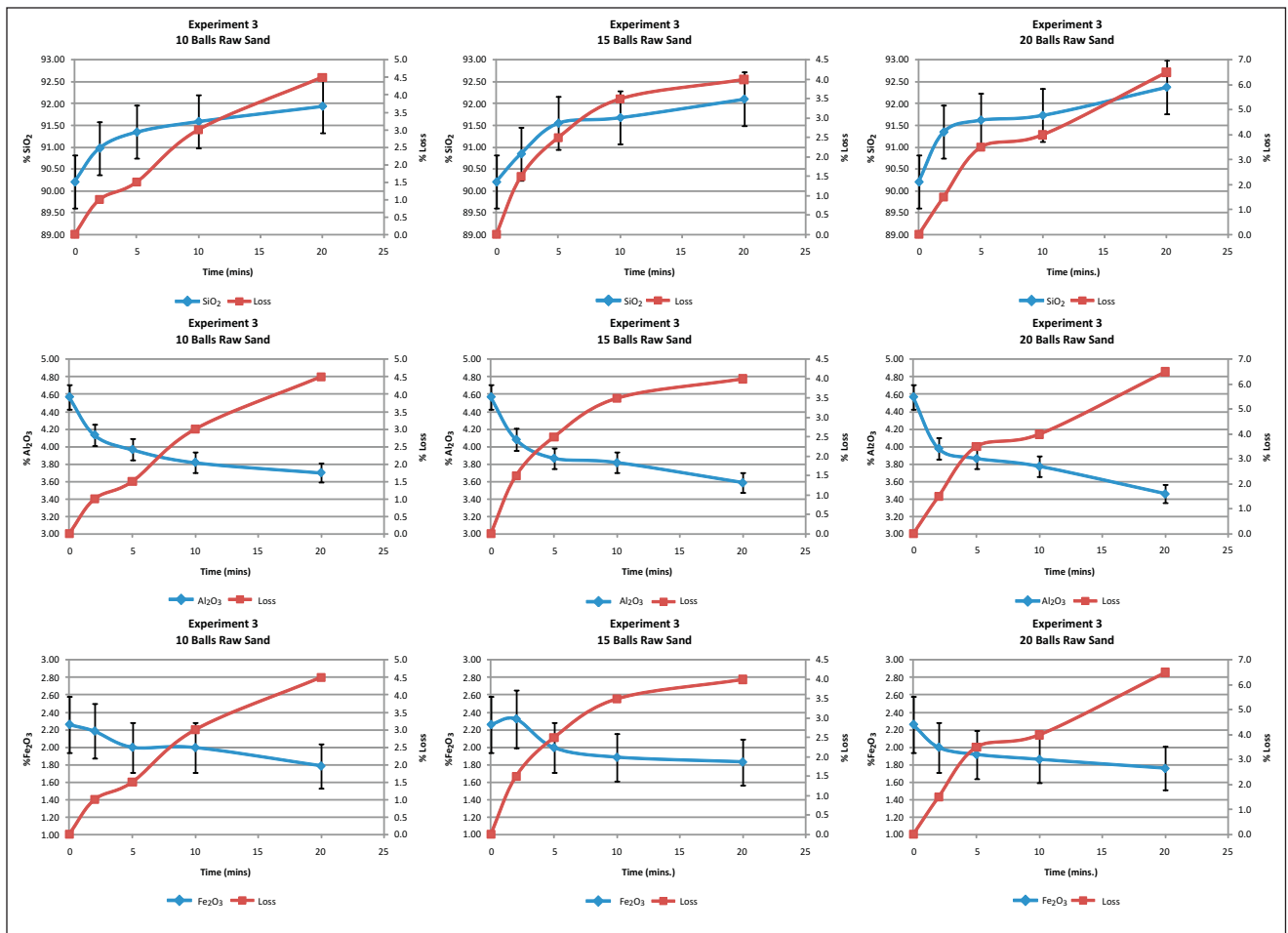


Figure 9. Chart of the percentage mass lost and the  $\text{SiO}_2$ ,  $\text{Al}_2\text{O}_3$  and  $\text{Fe}_2\text{O}_3$  analysis versus time from experiment 3.

Experiment 1, part 2 focused specifically on the impact of attrition on the 70/140 mesh size fraction within a raw sand sample. The experiment shows the addition of mass after 5 minutes of attrition, indicating the generation of grains in the 70/140 size fraction (Figure 7). This, presumably, was from the breakage of larger grains. The inflection in the  $\text{SiO}_2$  curve at 5 minutes (the time when the mass began to increase) suggests larger quartz grains began to fracture into smaller grains at this time. This is significant because angular grains are not desirable for frac sand, so although attrition may improve silica content, the fracturing of grains may degrade the suitability of the sand. The relatively limited and slow decrease in  $\text{Al}_2\text{O}_3$  suggests that  $\text{Al}_2\text{O}_3$ -bearing grains, possibly feldspar and hard (silicified) clay-rich lithic grains, resisted degradation during the course of the experiment. The rapid reduction in  $\text{Fe}_2\text{O}_3$  after 2 minutes suggests that Fe-bearing grains degraded early in the experiment. Although there was a relatively significant increase in the proportion of  $\text{SiO}_2$  from 87.71% in the unprocessed sample to 90.12%, it is well below the suggested  $\text{SiO}_2$  content used in frac sand.

Experiment 2 was designed to test if separating the 70/140 fraction from the raw sand sample would improve

results. The experiment produced a loss of 7.8% and the curve suggests that if the experiment were continued, there may be additional loss of material. The proportion of  $\text{SiO}_2$  in the unprocessed 70/140 size fraction is 87.71% and after processing, the sample had a maximum  $\text{SiO}_2$  content of 90.01%, an increase that mostly occurred in the first 2 minutes. Although this represents a relatively large improvement, it fails to achieve content that meets industry specifications. The flattening of the  $\text{SiO}_2$  curve signifies that continuing the experiment would likely not increase the silica content significantly, probably because quartz grains are being milled in the later stages of the experiment. The  $\text{Al}_2\text{O}_3$  shows an initial rapid decline and then a second drop between 5 and 15 minutes; however, the total reduction of  $\text{Al}_2\text{O}_3$  from 4.76% to 4.28% represents a small improvement. The percentage of  $\text{Fe}_2\text{O}_3$  dropped rapidly, in the first 2 minutes, followed by negligible improvement over the remaining 18 minutes.

Experiment 3 was aimed at testing if the experimental design was more aggressive, there would be an appreciable improvement in the  $\text{SiO}_2$  content. In the 10 ball scenario, there was a 4.5% mass loss and the percent loss curve suggests that additional material would be lost if the

experiment was prolonged. Although most of the increase in  $\text{SiO}_2$  and decrease in  $\text{Al}_2\text{O}_3$  occurred in the first 2 minutes, the curves suggest that if the experiment persisted, there may have been additional improvements. Nonetheless, the maximum  $\text{SiO}_2$  value of 91.94% is only marginally better than the unprocessed sand. The 15 ball experiment was slightly more successful with the  $\text{SiO}_2$  proportion, reaching 92.11%. The percent loss curve flattened over 20 minutes, although material would continue to be lost if the experiment was allowed to continue. Similarly,  $\text{SiO}_2$  would increase and  $\text{Al}_2\text{O}_3$  would decrease if time were extended. The  $\text{Fe}_2\text{O}_3$ , however, shows very little change between 5 and 20 minutes. The 20 ball experiment, considered the most aggressive in these tests, caused the greatest improvement in the sample, and the curves suggest that continuing the experiment may result in additional enhancement. The  $\text{SiO}_2$  content reached 92.38% and the  $\text{Al}_2\text{O}_3$  and  $\text{Fe}_2\text{O}_3$  were reduced to 3.46% and 1.76%, respectively; however, the experiment did produce an abundance of broken, angular quartz grains. Either the time duration should be limited or additional processing would be required to round the grains to meet the well rounded/spherical shape requirements suggested by the industry specifications.

In general, the experiments resulted in limited beneficiation. This, in part, is attributed to the limited scope of the experimental design. Nonetheless, the findings suggest that attrition alone is not sufficient to improve the content of the sand samples to an acceptable level and other beneficiation (magnetic separation, floatation, acid dissolution, etc.) is likely required. Attrition may offer some economic benefit early in processing, initially reducing the highly deleterious grains before more expensive and intensive physical, physiochemical or chemical processing is conducted. In these experiments, the unprocessed sample was relatively high in  $\text{SiO}_2$ , so the improvements were meagre. Attrition may be an appreciable process where the sand has a lower initial  $\text{SiO}_2$  content. Regardless, some form of attrition and washing should be included in any processing circuit. The duration of attritions will need to be optimized for industrial-scale beneficiation. In these experiments, the majority of improvement occurred in the early stages of the experiments (<5 minutes). Extending the attrition process may have adverse affects on the grain shape because of breakage.

Although silica content is an important factor in the suitability of sand for use as a proppant, other parameters, such as crush strength, acid solubility and grain shape are also critical. Silica content may not meet standards, but if the sand is satisfactory in the other parameters, it should still be considered for use as a proppant or proppant blend. Ultimately, further evaluation of the deposits' qualities is necessary to design and optimize a beneficiation process.

## CONCLUSION

- These attrition experiments show that light milling of the sand sample will result in the degradation of deleterious sand grains; however, attrition alone was insufficient to elevate the  $\text{SiO}_2$  content to industry standards. Attrition may be an effective early step in a processing circuit, removing highly deleterious grains in lower-grade samples. Other physical, physiochemical and chemical processing will be required to upgrade deposits for use as industrial proppants.
- Much of the improvement in the silica content was achieved early in the experiments. Consequently, a short duration of attrition would benefit the quality of the sample and would only add a brief processing step.
- Aggressive milling and longer durations tended to produce the greatest increase in  $\text{SiO}_2$  and the greatest decrease in  $\text{Al}_2\text{O}_3$  and  $\text{Fe}_2\text{O}_3$ . Aggressive milling and extending the experiments beyond approximately 5 minutes produced abundant angular grains that are detrimental to the quality of the proppant. Optimizing the time and intensity of attrition must be explored at the industrial scale to maximize the effectiveness of the processing step.

## ACKNOWLEDGMENTS

This project has benefitted from extensive collaboration between the BC Ministry of Energy and Mines and the Geological Survey of Canada. Rod Smith is thanked for directing us to the Fontas Dune Field. Transportation for sampling was provided by Great Slave Helicopters. The authors appreciate the review and comments from Ray Lett and Jeff Bond, which improved the manuscript.

## REFERENCES

- American Petroleum Institute (1995a): Recommended practices for testing sand used in hydraulic fracturing operations; *American Petroleum Institute*, API RP 56, 12 pages.
- American Petroleum Institute (1995b): Recommended practices for testing high-strength proppants used in hydraulic fracturing operations; *American Petroleum Institute*, API RP 60, 14 pages.
- Dumont, M. (2007): Silica/quartz; in Canada Mineral Yearbook, Godin, E., Editor, *Natural Resources Canada*, pages 47.1–47.12.
- Freeman, H.D., Gerber, M.A., Mattigod, S.V. and Serne, R.J. (1993): 100 area soil washing bench-scale test procedures; *Pacific Northwest Laboratory*, PNL-8520, 23 pages.
- Hickin, A.S., Ferri, F., Ferbey, F. and Smith, I.R. (2010): Preliminary assessment of potential hydraulic fracture sand sources and their depositional origin, northeast British Columbia; in Geoscience Reports, 2010, *BC Ministry of Energy and Mines*, pages 35–91.
- Huntley, D.H. and Hickin, A.S. (2010): Surficial deposits, landforms, glacial history and potential for granular aggregate and frac sand: Maxhamish Lake map area (NTS 94O), British Columbia; *Geological Survey of Canada*, Open File 6430, 17 pages.
- Huntley, D.H. and Hickin, A.S. (2011): Geo-Mapping for Energy and Minerals program (GEM-Energy): preliminary surficial geology, geomorphology, resource evaluation and geohazard assessment for the Maxhamish Lake Map Area (NTS 94O), northeastern British Columbia; in Geoscience Reports 2011, *BC Ministry of Energy and Mines*, pages 57-73.
- Huntley, D.H. and Sidwell, C.F. (2010): Application of the GEM surficial geology data model to resource evaluation and geohazard assessment for the Maxhamish Lake map area (NTS 94O), British Columbia; *Geological Survey of Canada*, Open File 6553, 22 pages.
- Huntley, D.H., Hickin, A.S. and Ferri, F. (2011): Provisional surficial geology, glacial history and paleogeographic reconstruction of the Toad River (NTS 94N) and Maxhamish Lake map areas (NTS 94O), British Columbia; in Geoscience Reports 2011, *BC Ministry of Energy and Mines*, pages 37-55.
- International Organization for Standards (2006): Petroleum and natural gas industries – completion fluids and materials – part 2: measurement of properties of proppant used in hydraulic fracturing and gravel-packing operations; *International Organization for Standards*, Report Number ISO 13503-2, 28 pages.
- Sundararajan, M., Ramaswamy, S. and Raghavan, P. (2009): Evaluation for the beneficiability of yellow silica from the overburden of lignite mine situated in Rajpardi District of Gujarat, India; *Journal of Minerals and Materials Characterization and Engineering*, Volume 8, pages 569–581.
- Taxiarchaou, M., Pnias, D., Douni, I., Paspaliaris, I. and Kontopoulos, A. (1997): Removal of iron from silica sand by leaching with oxalic acid; *Hydrometallurgy*, Volume 46, pages 215–227.
- Wentworth, C.K. (1922): A scale of grade and class terms for clastic sediments; *Journal of Geology*, Volume 30, pages 377–392.
- Zdunczyk, M. (2007): The facts of frac; *Industrial Minerals*, January 2007, pages 58–61.





